

GEOTHERMOMETRY - GEOBAROMETRY AND  
 $^{40}\text{Ar}/^{39}\text{Ar}$  INCREMENTAL RELEASE DATING  
IN THE SANDWICH BAY AREA, GRENVILLE  
PROVINCE, EASTERN LABRADOR

CENTRE FOR NEWFOUNDLAND STUDIES

**TOTAL OF 10 PAGES ONLY  
MAY BE XEROXED**

(Without Author's Permission)

TIMOTHY STUART van NOSTRAND





National Library  
of Canada

Bibliothèque nationale  
du Canada

Canadian Theses Service

Service des thèses canadiennes

Ottawa, Canada  
K1A 0N4

## NOTICE

The quality of this microform is heavily dependent upon the quality of the original thesis submitted for microfilming. Every effort has been made to ensure the highest quality of reproduction possible.

If pages are missing, contact the university which granted the degree.

Some pages may have indistinct print especially if the original pages were typed with a poor typewriter ribbon or if the university sent us an inferior photocopy.

Previously copyrighted materials (journal articles, published tests, etc.) are not filmed.

Reproduction in full or in part of this microform is governed by the Canadian Copyright Act, R.S.C. 1970, c. C-30.

## AVIS

La qualité de cette microforme dépend grandement de la qualité de la thèse soumise au microfilmage. Nous avons tout fait pour assurer une qualité supérieure de reproduction.

S'il manque des pages, veuillez communiquer avec l'université qui a conféré le grade.

La qualité d'impression de certaines pages peut laisser à désirer, surtout si les pages originales ont été dactylographiées à l'aide d'un ruban usé ou si l'université nous a fait parvenir une photocopie de qualité inférieure.

Les documents qui font déjà l'objet d'un droit d'auteur (articles de revue, tests publiés, etc.) ne sont pas microfilmés.

La reproduction, même partielle, de cette microforme est soumise à la Loi canadienne sur le droit d'auteur, SRC 1970, c. C-30.

GEOOTHERMOMETRY - GEOBAROMETRY AND  $^{40}\text{Ar}/^{39}\text{Ar}$  INCREMENTAL RELEASE  
DATING IN THE SANDWICH BAY AREA, GRENVILLE PROVINCE, EASTERN  
LABRADOR.

by

© Timothy Stuart van Nostrand (B.Sc. Hons.)

A thesis submitted in partial fulfillment of the requirements of  
Master of Science

Department of Earth Sciences  
Memorial University of Newfoundland

June 1987

St. John's

Newfoundland



Permission has been granted to the National Library of Canada to microfilm this thesis and to lend or sell copies of the film.

The author (copyright owner) has reserved other publication rights, and neither the thesis nor extensive extracts from it may be printed or otherwise reproduced without his/her written permission.

L'autorisation a été accordée à la Bibliothèque nationale du Canada de microfilmer cette thèse et de prêter ou de vendre des exemplaires du film.

L'auteur (titulaire du droit d'auteur) se réserve les autres droits de publication; ni la thèse ni de longs extraits de celle-ci ne doivent être imprimés ou autrement reproduits sans son autorisation écrite.

ISBN 0-315-43353-1

# ABSTRACT

Three major lithotectonic units have recently been defined in the Grenville Province of eastern Labrador on the basis of contrasting lithologic associations, structural style and metamorphic grade. Two of these units, the Groswater Bay and Lake Melville Terranes are interpreted to represent parts of the parautochthonous and allochthonous units, respectively, which are two regional subdivisions of the Grenville Province in Labrador.

Geothermometry and geobarometry estimates derived from garnet - biotite - plagioclase -  $Al_2SiO_5$  - quartz and garnet - orthopyroxene - clinopyroxene - plagioclase - quartz equilibria of selected paragneiss and mafic lithologies in the Sandwich Bay area suggest contrasting metamorphic P-T conditions of the two terranes. Estimates determined from the Groswater Bay Terrane range from 615°C to 850°C and 10 - 12 kbar, suggesting derivation from depths on the order of 30 to 40 km. In contrast estimates from the Lake Melville Terrane range from 650°C to 900°C and 6 - 10 kbar implying crustal derivation from 20 to 30 km. Microstructural relationships and mineral chemistry of the assemblages in each terrane suggest that the P-T estimates obtained from each terrane are representative of Grenvillian metamorphic conditions.

Equilibrium P-T paths constructed from the geothermobarometry estimates are interpreted to represent a portion of the uplift trajectory for both the Groswater Bay and Lake Melville Terranes. These paths suggest that both terranes followed a near isothermal

uplift path, implying rapid decompression during cooling.

$^{40}\text{Ar}/^{39}\text{Ar}$  incremental release radiometric dating of hornblende concentrates from orthogneiss and associated mafic dikes from the study area reveal contrasting ages from both terranes. Age spectra from the Groswater Bay Terrane are generally discordant and are interpreted to result from a combination of the presence of excess argon components and partial gas loss as a result of thermal resetting of the argon system. One sample from the Groswater Bay Terrane yields a reasonably defined plateau age of  $1260 \pm 5$  Ma. A similar plateau age of  $1241 \pm 3$  Ma is obtained from a sample immediately south of the Rigolet thrust zone in the Lake Melville Terrane. The significance of these pre-Grenvillian ages is at present not understood since they do not correlate with any major event (thermal or cooling) previously known in the Grenville Province. However, they are tentatively interpreted to date a closure of argon in hornblende at ca. 1250 Ma. Spectra obtained from samples from the southern Lake Melville Terrane record reasonably well defined  $^{40}\text{Ar}/^{39}\text{Ar}$  plateaux. One sample yields a plateau age of  $1070 \pm 50$  Ma, which is in broad agreement with the 1030 Ma age suggested for the culmination of Grenvillian metamorphism in the Lake Melville Terrane and is thus interpreted to represent the very rapid uplift following Grenvillian thermal overprinting. The most southerly samples yield younger ages of  $1020 \pm 8$  Ma and  $980 \pm 12$  Ma and are interpreted to results from slower post-Grenvillian uplift and subsequent cooling through the retention temperature required for argon in the hornblende crystal lattice.

## ACKNOWLEDGEMENTS

Field work for this thesis was carried out during the summers of 1984 and 1985 when the author was employed with the Newfoundland Department of Mines and Energy. I wish to thank Dr. Toby Rivers of the Memorial University of Newfoundland, who acted as supervisor for this project and who provided greatly appreciated guidance, suggestions and discussions throughout. Dr. Charles F. Gower of the Newfoundland Department of Mines and Energy is thanked for his ongoing interest in the project, for numerous discussions and guidance, both in and out of the field and for contributing many of the samples used in the study. Dr. Henry Longerich is thanked for his instruction on the use of the electron microprobe and for helpful discussion. A special thanks is given to Dr. Peter Reynolds and Keith Taylor of Dalhousie University who guided me through the radiometric dating analyses. Appreciation is extended to Flemming Mengel who both encouraged and helped me with useful discussions and in addition allowed me access to his most useful computer programs. Finally, I thank my family and friends for their patience and encouragement during my studies at Memorial.

## CONTENTS

iv

ABSTRACT .....	1
ACKNOWLEDGEMENTS .....	iii
CONTENTS .....	iv
TABLES .....	viii
FIGURES .....	ix
ABBREVIATIONS .....	xii
<u>CHAPTER 1 INTRODUCTION</u> .....	1
1.1 Purpose and Scope .....	1
1.2 The Grenville Province .....	3
1.3 Subdivisions of the Grenville Province in Labrador .....	5
1.3.1 Western Labrador .....	5
1.3.2 Central Labrador .....	8
1.3.3 Eastern Labrador .....	10
<u>CHAPTER 2 LITHOLOGIC UNITS</u> .....	13
2.1 Introduction .....	13
2.2 Groswater Bay Terrane .....	13
2.3 Lake Melville Terrane .....	18
<u>CHAPTER 3 STRUCTURE</u> .....	20
3.1 Introduction .....	20
3.2 Groswater Bay Terrane .....	20
3.3 Lake Melville Terrane .....	23
3.4 The Rigolet thrust zone .....	26
3.5 Grenvillian Effects .....	28
3.6 Pre-Grenvillian Effects .....	29



<b>CHAPTER 4 METAMORPHISM</b> .....	31
4.1 Introduction .....	31
4.2 Mineral Assemblages in the Groswater Bay Terrane .....	31
4.3 Mineral Assemblages in the Lake Melville Terrane .....	32
4.4 The Petrogenetic Grid .....	35
4.4.1 P-T Estimates from Paragneiss Isograds .....	35
4.4.2 P-T Estimates from Mafic Isograds .....	44
4.4.3 Microstructural Relationships .....	49
<b>CHAPTER 5 GEOTHERMOMETRY - GEOBAROMETRY</b> .....	64
5.1 Introduction .....	64
5.2 Methods .....	65
5.3 Geothermometry - Geobarometry Results .....	65
5.3.1 Calculation of P-T Estimates .....	65
5.3.2 Geothermometry Results .....	66
5.3.2.1 Garnet-Biotite .....	66
5.3.2.2 Garnet-Clinopyroxene-Orthopyroxene .....	70
5.3.3 Geobarometry Results .....	73
5.3.3.1 Garnet-Plagioclase- $\text{Al}_2\text{SiO}_5$ -Quartz .....	73
5.3.3.2 Garnet-Orthopyroxene-Clinopyroxene Plagioclase-Quartz .....	79
5.3.4 Comparison of P-T results from basic rocks and paragneisses .....	82
5.4 Interpretation of Geothermobarometry Results .....	83
5.4.1 Garnet-Biotite-Plagioclase- $\text{Al}_2\text{SiO}_5$ -Quartz .....	83
5.4.2 Garnet-Orthopyroxene-Clinopyroxene-Plagioclase Quartz .....	88
5.4.3 Regional Interpretation of Geothermobarometry Results .....	89

5.4.4	Equilibrium Pressure-Temperature Paths .....	99
CHAPTER 6	$^{40}\text{Ar}/^{39}\text{Ar}$ DATING .....	107
6.1	Introduction .....	107
6.2	Previous Geochronology .....	108
6.3	Statement of Problem .....	112
6.4	$^{40}\text{Ar}/^{39}\text{Ar}$ Results .....	113
6.4.1	Introduction .....	113
6.4.2	$^{40}\text{Ar}/^{39}\text{Ar}$ Spectra in the Groswater Bay Terrane ....	119
6.4.3	$^{40}\text{Ar}/^{39}\text{Ar}$ Spectra in the Lake Melville Terrane ....	122
6.5	Interpretation of $^{40}\text{Ar}/^{39}\text{Ar}$ Results .....	124
6.5.1	Introduction .....	124
6.5.2	Groswater Bay Terrane .....	125
6.5.3	Lake Melville Terrane .....	126
6.5.4	Implications for geothermobarometry .....	130
6.5.5	Origin of Extraneous Argon Components .....	131
CHAPTER 7	SUMMARY AND CONCLUSIONS .....	134
REFERENCES	.....	140
APPENDICES	.....	148
A.1	Petrography .....	148
A.2	Sample location map .....	154
A.3	Geologic map of study area .....	156
A.4	Activity Composition Relations .....	157
A.5	Geothermobarometry Methods .....	159
A.5.1	Exchange Thermometers .....	159
A.5.1.1	Garnet-Biotite .....	159
A.5.1.2	Orthopyroxene-Clinopyroxene .....	164

A.5.1.3	Garnet-Clinopyroxene .....	165
A.5.1.4	Garnet-Orthopyroxene .....	166
A.5.2	Net Transfer Barometers .....	167
A.5.2.1	Garnet-Plagioclase- $\text{Al}_2\text{SiO}_5$ -Quartz .....	167
A.5.2.2	Garnet - Clinopyroxene-Orthopyroxene- Plagioclase-Quartz .....	171
A.6	Microprobe Procedure .....	174
A.7	$^{40}\text{Ar}/^{39}\text{Ar}$ Procedure .....	176
A.8	Compositional Data .....	178
A.8.1	Compositional Parameters of Garnet-Biotite- Plagioclase .....	178
A.8.2	Compositional Parameters of Garnet-Orthopyroxene- Clinopyroxene-Plagioclase .....	179
A.8.3	Activities of Garnet-Orthopyroxene-Clinopyroxene Plagioclase .....	180
A.8.4	Composition of Hornblendes used in $^{40}\text{Ar}/^{39}\text{Ar}$ Dating .....	181
A.8.5	Microprobe Analyses .....	182

TABLES

Table 1: Temperature estimates obtained from garnet -biotite thermometers in the Sandwich Bay area.....	68
Table 2: Temperature estimates obtained from garnet - clinopyroxene, garnet - orthopyroxene and two - pyroxene thermometers in the Sandwich Bay area.....	72
Table 3: Temperature and pressure estimates and thermodynamic properties derived from garnet - biotite and garnet - plagioclase - Al <sub>2</sub> SiO <sub>5</sub> - quartz calibrations.....	75
Table 4: Temperature and pressure estimates derived from mafic rocks.....	80
Table 5: Lithologies used in <sup>40</sup> Ar/ <sup>39</sup> Ar study.....	114
Table 6: Analytical data of <sup>40</sup> Ar/ <sup>39</sup> Ar dating.....	115

## FIGURES

Figure 1:	Location of study area and subdivisions of the Grenville Province in eastern Labrador ...	2
Figure 2:	Tectonic subdivision of the Grenville Province in western Labrador .....	6
Figure 3:	Lithotectonic subdivision in the Grenville Province .....	9
Figure 4:	Lithologic units in the Grenville Province of eastern Labrador .....	15
Figure 5:	Regional structural pattern in eastern Labrador .....	20
Figure 6:	Major structures and kinematic interpretation of the Lake Melville Terrane .....	24
Figure 7:	Petrogenetic grid for paragneiss assemblages in the Groswater Bay and Lake Melville Terranes .....	37
Figure 8a:	Relict kyanite and stable cordierite in garnet-sillimanite-biotite paragneiss in the Lake Melville Terrane (Sample CG81-170B) .....	42
Figure 8b:	Relict kyanite and unstable cordierite in garnet-sillimanite-biotite paragneiss in the Lake Melville Terrane (Sample CG81-170B) .....	42
Figure 9:	Orthopyroxene-sillimanite-bearing paragneiss in the Lake Melville Terrane (Sample 235B) .....	42
Figure 10:	Petrogenetic grid for mafic rocks in the Groswater Bay and Lake Melville Terranes .....	45
Figure 11:	Equilibrium textural relationships between garnet and biotite in Groswater Bay Terrane paragneiss (Sample CG81-299A) .....	51
Figure 12:	Disequilibrium relationships of biotite inclusions in garnet in Groswater Bay Terrane paragneiss (Sample GF81-21) .....	51
Figure 13:	Coarse biotite grains truncated by garnet porphyroblasts in Groswater Bay Terrane paragneiss (Sample GF81-16) .....	51
Figure 14:	Pre-tectonic garnet porphyroblasts wrapped by main gneissic fabric (Sample GF81-18) .....	55



Figure 15:	Equilibrium relationships between kyanite and muscovite in Groswater Bay Terrane paragneiss (Sample GF81-16) .....	55
Figure 16:	Dis-equilibrium relationships between kyanite and muscovite in Groswater Bay Terrane paragneiss (Sample GF81-21) .....	55
Figure 17:	Crenulation of fabric defined by muscovite in Groswater Bay Terrane (Sample CG81-756) .....	59
Figure 18:	Partial replacement of kyanite by stable sillimanite in paragneiss, immediately south of the Rigolet thrust zone (Sample CG81-170B) ...	59
Figure 19:	Retrograde hornblende rims on granoblastic opx and cpx grains in the Lake Melville Terrane (Sample VN84-422) .....	59
Figure 20:	Granoblastic textures in garnet-cpx-opx granulite in the Lake Melville Terrane (Sample VN84-229) .....	62
Figure 21:	Plot of P-T estimates obtained from pelitic assemblages, together with appropriate isograds .....	78
Figure 22:	Plot of P-T estimates obtained from mafic assemblages, together with appropriate isograds .....	81
Figure 23:	Distribution of temperature estimates derived from pelitic and mafic assemblages within the study area.....	85
Figure 24:	Distribution of pressure estimates derived from pelitic and mafic assemblages within the study area.....	87
Figure 25:	Plot of P-T estimates obtained from paragneiss and mafic assemblages .....	91
Figure 26:	Temperature-time path, of rocks buried at variable depths in relation to post-thrusting erosion .....	95
Figure 27a:	Phase equilibria for paragneisses in the Groswater Bay Terrane .....	102

Figure 27b: Phase equilibria for paragneisses in the Lake Melville Terrane .....	102
Figure 28: Equilibrium pressure-temperature paths for the Groschat Bay and Lake Melville Terranes ...	104
Figure 29: Previous $^{40}\text{Ar}/^{39}\text{Ar}$ and K/Ar dates in eastern Labrador.....	109
Figure 30: • Previous Rb/Sr, Nd/Sm and U/Pb dates in eastern Labrador.....	110
Figure 31: $^{40}\text{Ar}/^{39}\text{Ar}$ age spectra in the study area.....	118

## ABBREVIATIONS

The following abbreviations are used in this text

$a_j$ : activity of component j in phase i

$\gamma_j$ : activity coefficient (component j in phase i)

$X_j$ : molar proportion of component j in phase i

ab: albite component in plagioclase

alm: almandine component in garnet

an: anorthite component in plagioclase

Ar: argon

bi: biotite

cord: cordierite

cpx: clinopyroxene

en: enstatite

fs: ferrosilite

GBT: Groswater Bay Terrane

gr: grossular component in garnet

ga: garnet

hbl: hornblende

ksp: potassium feldspar

ky: kyanite

LMT: Lake Melville Terrane

mag: magnetite

mu: muscovite

opx: orthopyroxene

P-T: pressure-temperature

P-T-t: pressure-temperature-time

pl: plagioclase

py: pyrope component in garnet

qtz: quartz

RTZ: Rigolet thrust zone

sa: sapphirine

sill: sillimanite

sp: spessartine component in garnet

## CHAPTER 1.

### INTRODUCTION

#### 1.1 Scope and Purpose

This thesis project is a contribution to the regional study of the Grenville Province in eastern Labrador, which is being conducted by C.F. Gower, and was initiated when the author was employed as a senior assistant with the Newfoundland Department of Mines and Energy during the 1984 and 1985 field seasons. The study involves an examination of parts of two lithotectonic terranes, the Groswater Bay and Lake Melville Terranes in the Sandwich Bay area, eastern Labrador (Figure 1).

The first purpose of the study is to outline the tectono - metamorphic evolution of the two terranes in terms of pre-Grenvillian and Grenvillian histories, in particular with regard to the conditions and timing of metamorphism within and at the boundary of the terranes. Emphasis is placed on the quantitative determination of pressure and temperature conditions with the application of recently calibrated geothermobarometers derived for both pelitic and basic assemblages. Estimates are used to interpret P-T gradients in an attempt to distinguish pre-Grenvillian from Grenvillian metamorphic conditions.

A second aspect of this study involves  $^{40}\text{Ar}$ - $^{39}\text{Ar}$  incremental release radiometric dating of hornblende concentrates separated from several samples collected within the map area. These data are used to supplement previous geochronology in the eastern Grenville Province

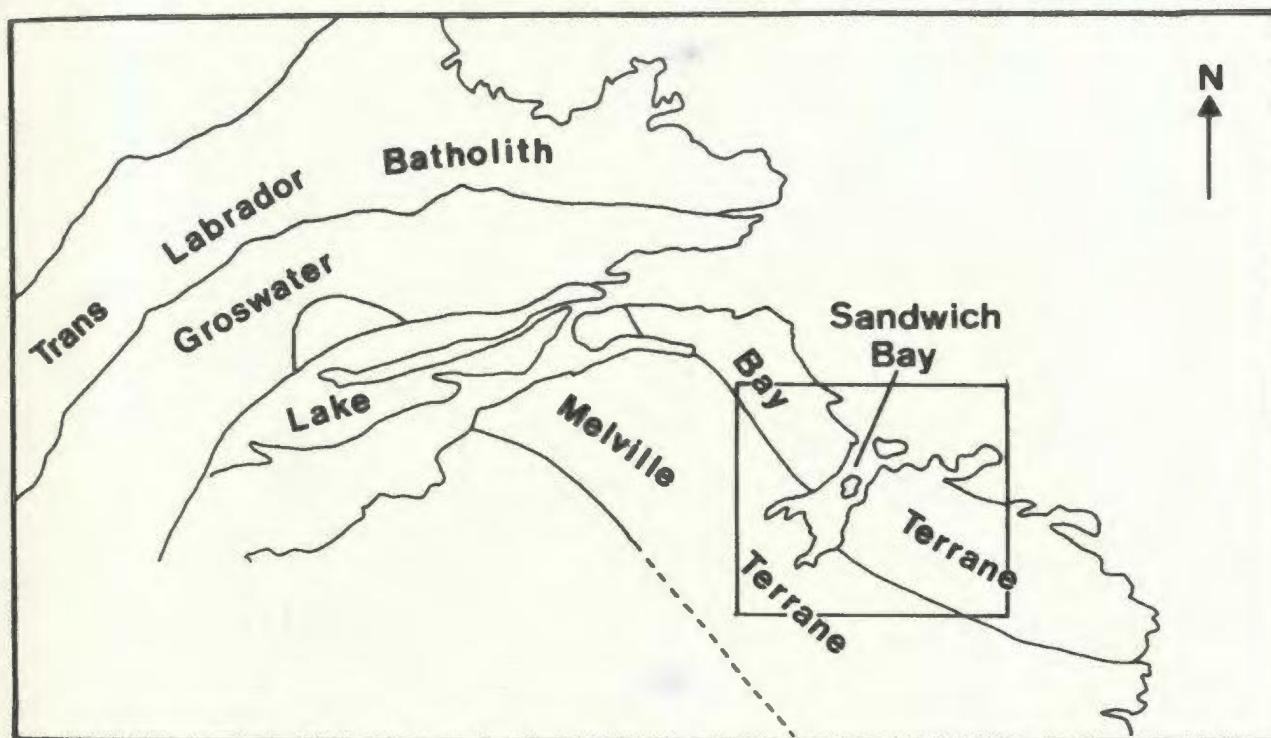


Figure 1. Location of study area and subdivisions of the Grenville Province in eastern Labrador, after Gower and Owen (1984).



in an attempt to interpret the thermal and uplift history in the region.

Laboratory analyses involved extensive petrography and the acquisition of mineral chemistry using the electron probe microanalyzer. Radiometric dating involved isotopic analyses of argon in hornblende concentrates using the incremental step-wise heating method.

The Sandwich Bay region in eastern Labrador (Figure 1) lies entirely within the Grenville Province and straddles a major thrust fault, known as the Rigolet thrust zone (Gower and Owen, 1984), which has been defined as the boundary between the Groswater Bay and Lake Melville Terranes. Field work for the project involved assisting in 1:100,000 scale geological mapping of N.T.S map sheets 13H/3,4,5,6 (Gower et al., 1985) and 13H/1,2,7,8 (Gower et al., 1986). Samples for microprobe and geochronological analyses were collected from the above areas, and in addition from 13H/11,12,14,15,16 (Gower et al., 1982).

## 1.2 The Grenville Province

Knowledge of the geology of the Grenville Province in Labrador prior to 1977 was based largely on 1:250 000 scale reconnaissance mapping completed by the Geological Survey of Canada during the early 1970's, (summarized by Greene, 1972) and the geological evolution of this segment of the Canadian Shield was in general poorly understood. According to Wynne-Edwards (1972), who summarized the state of knowledge at that time, much of the eastern and central Grenville

Province is underlain by quartzofeldspathic gneisses, of both granitic and sedimentary protolith, which range from Archean to Mid-Proterozoic in age. These gneisses were considered to be, at least in part, originally part of the adjacent older tectonic provinces which were subsequently incorporated and reworked during the Grenvillian Orogeny. Before their reworking, these rocks had acted as a basement for Lower and Middle Proterozoic supracrustal sequences, remnants of which were recognized across the orogen. Additionally, plutonism was known to be extensive in the Grenville Province of Labrador with the intrusion of a variety of granitic, gabbroic and anorthositic plutonic suites, thought to be predominantly of Middle Proterozoic age. At that time, however, lithologic, structural, metamorphic and age relationships between the various units were largely unknown and much of the interpretation with respect to pre-Grenvillian and Grenvillian tectonic events was speculative.

In 1977 however, the Newfoundland Department of Mines and Energy, in cooperation with the Geological Survey of Canada, began the process of remapping the Grenville Province in Labrador at 1:100 000 and 1:50 000 scales, and associated studies have included comprehensive geochronological and bedrock geochemical analyses. The objective of this work has been to develop a better understanding of the supracrustal sequences and of the metamorphic, plutonic and tectonic history and mineral potential of the belt as a whole.

Recent work has shown that the Grenville Province is composed of a collage of lithotectonic terranes with both pre-Grenvillian and Grenvillian histories, which can be distinguished on the basis of

the character and age of the rocks, together with their structural style and metamorphic grade. These terranes were emplaced together during the Grenvillian Orogeny along major thrust faults (Gower and Owen, 1984)

### 1.3 Subdivisions of the Grenville Province

#### 1.3.1 Western Labrador

In western Labrador, Rivers and Nunn (1985), Rivers and Chown (1986) have proposed a subdivision of the Grenville Province, which is purely tectonic in concept. The orogen is divided into three tectonic units: an autochthon, a parautochthon and several allochthons (Figure 2). The autochthon, which lies immediately south of the Grenville Front, is composed primarily of the reworked equivalents of older, adjacent provinces and is interpreted to have been deformed "in situ" during the Grenvillian Orogeny (Rivers and Nunn, 1985). Further south, towards the interior of the Grenville Province, a parautochthonous unit has been defined which is underlain by several major thrust faults, and interpreted to be composed of imbricate thrust nappes. Structural and lithological continuity suggests that overall movement along these thrust faults was not extensive, although crustal thickening was considerable. Structurally overlying, and in thrust contact with the parautochthon are a series of allochthonous units, interpreted to be tectonically emplaced thrust nappe structures. Lack of structural, lithological and metamorphic correlation suggests a significant amount of transport along the thrust faults bounding the allochthons.

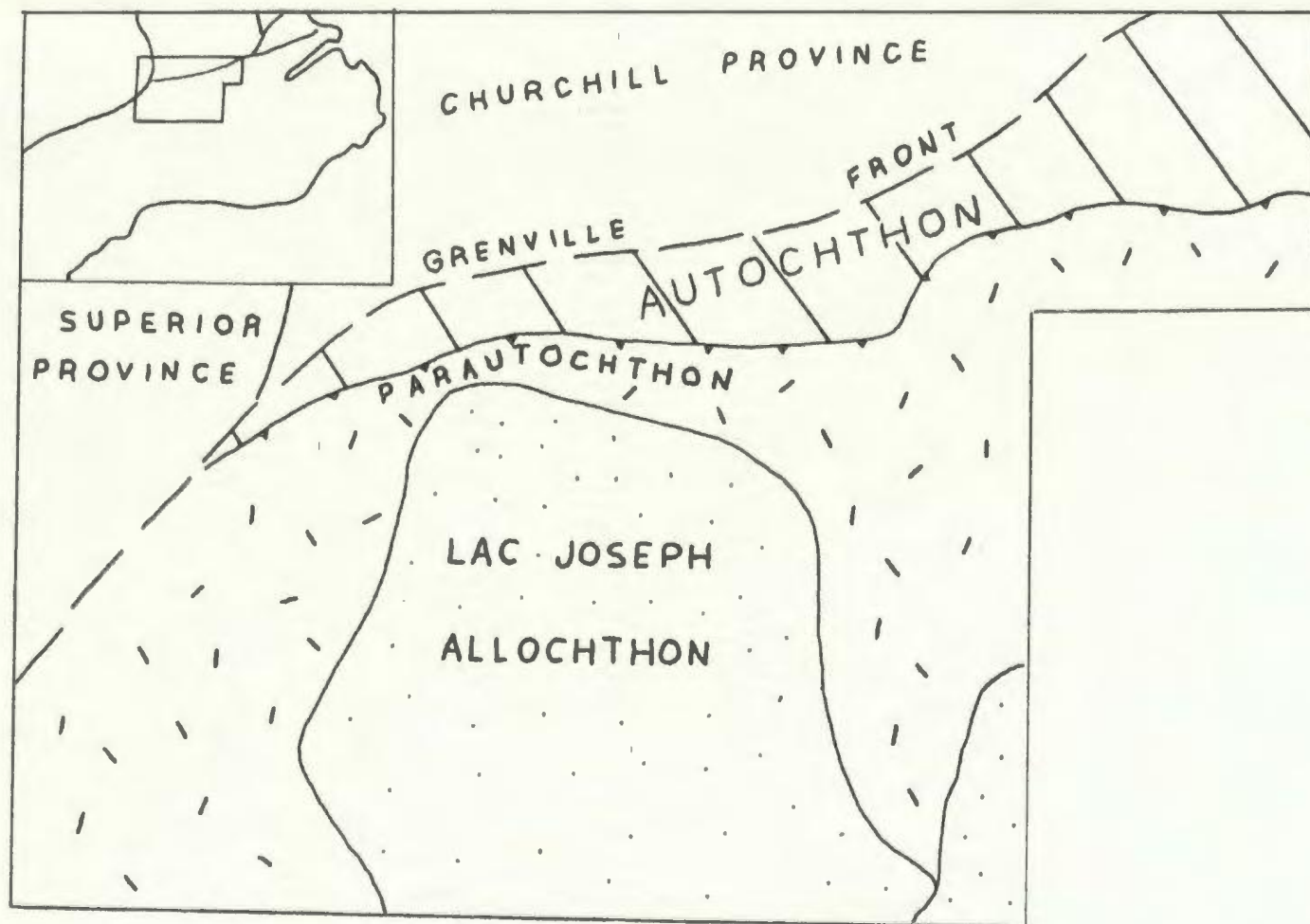


Figure 2. Tectonic subdivision of the Grenville Province in western Labrador, after Rivers and Nunn (1985).

The structural, lithologic and metamorphic relationships between the autochthon, parautochthon and allochthons are well developed in western Labrador, and may be used as a model of the tectonic style in the eastern Grenville Province. In western Labrador, the western part of the foreland is composed of Archean gneisses of the Superior Province which form the basement to an unmetamorphosed to greenschist facies, lower Proterozoic platformal supracrustal sequence known as the Knob Lake Group (Rivers and Nunn, 1985). The autochthon, to the south of the Grenville Front, represents the continuation of these rocks where they display a well developed Grenvillian overprint (generally a cleavage or schistosity), but no evidence of translation by thrusting.

The parautochthon comprises rocks with distinct pre-Grenvillian histories which were subsequently overprinted by Grenvillian metamorphism and tectonism. In the west, the previously unmetamorphosed southerly extension of the lower Proterozoic Knob Lake Group was metamorphosed during the Grenvillian Orogeny resulting in the development of a progressive metamorphic sequence from greenschist facies in the north to upper amphibolite facies in the south (Rivers, 1983a). In the eastern portion of the parautochthon, in Figure 2, high grade gneisses and granitoid rocks which were formed and emplaced during the recently defined Labradorian Orogeny at 1650 Ma (Nunn and Christopher, 1983), were reworked under amphibolite facies conditions during the Grenvillian Orogeny. Thus the Grenvillian metamorphic overprint was at amphibolite facies in most of the parautochthon, and was associated with regional imbrication by thrusting, giving rise to extensive crustal



thickening.

Structurally overlying, and in thrust contact with the parautochthon are rocks interpreted to be allochthonous, termed the Lac Joseph Allochthon, in western Labrador (Rivers and Nunn, 1985). Presently available evidence suggests that this unit has a negligible Grenvillian metamorphic overprint. Rivers and Nunn noted that the progressive metamorphic sequence present in the parautochthon is truncated by the allochthon. Lithologic units which can be correlated from the autochthon into the parautochthon cannot be traced across the parautochthon-allochthon boundary. Radiometric U-Pb dating of zircon and monazite within the allochthon yields consistent ages of about 1650 Ma. This implies that the last significant thermal event experienced by the allochthon was at 1650 Ma and suggests that Grenvillian reworking was minor. Rivers and Nunn considered that structural emplacement of the allochthon occurred during the Grenvillian Orogeny and that although the interior of the allochthon may have a negligible metamorphic overprint, the basal portion may in fact have been considerably reworked during the Grenvillian Orogeny (Rivers and Nunn, 1985).

This regional subdivision, established in western Labrador, (Rivers and Nunn, 1985) has been shown to be compatible with divisions throughout the entire Grenville Province in Labrador (Figure 3) and into Quebec (Rivers and Chown, 1986).

#### 1.3.2 Central Labrador

In central Labrador, middle Proterozoic greenschist facies

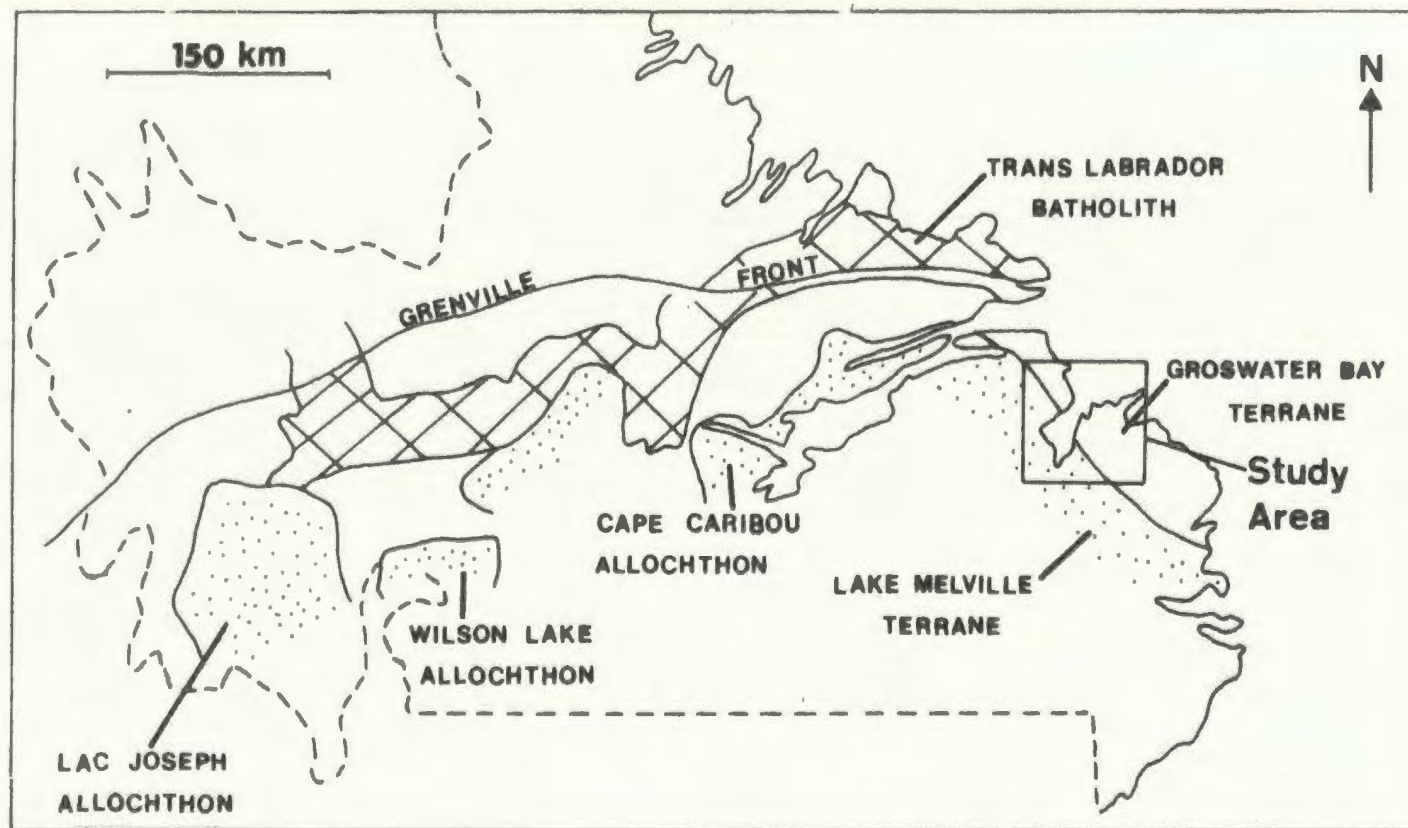


Figure 3. Lithotectonic subdivisions in the Grenville Province in Labrador, after Rivers and Chown (1986).

supracrustal and granitoid rocks with minor remnants of amphibolite facies Hudsonian gneisses define the parautochthonous unit (Thomas, 1985). The southern limit of the parautochthon is marked by major south-dipping thrust zones. The parautochthon contains greenschist to upper amphibolite facies lithologies of predominantly calc-alkaline granitoids and semi-pelitic migmatitic paragneiss. The allochthon to the south, known as the Wilson Lake Allochthon (Figure 3) is composed of quartzofeldspathic paragneiss containing hypersthene, sapphirine and sillimanite, and is interpreted to be a deep-seated crustal fragment, tectonically emplaced over the parautochthon as a klippe.

### 1.3.3 Eastern Labrador

In eastern Labrador, the Grenville Province is divided into three major lithotectonic terranes, (Gower, 1981; Gower and Owen, 1984), defined on the basis of distinct lithological, structural and metamorphic characteristics (Figure 1). Although the subdivision of the three terranes is based primarily on lithological and metamorphic distinctions, a partial correlation can be made with the tectonic division proposed by Rivers and Chown in western Labrador.

The northern most terrane, the Trans-Labrador Batholith is a major belt of post-orogenic granitoid rocks associated with the newly defined Labradorian Orogeny (Thomas et al., 1985; Rivers and Nunn, 1985) which extends along the northern margin of the Grenville Province in Labrador. U-Pb and Rb-Sr dating yields 1650 ma. to 1600 ma. ages, the U-Pb ages being almost concordant. Variably deformed granodiorite, granite, quartz monzonite and quartz syenite are the

predominant lithologies and are characterized by greenschist facies sub assemblage of chlorite, albite and epidote.

South of the Trans-Labrador Batholith, Gower (1981) and Gower and Owen (1984) describe a major lithotectonic unit, the Groswater Bay Terrane, which is a large arcuate belt extending 350 km through eastern Labrador. Its northern extent is defined as the southern boundary of the Trans-Labrador Batholith. Rock types include predominantly tonalitic to granodioritic orthogneiss, mafic intrusions, various granitoid rocks and minor pelitic paragneiss. Metamorphic grade is at middle to upper amphibolite facies with local retrogression to greenschist facies. Radiometric age dates imply that the region underwent a major tectonothermal event at 1650 Ma. and a weaker Grenvillian event at 1100 Ma. (Gower and Owen, 1984). Regional correlation with the 3-fold subdivision of the Grenville Province in Labrador discussed previously suggests that the Groswater Bay Terrane is part of the Grenvillian parautochthon.

A third lithotectonic unit, the Lake Melville Terrane, recently defined in the Grenville Province of eastern Labrador is a 60 km wide and 250 km long crustal segment which is bounded in the north by the Groswater Bay Terrane and in part by the Mealy Mountains Terrane to the south. Major rock types include pelitic and semi-pelitic paragneiss, K feldspar megacrystic and non-megacrystic granodiorite and layered mafic complexes. Metamorphic grade is at upper amphibolite to granulite facies, with the development of greenschist facies assemblages along fault zones. Field evidence suggests that the Lake Melville Terrane is allochthonous and has been tectonically juxtaposed upon the Groswater Bay Terrane along the Rigolet thrust

zone, during the Grenvillian Orogeny (Gower and Owen, 1984)

The lithologic association, metamorphic grade and tectonic nature of both the Groswater Bay and Lake Melville Terranes in eastern Labrador suggests a strong correlation with the parautochthon - allochthonous units respectively in western and central Labrador. The Groswater Bay Terrane comprises rocks with distinct pre-Grenvillian histories which have been overprinted by widespread Grenvillian amphibolite facies metamorphism and associated tectonism.

Structurally overlying and in thrust contact with the Groswater Bay Terrane, the Lake Melville Terrane is interpreted by Gower and Owen (1984) to represent an allochthonous segment, which was transported northward during the Grenvillian Orogeny.

## CHAPTER 2

### LITHOLOGIC UNITS

#### 2.1 Introduction

The delineation of the parautochthon and the allochthon in eastern Labrador is reflected in a contrast in lithologic associations. Although some similarities in the compositions of lithologies exist between the Groswater Bay and the Lake Melville Terranes, relative proportions and field characteristics are used as a basis to classify rock types into their respective terranes (Gower and Owen, 1984). The Groswater Bay Terrane is composed predominantly of granitic orthogneiss, foliated granitoids and mafic rocks, with semi-pelitic paragneiss being a minor rock type, whereas in the Lake Melville Terrane, pelitic and semi-pelitic paragneiss, layered mafic intrusions and foliated granitoids are the major lithologies.

#### 2.2 Groswater Bay Terrane

Major rock types occurring within the Groswater Bay Terrane include granodiorite to tonalite orthogneiss, diorite to quartz diorite, K feldspar megacrystic and non-megacrystic granodiorite, pyroxene-bearing granitoids, various mafic lithologies and pelitic and semi-pelitic paragneiss (Figure 4). Field relationships between the orthogneiss and the foliated granitoid rocks in some areas indicate that the gneisses are basement rocks occurring as enclaves within the granitoids, which are themselves intruded by Helikian

Figure 4. Lithologic units in the Grenville Province of eastern Labrador, after Gower and Owen, 1984; Gower et al., 1985, 1986.

MM - Mealy Mountains Terrane (anorthosite and related rocks)  
 MGGB - Mount Gnat Granulite Belt; EID - Earl Island Domain;  
 RTZ - Rigolet thrust zone; PMGB - Paradise Metasedimentary Gneiss Belt; SHBP - Sand Hill, Big Pond gabbro-norite; WBAC - White Bear Arm Complex.

MAKKOVIK PROVINCE AND TRANS-LABRADOR BATHOLITH



Bruce River Group (1.63 Ga.)



Trans-Labrador Batholith (1.65 - 1.60 Ga.)



Upper Aillik Group (1.8 - 1.6 Ga.)



Syn-Makkovikian granitoid plutons (1.85 - 1.75 Ga.)



Lower Aillik and Moran Lake Groups (1.9 Ga.)



Tonalitic to granodioritic gneiss, amphibolite (ca. 1.76 Ga.)

GROSWATER BAY AND LAKE MELVILLE TERRANES (GRENVILLE PROVINCE)



Double Mer Formation (0.8 Ga.)



Undivided granitoid plutons (1.65 - 1.25 Ga.)



Undivided mafic intrusions (1.65 - 1.40 Ga.)



Layered gabbro-anorthosite-monzonite (granulite facies 1.65 Ga.)



Diorite to quartz monzonite (1.65 Ga.)

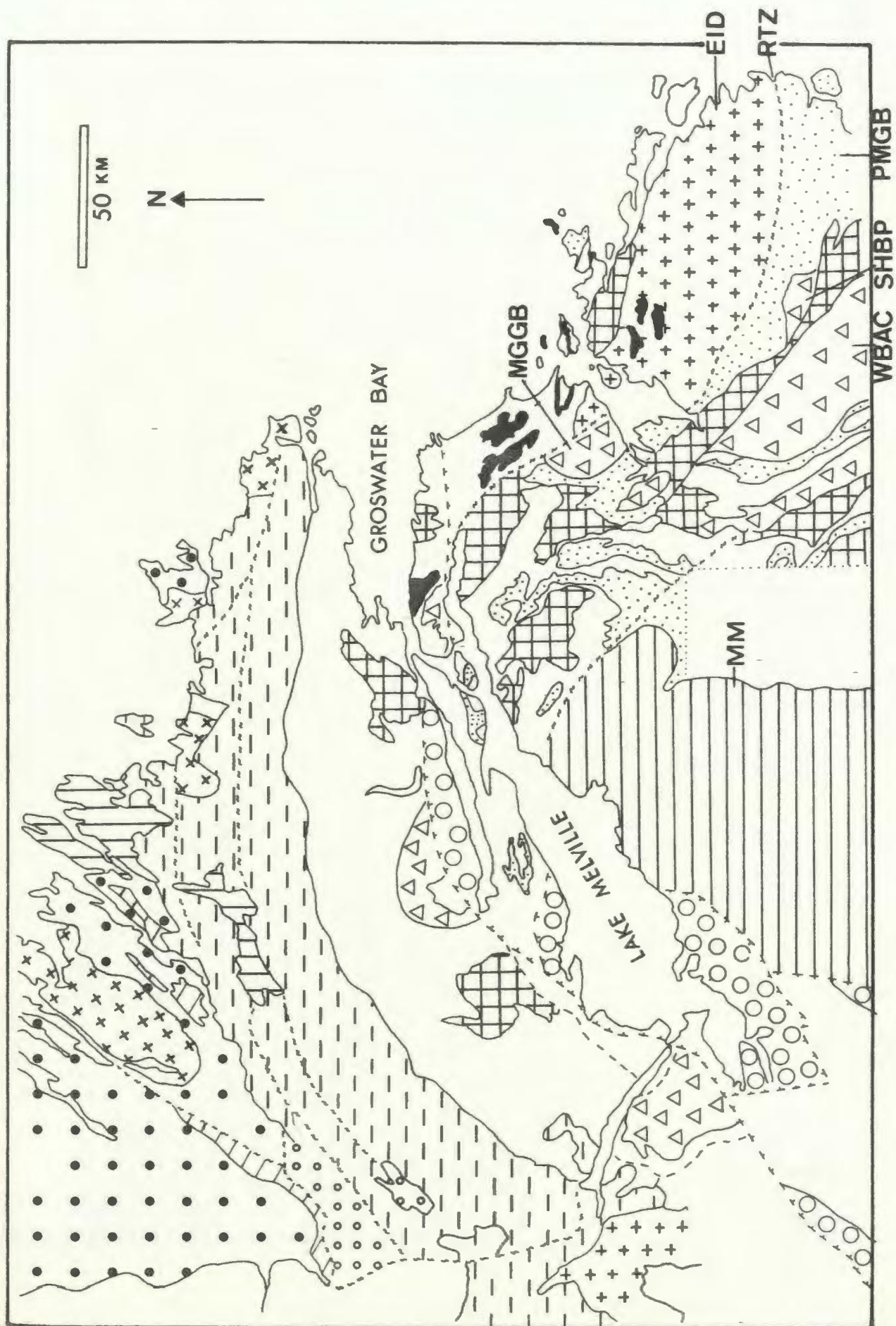


Tonalitic to granodioritic gneiss (1.65 Ga. and older)



Metasedimentary gneiss (1.90 Ga.)







gabbros. In other areas, a gradational contact between the gneisses and the granitoids implies a variation in the Grenvillian deformational overprint (Gower and Owen 1984). Younger granitoids are interpreted as having been emplaced partly coeval with and partly postdating the 1650 Ma thermotectonism in the supracrustal rocks which were deposited on or adjacent to the inferred gneissic basement.

The orthogneiss is characterized by well developed migmatitic banding, locally grading into strongly foliated granodiorite and tonalite. Biotite is the dominant mafic phase although hornblende and garnet are common.

Paragneisses in the Groswater Bay Terrane are divided into 2 major groups by Gower and Owen (1984). These are medium and high grade pelitic paragneiss and low grade metasedimentary rocks with recognizable primary structures. Medium to high grade metasediments characteristically contain biotite-garnet-quartz-plagioclase-K feldspar with kyanite as the aluminosilicate polymorph, locally partially retrogressed to muscovite. Migmatitic fabrics are widespread and the unit displays a range from schistose to gneissic fabrics. In many areas, concordant aplitic dikes and enclaves enhance the gneissic appearance. The restite is composed of fine-grained aggregates of kyanite, biotite and magnetite. The leucosome component is composed of recrystallized quartz, plagioclase and K feldspar. Minor biotite and magnetite are commonly present. The low grade metasediments are dominantly greywacke and siltstone and although a strong fracture cleavage is developed, primary sedimentary bedding is commonly preserved. Gower and Owen (1984) consider that the low grade

metasediments post-date the regional medium to high grade metamorphism of Labradorian (1650 Ma) age.

Dioritic to quartz monzonitic rocks are predominant in the south-eastern portion of the Groswater Bay Terrane (Figure 4). The major rock type is a medium to coarse-grained diorite to quartz diorite characterized by a weakly foliated to gneissic fabric. Hornblende and biotite are ubiquitous and locally the rock contains K feldspar megacrysts. Associated with the quartz diorite unit are intrusions of medium-grained commonly megacrystic biotite granodiorite, which in some areas appear to be gradational with the quartz diorite. The diorite to quartz diorite and associated biotite granodiorite are collectively grouped into a major intrusive body which occupies the Earl Island Domain (Gower, 1981).

Mafic rocks comprise a significant proportion of the Groswater Bay Terrane. Gower and Owen (1984) subdivide them into 2 distinct suites, the older consisting predominantly of layered intrusions, the younger composed of mafic dikes. The older suite includes olivine gabbro, anorthosite, leucogabbro, pyroxenite and associated monzonites and syenites. These rocks are comparable both in age and lithologic affinity to the Adlavik Intrusive Suite of the Makkovik Province dated at 1650 to 1600 Ma and Gower and Owen (1984) and have tentatively correlated them with it. The younger suite of mafic intrusions which is composed of olivine-bearing ophitic to corona textured metagabbros, has been assigned to the 1400 Ma Michael gabbro (Gower and Owen, 1984). Other mafic rocks include several suites of dikes which pre-date intrusion of the 1400 Ma gabbro and post-date early Helikian granitoids (Gower et. al., 1982). Two generations of

diabase dikes of Phanerozoic age have also been recognized.

### 2.3 Lake Melville Terrane

In contrast to the Groswater Bay Terrane, the Lake Melville Terrane is dominated by pelitic and semi-pelitic paragneiss, foliated granitoids and layered mafic intrusions; granitic orthogneiss is a relatively minor rock type.

Supracrustal rocks in the Lake Melville Terrane comprise 5 distinct compositional groups; these are pelitic to semi-pelitic gneiss, psammitic gneiss, quartzite, calc-silicate rocks and mafic gneiss. (1) Semi-pelitic schlieric banded paragneiss is the dominant rock type and is characterized by sillimanite + K feldspar subassemblages. Layering is defined by segregation of leucosome and mafic restite components. Transposition of these layers is common and in some areas extremely complex. Diatexites, interpreted as strongly migmatized equivalents of the semi-pelitic gneisses, occur as large bodies intercalated with the pelitic rocks. (2) Psammitic gneiss is commonly pyritic with a distinct rusty-brown weathering color. Garnet and biotite are widespread and sillimanite and muscovite occur locally. Where not associated with other supracrustal rocks the distinction between psammitic gneiss and granodioritic orthogneiss may be difficult. (3) Calc-silicate zones within pelitic and psammitic gneiss range from layers of 10 cm up to 300 m wide and contain diopside + grossular + amphibole + plagioclase as constituent phases. (4) Quartzite is a minor rock type, although layers up to 50 m wide occur in a few localities. Mineral assemblages include: quartz

+ plagioclase + magnetite + garnet + graphite + diopside + biotite.

(5) Mafic rocks interlayered within the supracrustal sequence are present in a few areas. They contain epidote + diopside + grossular + plagioclase + calcite as characteristic mineral phases and are interpreted to be strongly deformed pillow basalts.

The predominant composition of the orthogneiss is granodiorite. These rocks are variably migmatitic with the fabric ranging from strongly foliated to a well developed banding. In some areas the presence of flattened enclaves and dikes enhances the overall gneissic texture. Biotite, hornblende and garnet are the common mafic phases and locally orthopyroxene is developed in the leucosome. In some areas the fabric is weak to moderately foliated with local gradations to strongly foliated and gneissic. Gradational contacts between strongly tectonized and more massive granodiorite suggest that the variation is a result of strain heterogeneities during deformation.

Mafic intrusive rocks occur predominantly in the Mount Gnat Granulite Belt (Gower et al., 1981) and the White Bear Arm Complex (Figure 4). These rocks are interpreted to be large fractionated layered mafic intrusions of gabbro - leucogabbro - leuconorite - anorthosite - monzonite and granite. Locally igneous layering is preserved; however layering as a result of metamorphic differentiation is more common. Gabbros with both single and double coronas of olivine-orthopyroxene and olivine-orthopyroxene-amphibole occur throughout both units. Minor fine-grained leucogabbro-norite which occurs in isolated and discontinuous outcrops may be dikes related to the layered complexes.

## CHAPTER 3

### STRUCTURAL GEOLOGY

#### 3.1 Introduction

In this section the structural development of the Groswater Bay and the Lake Melville Terranes will be considered within the framework of the tectonic model for the Grenville Province presented in Chapter 1. A regional interpretation of structures in eastern Labrador is given by Gower and Owen (1984) and Gower et al. (1985, 1986). These authors have interpreted the complex to be due to a combination of pre-existing Labradorian features widely overprinted by Grenvillian trends. (At the time of writing, Gower and Owen, 1984 were not really aware of the Labradorian Orogeny, and interpreted pre-Grenvillian features to be Makkovikian, however, we now know they are Labradorian). The majority of this section is a summary of this work to which the author contributed.

#### 3.2 Groswater Bay Terrane

The regional structural pattern in the eastern Groswater Bay Terrane is shown in Figure 5. Foliations trend northwesterly in the Sandwich Bay area and swing towards the northeast in the Groswater Bay area. Dips are towards the southwest near Sandwich Bay and generally northwest north of Groswater Bay.

Owen and Rivers (1983), Gower and Owen (1984) and Owen (1985) have described the progressive overprinting and obliteration of NE

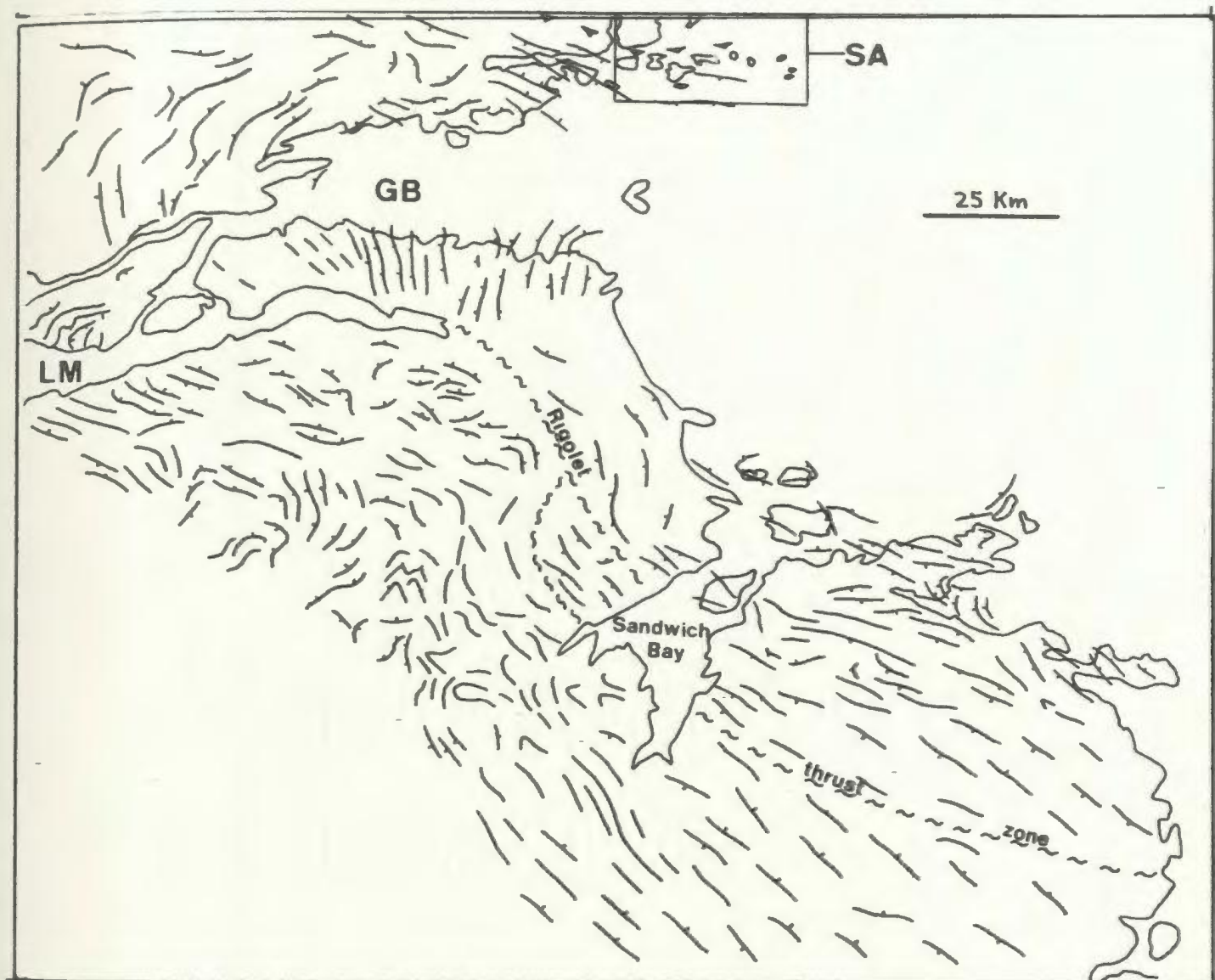


Figure 5. Regional structural pattern in eastern Labrador, after Gower and Owen (1984); Gower et al. (1984, 1985).

The Rigolet thrust zone separates the Groswater Bay and Lake Melville Terranes.

The thrust symbol in the Smokey Archipelago is the Grenville Front.

SA - Smokey Archipelago  
 GB - Groswater Bay  
 LM - Lake Melville

trending Makkovik fabrics in the Smokey Archipelago, just to the south of the Grenville Front on the coast of Labrador (Figure 5) and on this basis interpret the present structural pattern to be a result of the overprinting and re-orientation of pre-existing Makkovik NNE trending fabrics by widespread EW Grenvillian fabrics. However, in a small structural domain on the south shore of Groswater Bay (Figure 5) fabrics trend north to north-east and are interpreted to be relict Makkovikian features which were essentially unaffected by Grenvillian deformation (Gower and Owen, 1984).

Fabrics in the Groswater Bay Terrane are represented by well developed foliations in paragneiss and orthogneiss and moderately developed fabrics in granitoid and mafic rocks. Migmatitic banding in semi-pelitic paragneiss is well developed and defined by layers of granitic leucosome alternating with restite layers consisting of kyanite - biotite - garnet - muscovite. Fabrics in granitoid and mafic rocks are defined by elongate aggregates of biotite and hornblende. Down dip mineral lineations, defined by the preferred orientation of inequant minerals and elongate mineral aggregates, are well developed in paragneiss and orthogneiss, particularly in zones of shearing or intense deformation.

Numerous faults are present in the Groswater Bay Terrane, the majority of these being interpreted as brittle strike-slip faults. They have been mapped on the basis of fault breccia, extreme alteration and on aerial photograph lineaments. Only rarely is there evidence of displaced lithologic contacts. Thrust faults in the region are recognized by their well developed mylonitic fabrics and intense recrystallization. Rotated K-feldspar megacrysts are common,

their sense of rotation combined with lineation orientations suggest a general north to north-east directed transport direction.

### 3.3 Lake Melville Terrane

The regional structural pattern in the Lake Melville Terrane is more complex than that in the Groswater Bay Terrane (Figure 5). In the southeast part of the Lake Melville Terrane, foliations trend predominantly south-east, and dip towards the north-east. In some areas, this fabric is interpreted to have been deflected as a result of deformation along Grenvillian shear zones (Gower and Owen, 1984; Figure 6). In the central Lake Melville Terrane, west of Sandwich Bay, variable foliation trends and dip directions reflect a complex structural pattern. In the western portion of the terrane, east of Lake Melville, foliations trend essentially east-west and dip consistently towards the north to north-east. The variability of foliations and dip directions in the Lake Melville Terrane appears to be consistent with a model of pre-Grenvillian (Labradorian) fabrics variably modified during the Grenvillian orogeny. Near the Rigolet thrust zone, folds with axes parallel to the fault are considered to be of Grenvillian age, although elsewhere, relationships are more difficult to establish.

Planar fabrics in the Lake Melville Terrane range from gneissic layering developed in most paragneiss and orthogneiss lithologies to weakly developed foliations in granitoids and mafic rocks. In some areas, planar fabrics are generally absent in plutonic rocks which are characterized by primary igneous textures. Gneissic fabrics are



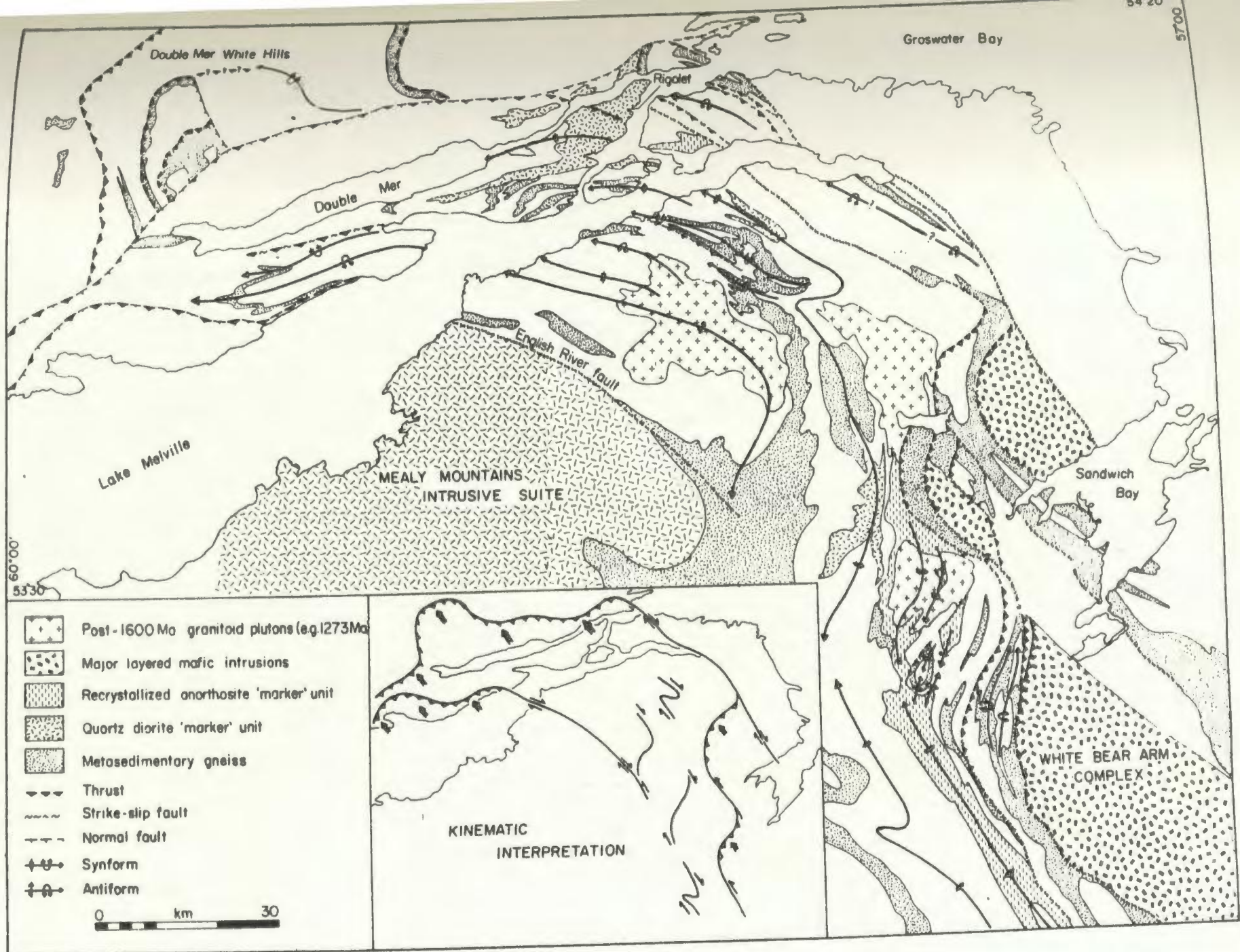


Figure 6. Major structures and kinematic interpretation (inset) of the Lake Melville Terrane, after Gower et al. (1985).

generally defined by alternating leucosome layers consisting of plagioclase - K feldspar - quartz with minor mafic phases and restite layers consisting of various combinations of sillimanite - biotite - magnetite - garnet - cordierite - orthopyroxene in paragneiss and biotite - hornblende - orthopyroxene - clinopyroxene - garnet - magnetite in orthogneiss. Minor folds associated with the migmatitic fabric are tight to isoclinal and indicate extensive transposition and tight folding.

Granitoid rocks are characterized by a strong to weakly developed foliation defined by alignment of biotite + hornblende selvages and commonly K feldspar megacrysts. Strongly foliated granitoid rocks locally become gneissic near shear zones and thrusts. Mafic lithologies are commonly moderately to strongly foliated, although in general, granulite facies rocks have a granoblastic fabric implying subsequent recrystallization. Linear fabrics are well developed in paragneiss, orthogneiss and granitoid rocks, although are rare in mafic lithologies. Mineral stretching lineations and rodding structures are generally down dip and parallel to the orientations of fold axes, suggesting an extensional strain regime in which lineations were rotated into parallelism with fold axes during deformation.

Mylonite zones in the Lake Melville Terrane are characterized by variably recrystallized mylonitic foliations. Quartzofeldspathic mylonites commonly exhibit ribbon textures where quartz grains reach aspect ratios of 30:1 implying no annealing after their formation. Thin pseudotachylite zones, which cross-cut the mylonitic fabric occur locally in areas of intense shearing. Rotated K feldspar

megacrysts in granitoid rocks together with down dip mineral lineations indicate north-east to north-west transport direction. Mylonites in mafic rocks exhibit extreme recrystallization with the development of blastomylonitic textures. All these mylonites, which range from less than 1m up to 100m wide, are interpreted to be moderate to shallowly dipping thrust faults in which the hanging wall has been transported northward.

#### 3.4. Rigolet Thrust Zone

A prominent structural feature in the area is a major east to south-east trending thrust fault which extends from the north west shore of Lake Melville to the south-east coast of Labrador. (Figure 6). This feature, termed the Rigolet thrust zone (Gower et al., 1982) defines the boundary between the Groswater Bay Terrane and the Lake Melville Terrane. Where exposed, the Rigolet thrust is defined by shallow south to south-east dipping zones of mylonite, pseudotachylite and cataclasite. Where exposure is lacking the thrust has been extrapolated on the basis of its linear negative aeromagnetic signature. The morphology and inferred kinematic signature of the Rigolet thrust zone vary along its length (Figure 6, inset). In the Double Mer-White hills region, near Rigolet, where there is an extension of the Lake Melville Terrane in the form of a thrust lobe, it is characterized by multiple thrust faults with down dip (south-east plunging) extension mineral lineations. In this area, Gower and Owen (1984) propose a northward translation of the Lake Melville Terrane over the Groswater Bay Terrane. Further to the

south-east the Rigolet thrust zone is interpreted to be a predominantly strike-slip fault with only a minor thrust component (Gower et al., 1985). East of Sandwich Bay, the extension of the Rigolet thrust zone is predominantly an intrusive contact between the Earl Island Domain and the Paradise Metasedimentary Belt (Gower et al., 1985) and the structural significance of the zone in this area is at present uncertain.

Gower et al. (1985) have proposed that the Lake Melville Terrane was transported in a northwest to north-northwest direction along the Rigolet thrust zone (Figure 6). The kinematic interpretation (Figure 6, inset), shows that east to north-east trending portions of the Rigolet thrust zone have a major thrust component, whereas north-west striking structures are essentially right lateral strike-slip faults with only a minor thrust component. In the Double Mer-White Hills region (Figure 6), the Rigolet thrust zone is in the form of a thrust lobe, which is comparable in lithologic association, structural style and metamorphic grade to the Lac-Joseph, Wilson Lake and Cape Caribou allochthons to the west (Figure 3).

Within the Lake Melville Terrane, several northwest facing frontal thrusts with marginal strike-slip faults are developed. South-west of Sandwich Bay, these thrusts are interpreted to be a result of a combination of right lateral movement along the English River fault, which bounds the north-east side of the Mealy Mountains Terrane and movement along the northeastern margin of the Lake Melville Terrane (Figure 6, Gower et al., 1985.).

### 3.5 Grenvillian Effects

The most obvious effect of the Grenvillian Orogeny in eastern Labrador was the regional slicing and stacking of pre-Grenvillian rocks into major thrust bound crustal segments along the Rigolet thrust zone and other minor intra-terrane mylonites. The regional structural pattern suggests a north to north-west transport of an exhumed deep level allochthon (Lake Melville Terrane) over a parautochthonous unit (Groswater Bay Terrane).

On a smaller scale, there is evidence that Grenvillian deformation was polyphase. Owen (1985), describes 3 phases of deformation attributed to the Grenvillian Orogeny in the Smokey Archipelago just south of the Grenville Front in eastern Labrador. The first period of Grenvillian deformation (GD1) resulted in the development of east trending inclined folds which are seen to deform pre-Grenvillian fabrics. Gower (1981) describes a regional west plunging GF1 antiform with an east-west trending axial trace passing through Groswater Bay, which is considered to be a major structural feature of the Groswater Bay Terrane; and Owen (1985) describes the development of GS1 fabric along the limbs of GF1 folds. Several major GF1 folds have been interpreted to occur west of Sandwich Bay in the Lake Melville Terrane (Figure 6). A regional synform has been interpreted to extend from south of Sandwich Bay to west of Rigolet, the axial trace of which is defined by folded quartz diorite bodies in some areas (Figure 6). To the west and south of this synform, a large domal structure defined by antiforms is outlined by paragneiss. A second

period of Grenvillian deformation produced SE to SSW plunging GP2 folds, which locally are seen to deform GP1 folds. GP2 Folding was accompanied by the development of a south dipping axial planar foliation. GD2 deformation associated with northwest transport of the Mealy Mountains terrane, resulted in tightening of the northwest end of the domal structure into north verging folds and refolding of the regional synform in the Paradise River area into minor open Z folds (Gower et al., 1985).

GD3 is represented by local deformation of GS2 fabrics giving rise to SSW plunging folds. Owen (1985) suggests a NNW-SSE oriented direction of maximum compression during GD1 and GD2 in the Grenville Front region, which culminated in north-directed thrusting along the Benedict and Cut Throat Island Faults near Smokey (Figure 5). A similar kinematic interpretation appears applicable for the western Rigolet thrust zone, in the Double-Mer White Hills area, where a frontal lobe of the Lake Melville Terrane is thrust onto the Groswater Bay Terrane.

### 3.6 Pre-Grenvillian Effects

The recognition of distinct older fabrics in the Groswater Bay and Lake Melville Terranes is generally difficult, although locally in the Groswater Bay Terrane, a NNE trending Makkovikian fabric is preserved in gneissic rocks, which are essentially unaffected by Grenvillian deformation. Elsewhere, relict Makkovikian trends are interpreted by Gower and Owen (1984) to have been deflected towards a northeast direction as a result of translation along Grenvillian

strike-slip faults.

This interpretation implying a widespread Grenvillian structural overprint in both the Groswater Bay and Lake Melville Terranes in eastern Labrador differs from the structural relationships in the parautochthon-allochthon units in western Labrador. Rivers and Chown (1986) and Rivers and Nunn (1985) noted that although the degree of Grenvillian structural reworking of the allochthon was largely unknown the preservation of 1650 Ma U/Pb ages on or almost on concordia suggested that Grenvillian overprinting was likely minimal there.

In summary, the regional structural pattern of the Grenville Province in eastern Labrador suggests widespread Grenvillian overprinting of older crustal segments with pre-existing structural histories. Strong Grenvillian reworking of older Makkovikian and Labradorian fabrics resulting in a variably trending Grenvillian overprint is evident in both the Groswater Bay and Lake Melville Terranes. The kinematic framework in eastern Labrador is based on regional ductile thrusting of a series of nappe structures with both pre-Grenvillian and Grenvillian histories. In the Sandwich Bay area, this thrusting is represented by transport of the allochthonous Lake Melville Terrane onto the parautochthonous Groswater Bay Terrane and thrusting of both the Mealy Mountains Terrane and the White Bear Arm Complex over the Lake Melville Terrane.

## CHAPTER 4

### METAMORPHISM

#### 4.1 Introduction

Distinction between the Groswater Bay and Lake Melville Terranes in eastern Labrador is based in part on the variation in metamorphic grade across the Rigolet thrust zone, which separates the two terranes. Mineral assemblages in the Groswater Bay Terrane show middle to upper amphibolite facies conditions, whereas upper amphibolite to granulite facies is recorded in the Lake Melville Terrane. This chapter describes mineral assemblages in paragneisses and granitoid and basic rocks of both terranes. In addition, metamorphic conditions in both terranes are estimated qualitatively on the basis of comparisons with experimentally investigated reactions in petrogenetic grids.

#### 4.2 Mineral Assemblages in the Groswater Bay Terrane

Complete mineral assemblages for samples used in this study are listed in Appendix 1. Mineral assemblages in paragneissic, granitoid and mafic lithologies in the Groswater Bay Terrane indicate that the prevailing grade of metamorphism is middle to upper amphibolite facies. There is also evidence of partial retrogression under lower amphibolite facies conditions, particularly the development of muscovite and epidote in paragneissic and granitoid rocks respectively and locally, along zones of ductile thrusting and



faulting, chlorite and hematite are extensively developed.

The assemblage plagioclase + K feldspar + quartz + biotite + kyanite + garnet + granitic veins is common in semi-pelitic gneiss. In some samples, minor retrogression is indicated by the presence of muscovite and/or by the local alteration of kyanite and K feldspar assemblages to produce muscovite + quartz. Partial melting of pelitic gneiss formed granitic veins, resulting in the development of widespread intense migmatitic schlieric banding which locally is accentuated by the intrusion of minor aplitic veins, parallel to the banding.

Orthogneiss and foliated granitoid rocks typically contain biotite + hornblende + garnet subassemblages. Retrograde epidote is ubiquitous and occurs throughout granitoid rocks in the Groswater Bay Terrane. East of Cartwright, monzonitic to syenitic rocks contain metamorphic subassemblages of clinopyroxene + hornblende + garnet.

Mafic rocks in the Groswater Bay Terrane are characterized by hornblende + plagioclase + garnet + biotite subassemblages, although metamorphic orthopyroxene and clinopyroxene have been found locally.

#### 4.3 Mineral Assemblages in the Lake Melville Terrane

Mineral assemblages in the Lake Melville Terrane suggest that metamorphic grades of upper amphibolite to lower granulite facies were attained. Locally retrograde greenschist facies assemblages occur along fault zones. The most significant contrast in metamorphic parageneses occurs within the paragneiss lithologies. As opposed to the kyanite + K feldspar-bearing pelites in the Groswater Bay

Terrane, paragneisses in the Lake Melville Terrane are characterized by K feldspar + sillimanite + biotite + garnet + granitic liquid subassemblages.

In the Paradise metasedimentary gneiss belt (PMGB, Gower et al., 1986), a zone of predominantly pelitic and semi-pelitic paragneisses extending from west of Sandwich Bay to the coast of Labrador (Figure 4), pelitic rocks containing subassemblages of stable muscovite + biotite + garnet and cordierite + sillimanite + granitic liquid occur.

In the Sand Hill River area, adjacent to the Sandhill Big Pond gabbro-norite complex (SHBP, Figure 4), (Gower et al., 1986), a narrow zone of paragneiss is characterized by the high grade subassemblage sillimanite + orthopyroxene + sapphirine + osumilite (C.F. Gower personal communication, 1986). This assemblage is interpreted to be a result of local contact metamorphism due to the intrusion of the SHBP gabbro-norite body. [Recent work by Valley et al. (1986) in the Adirondacks has shown that mineral assemblages in the contact metamorphic aureole of the Marcy anorthosite remained stable during subsequent Grenvillian granulite facies metamorphism, because fluid activity was close to 0 during the latter event (i.e. it was completely driven off during contact metamorphism). This model may also be applicable to the osumilite-bearing assemblages present in paragneiss adjacent to the SHBP gabbro-norite].

Coexisting kyanite and sillimanite have been discovered in a few localities immediately south of the Rigolet thrust zone, on the White Bear River. Petrographic inspection reveals that kyanite is being replaced by stable sillimanite, and the reaction is thus prograde.

The location of the kyanite-sillimanite isograd thus approximately coincides with the boundary between the Groswater Bay Terrane and the Lake Melville Terrane.

Evidence of partial melting in paragneisses from the Lake Melville Terrane is widely developed, with migmatization ranging from 20 to 70 volume % in the rock. Mineral assemblages developed in orthogneiss and foliated granitoid rocks contain biotite + hornblende + garnet; partial retrogression to chlorite occurs locally. In the central Lake Melville Terrane, large intrusions of hornblende + pyroxene-bearing granodiorite (Gower and Owen, 1984) are commonly highly strained and migmatized, implying that conditions required for partial melting were reached.

Mafic lithologies in the Lake Melville Terrane are characterized by rather variable assemblages. Gabbroic and anorthositic rocks commonly contain relict primary igneous mineralogies along with metamorphic amphibole-bearing assemblages in which partial recrystallization of igneous phases is widespread. In the Mount Gnat Granulite Belt (Gower et. al., 1981) and the White Bear Arm Complex (Gower et. al., 1985, Figure 4) igneous olivine is preserved in cores of coronas with rims of either amphibole or hypersthene + amphibole. However, the significance of these coronas is not clear, as it is not known whether the coronas are a metamorphic or subsolidus cooling feature. Elsewhere in the Lake Melville Terrane granulite facies assemblages of hypersthene + diopside + garnet + hornblende occur throughout in mafic lithologies.

In summary, the development of sillimanite + K feldspar + melt and kyanite + K feldspar + melt assemblages in paragneisses in the Lake

Melville and Groswater Bay Terranes, respectively, suggests a distinct variation in metamorphic conditions across the Rigolet thrust zone.

#### 4.4 The Petrogenetic Grid

Metamorphic pressure and temperature conditions can be approximated within the study area on the basis of comparisons with experimentally determined equilibria. In this section petrogenetic P-T grids with relevant equilibria for pelitic and basic rocks in the Groswater Bay and Lake Melville Terranes are presented.

##### 4.4.1 Paragneiss Assemblages

Figure 7 shows various reactions relevant for pelitic rocks in the study area. Reactions representing formation of minimum melts may be modelled in the eight component model pelitic system  $\text{SiO}_2 - \text{Al}_2\text{O}_3 - \text{K}_2\text{O} - \text{MgO} - \text{FeO} - \text{H}_2\text{O} - \text{CaO} - \text{Na}_2\text{O}$  (Thompson & Algor, 1977; St. Onge, 1981). These authors have demonstrated the existence of several melting reactions in the model system radiating from an invariant point defined by the intersection of the granite minimum melt curve and the curve representing breakdown of muscovite in the presence of quartz.

A number of these reactions have been investigated at various values of  $a\text{H}_2\text{O}$  by several authors, including, Kerrick (1972) and Thompson (1974). Experimental work on the muscovite + quartz =  $\text{Al}_2\text{SiO}_5 + \text{K feldspar} + \text{H}_2\text{O}$  reaction in the  $\text{K}_2\text{O} - \text{Al}_2\text{O}_3 - \text{SiO}_2 - \text{H}_2\text{O}$

Figure 7. Petrogenetic grid with appropriate reactions for paragneiss in the Groswater Bay and Lake Melville Terranes.

Cross-hatched area - minimum P-T conditions in the Groswater Bay Terrane.

Dotted area - minimum P-T conditions in the Lake Melville Terrane.

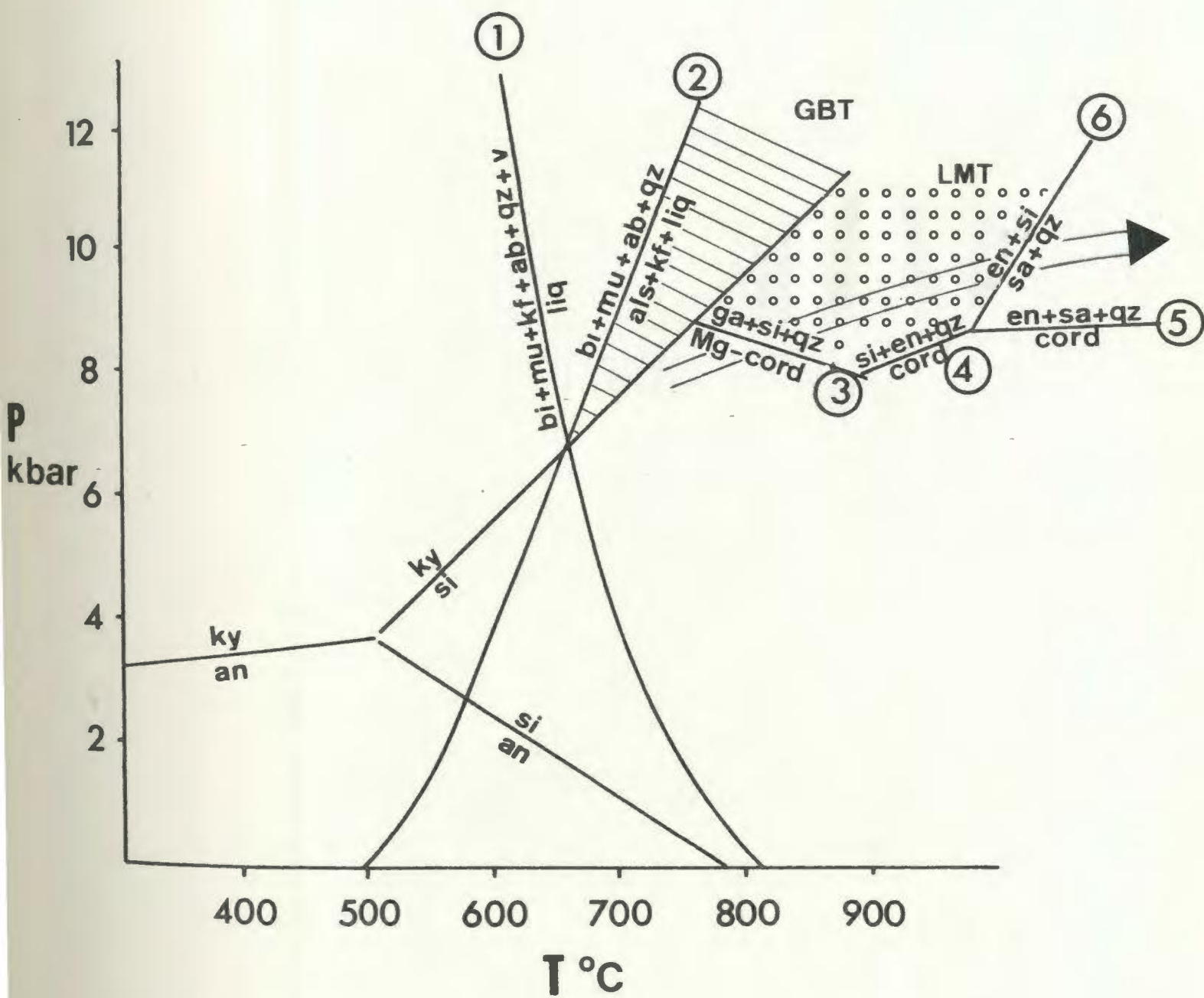
Arrow represents progressive metamorphic sequence in the Paradise Metasedimentary Gneiss Belt (LMT).

Curves 1 and 2 (for  $a_{H_2O} = 0.5$ ) after Kerrick (1972).

Curve 3 (for  $X_{Mg}$  in cord. = 0.71) after Newton (1972).

Curves 4, 5 and 6 (for  $X_{Mg}$  in cord. = 0.71) after Newton et al. (1974).

$Al_2SiO_5$  triple-point after Holdaway (1971).



(KASH) system has shown that the position of the reaction in P-T space migrates towards lower temperatures and pressures with a decrease in  $aH_2O$ .

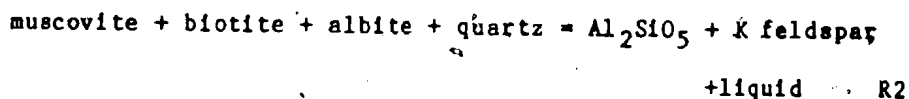
The granite minimum melting curve has been studied by Piwinski (1968) and Boettcher and Wyllie (1968) for various values of  $aH_2O$ . Experimental evidence shows that this reaction migrates to higher P-T conditions with a decrease in  $PH_2O$ . Kerrick (1972) summarized the effect of variable values of  $aH_2O$  on both the granite minimum melt and K feldspar -  $Al_2SiO_5$  forming reactions in the KASH system.

In the study area, it is most likely that anatexis occurred under water undersaturated conditions (i.e.  $PH_2O < P_{total}$ ). This assumption is supported by the anhydrous nature of paragneisses in some areas. To approximate this assumption conditions of  $aH_2O = 0.5$  are used for the positions of reactions involving the generation of granitic melts and the upper stability limit of muscovite in Figure 7. The absence of muscovite in the paragneisses, (except as locally developed retrograde phases), indicates that metamorphism occurred above the stability limit of muscovite.

In paragneisses of the Groswater Bay Terrane, coexistence of kyanite + K-feldspar in the restite component, is inferred to result from the vapour absent dehydration melting reaction, which can be modelled in the KASH system as:

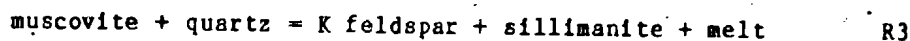


or in the eight component model system (reaction 2 in Figure 7):



Since this reaction has taken place within the stability field of kyanite, minimum metamorphic conditions in the order of 7 kbar and 650°C are implied (assuming  $a\text{H}_2\text{O} = 0.5$ ).

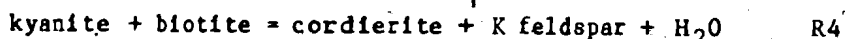
In the Lake Melville Terrane, more variable metamorphic mineral assemblages in paragneisses allow a more detailed interpretation of P-T conditions. The characteristic association of sillimanite + garnet + biotite + melt in these paragneisses implies (1) that the stability field of staurolite has been exceeded, and (2) that anatexis has occurred. The coexistence of sillimanite + K feldspar in the restite component of the rock suggests that the reaction:



has occurred. This is the same dehydration melting reaction as inferred for the Groswater Bay Terrane, except that the stable  $\text{Al}_2\text{SiO}_5$  is sillimanite rather than kyanite. In a few localities immediately south of the Rigolet thrust zone, relict kyanite occurs in addition to sillimanite + K feldspar + melt. The intersection of the kyanite = sillimanite and the K feldspar + melt isograds implies minimum P-T conditions on the order of 650°C and 7 kbar for  $a\text{H}_2\text{O} = 0.5$ . It is clear from Figure 7 that for a fixed value of  $a\text{H}_2\text{O}$ , the sillimanite bearing assemblages in the Lake Melville Terrane formed at either lower pressure or higher temperature than their kyanite bearing counterparts in the Groswater Bay Terrane.

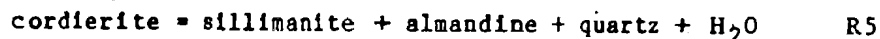


One locality (CG81-170B) in the Paradise Metasedimentary Belt, on the Eagle River (Figure 4), contains the assemblage sillimanite + garnet + biotite + melt + cordierite + (kyanite) + (muscovite), (minerals in brackets indicate unstable phases). In this sample, kyanite and biotite, occur as inclusions within cordierite porphyroblasts (Figure 8a). The resorbed nature of the inclusion phases, and the stable appearance of the cordierite suggests that the continuous reaction:



has occurred (after Newton, 1972).

The coexistence of cordierite, sillimanite, garnet and quartz in CG81-170B (Figures 8a and b) supports the operation of the net transfer reaction:



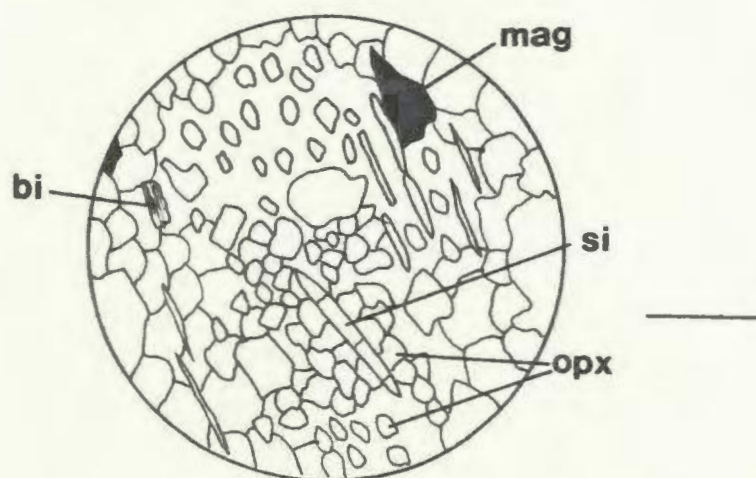
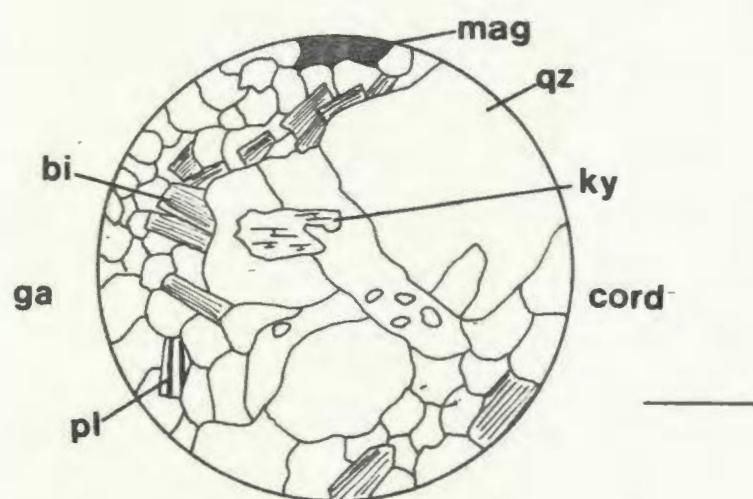
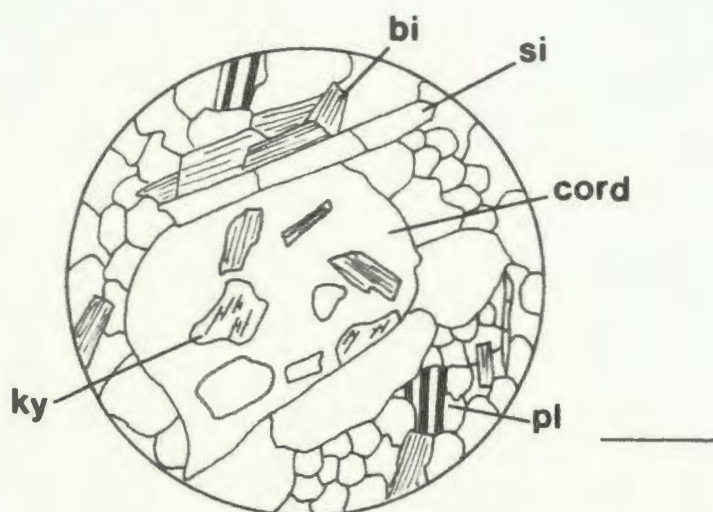
The development of this prograde metamorphic sequence allows estimation of P-T conditions within a petrogenetic grid. In Figure 7, the cordierite = almandine + sillimanite + quartz reaction is plotted (following Newton, 1980) for XMg in anhydrous cordierite of 0.71, obtained from microprobe analysis of cordierite in sample CG81-170B (Appendix 8). Since the assemblage represents the intersection of the kyanite = sillimanite equilibrium as well as the cordierite breakdown reaction, P-T conditions on the order of 775°C and > 8 kbar are

Figure 8a: Relict kyanite and stable cordierite in garnet - sillimanite-biotite paragneiss in the upper Eagle River area, Lake Melville Terrane (Sample CG81-170B).

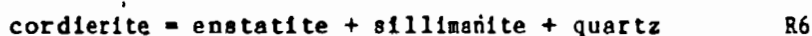
Figure 8b: Relict kyanite and altered cordierite in garnet-sillimanite-biotite paragneiss, upper Eagle River area, Lake Melville Terrane (Sample CG81-170B).

Figure 9: Orthopyroxene - sillimanite bearing paragneiss in the upper Eagle River area, Lake Melville Terrane (Sample CG81-235B).

Scale bar - 2 mm



implied for  $a_{H_2O} = 0.5$  (Figure 7). Sample CG81-285B, located immediately west of CG81-170 (see sample location map in Appendix 2), contains the assemblage sillimanite + hypersthene + melt (Figure 9). Although cordierite was not identified in this thin section, the similarity of the rock type and the proximity to sample CG81-170B, which does contain relict cordierite, suggests that the reaction:



after Newton (1972)

may have occurred (Figure 7). Since cordierite is absent, the composition of cordierite for this reaction is unknown, however, it has been assumed to be  $X_{Mg} = 0.71$  as in sample CG81-170B. The position of this reaction in the petrogenetic grid implies metamorphic conditions in the order of  $875^{\circ}\text{C}$  and 8. kbar.

Adjacent to the Sand Hill Big Pond gabbro-norite, paragneisses in the Paradise Metasedimentary Belt contain the assemblage sillimanite + hypersthene + sapphirine +/- osumilite + quartz (C. Gower, personal communication, 1986). Although these assemblages result from local contact metamorphism (Section 4.3) and are unrelated to the regional metamorphic gradient in the Lake Melville Terrane, reactions involving the formation of some of these assemblages have been included in Figure 7. The development of sapphirine + quartz is presumably a result of the reaction:



after Newton (1972).

In Figure 7, this reaction has been plotted for the Mg system (i.e.  $X_{Mg}(\text{opx}) = 1.0$ , and suggests that metamorphic conditions exceeded  $900^{\circ}\text{C}$  and 8 kbar. Newton (1982) notes that the assemblage hypersthene + sillimanite + quartz is stabilized at pressures of about 10 kbar in the Mg system and that the association sapphirine + quartz indicates pressures greater than 8 kbar.

The reactions which occurred within the Paradise Metasedimentary Belt of the Lake Melville Terrane represent a metamorphic field gradient, shown by the arrow in Figure 7. In the Eagle River area (Appendix 2), cordierite appears to have been formed at the expense of kyanite and biotite. At higher pressures, cordierite breaks down to produce enstatite + sillimanite + quartz. In the Sand Hill Big Pond area, an increase in temperature results in the formation of sapphirine + quartz at the expense of enstatite + sillimanite.

The latter reaction, however, is restricted to a narrow zone adjacent to the Sand Hill Big Pond gabbro-norite complex. The implications of these assemblages with respect to the regional metamorphic gradient are discussed in the Section 4.2

#### 4.4.2 Mafic Assemblages

Reactions in mafic rocks in amphibolite, granulite and eclogite facies rocks in the  $\text{CaO} - \text{MgO} - \text{Al}_2\text{O}_3 - \text{SiO}_2$  system are shown in Figure 10 (after Wells, 1979). The relationships in this system can be extended into complex natural systems by considering variations in  $a_{\text{H}_2\text{O}}$ ,  $X_{\text{Mg}}$  and  $X_{\text{Na}}$ . For a given value of  $a_{\text{H}_2\text{O}}$  all of the reactions

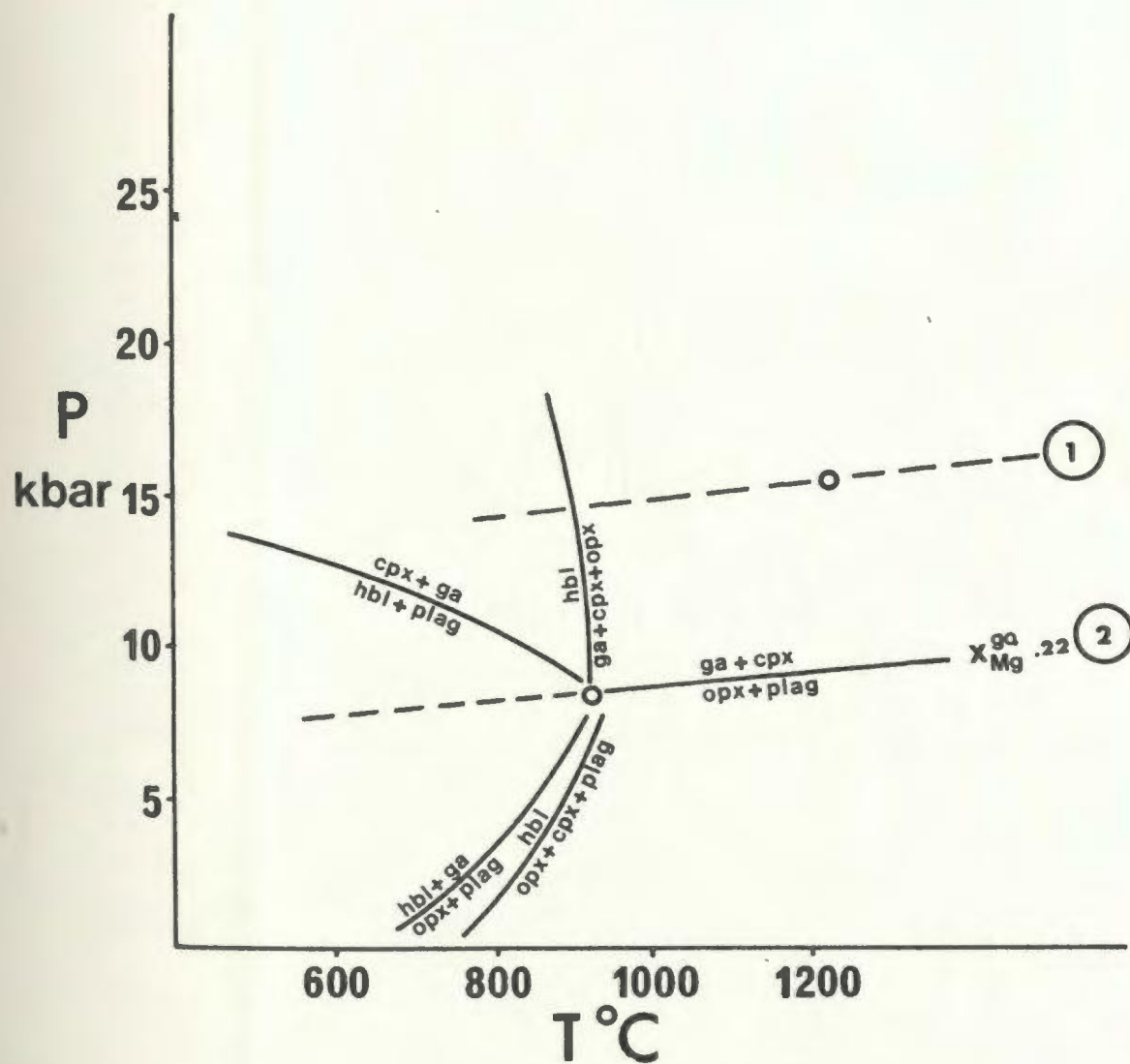
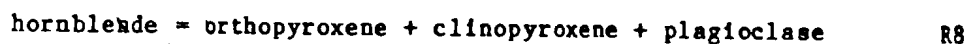


Figure 10. Petrogenetic grid for mafic rocks in the CMAS system, after Wells (1979). Position of the invariant point shown for  $a_{H_2O} = 1.0$  and  $X_{Mg}^{ga} = 1.0$  [1]; And for  $a_{H_2O} = 0.5$  and  $X_{Mg}^{ga} = 0.22$  (after Glassley and Sorensen, 1980) [2].

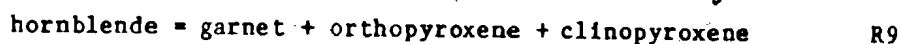
must pass through one invariant point which, with decreasing temperature traces out a univariant curve along the hornblende absent (hbl) reaction. The invariant point is shown at values of 1.0 and 0.5  $aH_2O$ . Hensen (1976) noted that the (hbl) reaction is sensitive to changes in Fe/Fe+Mg ratios. This reaction has been plotted at XMg in garnet of 0.22 (after Glassley and Sorensen, 1980). The effect of Na on the (hbl) reaction is to shift the reactions to higher pressures (e.g 1-2 kbar for  $X_{an} = 0.5$ , Wells, 1979).

Although neither of these reactions have been observed in the Groswater Bay or Lake Melville Terranes, the presence of orthopyroxene + garnet + clinopyroxene +/- hornblende assemblages allows a qualitative estimation of P-T conditions within the study area. Since  $aH_2O$  previously was assumed to be 0.5 (Section 4.4.1), a similar assumption is made for mafic assemblages (the value of  $aH_2O$  for assemblages in the study area is further discussed following the results of the geothermobarometry estimates, see Section 5.3.3.2). The average composition of garnet in garnet - clinopyroxene - orthopyroxene - hornblende assemblages for both Groswater Bay and Lake Melville Terranes ranges from 0.20 to 0.30 mole fraction of pyrope. Thus the position of the (hbl) reaction for the study area is approximated at 0.22 using the curve of Glassley and Sorensen (1980). Combined with the assumption of  $aH_2O = 0.5$  the position of the invariant point and the (hbl), (cpx) and (ga) reactions for mafic rocks in both the Groswater Bay and Lake Melville Terranes are shown in Figure 10.

The coexistence of orthopyroxene + clinopyroxene + plagioclase in the Groswater Bay Terrane is represented by the (ga) reaction:

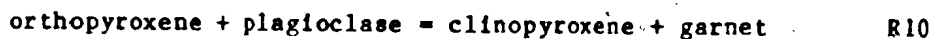


A second assemblage observed in the Groswater Bay Terrane is garnet + orthopyroxene + clinopyroxene and is represented in Figure 10 by the equilibrium:



From Figure 10, the coexistence of these assemblages, implies conditions on the order of 900°C and 7 kbar. However, this estimate is highly generalized, since Wells (1979) noted that if  $a_{\text{H}_2\text{O}}$  remains constant, the effect of addition of Fe to the system is to make the univariant reactions divariant fields and the invariant point traces out a univariant curve. Thus both the (hbl) and (ga) reactions would occur over a wider range of P-T estimates than depicted by the univariant curve in Figure 10. Secondly, the assumption of  $a_{\text{H}_2\text{O}} = 0.5$  in these assemblages is highly speculative, and if this value is different from 0.5 the positions of the various reactions in P-T space would change considerably.

In the Lake Melville Terrane the assemblage orthopyroxene + clinopyroxene + garnet + plagioclase + quartz, is observed in mafic rocks, and is represented by the reaction:



If the stability of hornblende-bearing assemblages has been



exceeded (i.e. to the high temperature side of the (cpx) and (ga) reactions) then metamorphic conditions in the order of 900°C and 7 kbar are implied (Figure 10). However, as noted above, since the variables which control the positions of the reactions (i.e.  $aH_2O$  and  $XFe$ ) are only approximate the implied conditions can only be regarded as speculative.

In summary, mineral equilibria in the Groswater Bay Terrane suggest that metamorphic grade is predominantly at middle to upper amphibolite facies with local development of retrograde lower amphibolite facies assemblages. Pressures and temperatures on the order of 8 kbar, and 750°C indicate crustal thicknesses of 28 km. Coexisting minerals in the Lake Melville Terrane indicate upper amphibolite to granulite facies metamorphism. Sillimanite + K feldspar assemblages imply minimum conditions of 650°C and 7 kbar, within the Paradise Metasedimentary Belt, and adjacent to the Sand Hill Big Pond gabbro-norite, the development of orthopyroxene + sillimanite + sapphirine assemblages suggests temperatures and pressures in the order of 850°C and 7 to 9 kbar. P-T estimates from mafic assemblages suggest conditions in the order of 900°C and 7 kbar.

#### 4.4.3 Microstructural Relationships

When attempting quantitative P-T studies of mineral equilibria, the evaluation of textural as well as chemical relationships is essential, particularly with respect to equilibrium / disequilibrium criteria, and the distinction of the relative ages of assemblages in polyorogenic terranes. In this section, the mineral equilibria of the Groswater Bay and Lake Melville Terranes are discussed in terms of microstructural relationships and chemical signatures, both within and between mineral phases. The purpose is to distinguish; (1) equilibrium and disequilibrium assemblages; and (2) whether the investigated assemblages represent pre-Grenvillian or Grenvillian signatures for each of the geothermometric and geobarometric equilibria. More generalized descriptions of the assemblages are given in Appendix 1.

##### Garnet-Biotite:

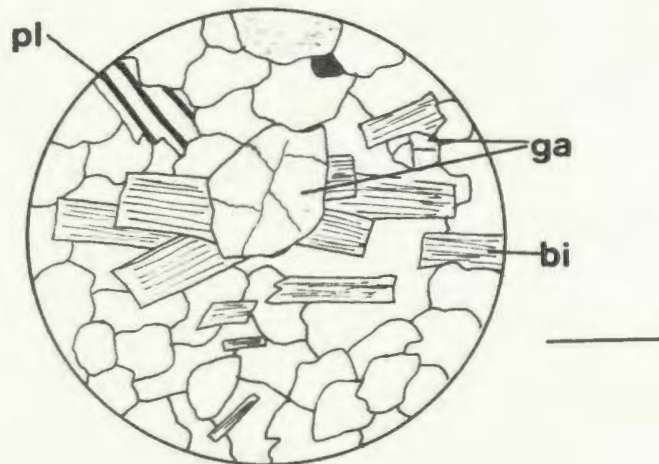
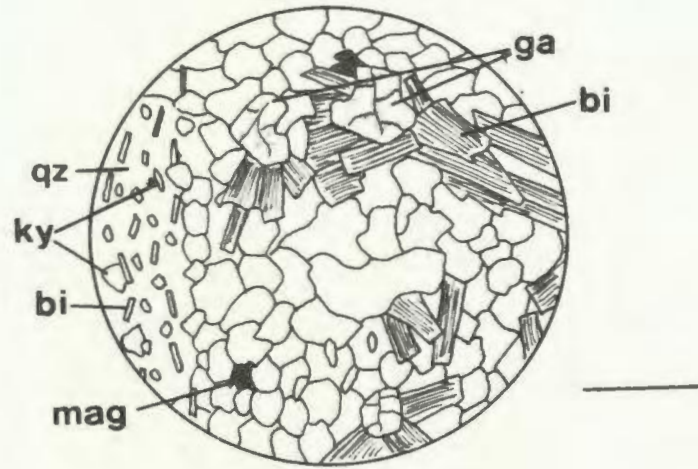
In the Groswater Bay Terrane, biotite in garnet-biotite pairs occurs in two distinct textural habits: (1) where fine-grained biotite inclusions occur within garnet porphyroblasts; and (2) where fine to medium grained, subidioblastic biotite laths wrap around pre-existing garnets. In the latter case, grain boundaries are sharp and straight, and the two minerals are interpreted to be in equilibrium (Figure 11). Grain contacts of biotite inclusions within host garnets, however, are generally irregular and serrated (Figure 12) and imply

Figure 11: Equilibrium textural relationships between garnet and biotite in the Groswater Bay Terrane (Sample CG81-299A).

Figure 12: Disequilibrium textural relationships between garnet and biotite in Groswater Bay Terrane paragneiss (Sample GF81-21).

Figure 13: Coarse biotite grains truncated by garnet porphyroblasts in Lake Melville Terrane paragneiss (Sample GF81-16).

Scale bar - 2 mm



garnet growth at the expense of biotite. Microprobe analyses of matrix biotites display a relatively consistent composition but biotite inclusions in garnet have a wide compositional range. This variation is probably a result of local re-equilibration of the biotite with adjacent garnet. Both textural and chemical evidence suggest that the matrix biotites are in equilibrium with other phases in the assemblage, whereas biotites which occur as inclusions within garnet porphyroblasts appear to be unstable. Only one generation of garnet has been identified in the Groswater Bay Terrane paragneisses, in appearance these are fine-grained, locally fragmented, subidioblastic porphyroblasts. Microprobe analyses of several grains within any one sample reveals a very consistent composition, implying that the single garnet generation is stable. Extensive microprobe analyses of 12 garnets from 5 samples from the Groswater Bay Terrane reveals no systematic zoning or inhomogeneity.

Textural relationships between garnet and biotite mineral pairs in the Lake Melville Terrane are more variable than in the Groswater Bay Terrane, in part due to the more extensive development of garnet - biotite assemblages. Two distinct biotite generations are present in the paragneisses, an earlier generation of coarse grained crystals which pre-dates garnet growth and a later fine - to medium grained phase defining a well developed fabric, which post-dates the garnet porphyroblasts. Only one generation of garnet has been identified, which occurs as subidioblastic to idioblastic, locally fragmented porphyroblasts as in the Groswater Bay Terrane.

The predominant textural relationship between biotite-garnet mineral pairs is where subidioblastic to idioblastic garnets truncate

a well developed gneissic fabric defined by the earlier coarse biotite grains (Figure 13), suggesting garnet post-dates biotite growth. In some samples, the main fabric, defined by fine-grained biotite, wraps around subidioblastic, inclusion free, commonly fragmented garnet porphyroblasts (Figure 14), implying both the biotite and the fabric post-date garnet growth. A third textural relationship, exhibited in two samples, shows subidioblastic, garnet porphyroblasts with fine-grained magnetite inclusion trails, suggesting syn-tectonic garnet growth. Straight grain boundaries of garnet and other co-existing phases, lack of alteration rims, and consistent composition of several garnet grains within any one sample suggests that garnet is a stable phase in all samples analyzed. Microprobe analyses of several biotites from the same sample, in which biotite post-dates garnet growth reveal a very consistent compositional range, suggesting that the younger biotites are in equilibrium with the older garnet phase. Biotites which pre-date garnet growth, however, reveal a wide range of composition between several grains within the same sample, suggesting that the older biotite generation is not in chemical equilibrium with the younger garnet phase. Texturally, however, both the earlier and later biotite phases exhibit well developed decussate aggregates in addition to sharp and straight grain boundaries where in contact with the garnet porphyroblasts.

#### Garnet-Plagioclase- $\text{Al}_2\text{SiO}_5$ -Quartz

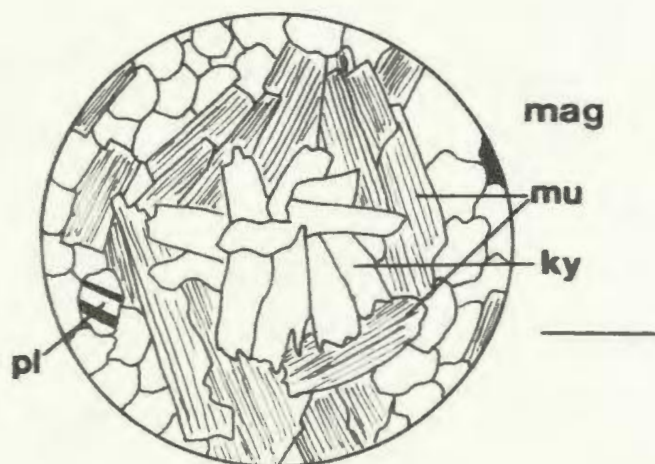
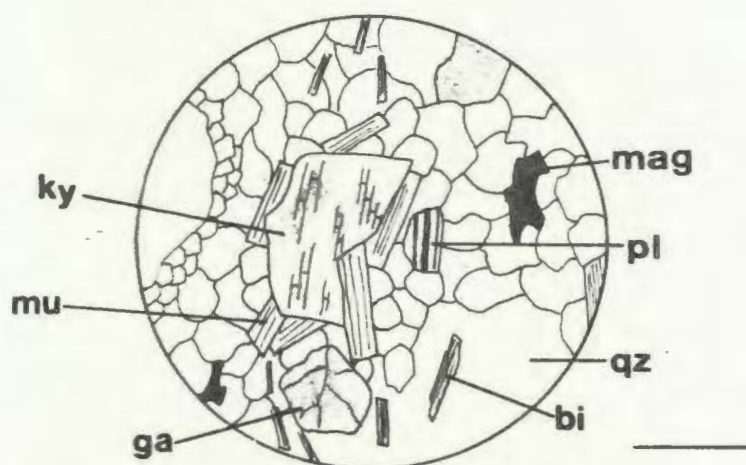
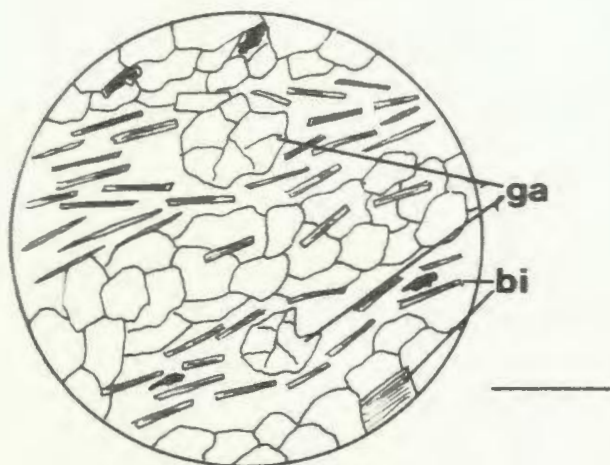
In the Groswater Bay Terrane, pelitic gneisses exhibit two dominant

Figure 14: Pre-tectonic garnet porphyroblasts wrapped by main gneissic fabric in Groswater Bay Terrane paragneiss (Sample GF81-18).

Figure 15: Equilibrium textural relationships between kyanite and muscovite in Groswater Bay Terrane paragneiss (Sample GF81-16).

Figure 16: Disequilibrium textural relationships between kyanite and muscovite in Groswater Bay Terrane paragneiss (Sample GF81-21).

Scale bar - 2 mm





mineral assemblages: (1) kyanite + garnet + K feldspar + melt and (2) kyanite + garnet + muscovite + melt. In the former case, all phases are texturally stable where in contact with one another. The restite component comprises fine-grained kyanite aggregates, along with fine-to medium grained garnet porphyroblasts and abundant fine biotite laths. The leucosome component consists of strongly recrystallized, polygonal grains of K feldspar, plagioclase and quartz, which exhibit well developed triple-points and straight grain contacts.

In the latter assemblage, textural relationships, particularly between kyanite and muscovite, are variable. In some samples both kyanite and muscovite appear to be texturally stable with both garnet and biotite in the same thin section (Figure 15). In other samples, muscovite is retrograde, and is either partially or totally pseudomorphing kyanite (Figure 16). In some samples in which muscovite is present in the fabric, either as a stable phase or a pseudomorph of kyanite, it has developed a strong tight to open crenulation (Figure 17), suggesting that following its formation, muscovite has undergone small scale folding.

On the basis of the microstructural relationships described above, two interpretations of the relative ages of the kyanite - garnet - K feldspar assemblages are proposed. Since the muscovite-bearing assemblage is retrogressed from the kyanite + garnet + K feldspar assemblage, the latter assemblage may be (1) a Grenvillian equilibrium with the development of retrograde muscovite, which is locally crenulated, is a result of post-Grenvillian uplift and associated tectonism; or (2) a pre-Grenvillian assemblage, with the

development of muscovite + quartz being an effect of Grenvillian retrogression. However, the former interpretation appears to be more reasonable since the main gneissic fabric which is defined by the kyanite + K feldspar assemblage is at least in part a Grenvillian feature, since as discussed in Chapter 3 (Structure) the regional structural pattern in the Groswater Bay Terrane is interpreted to be a result of a strong Grenvillian overprint of pre-existing (i.e. pre-Grenvillian) fabrics. Thus the kyanite + K feldspar assemblage is tentatively interpreted to be a Grenvillian feature with the development of retrograde muscovite + quartz being a result of post-Grenvillian uplift.

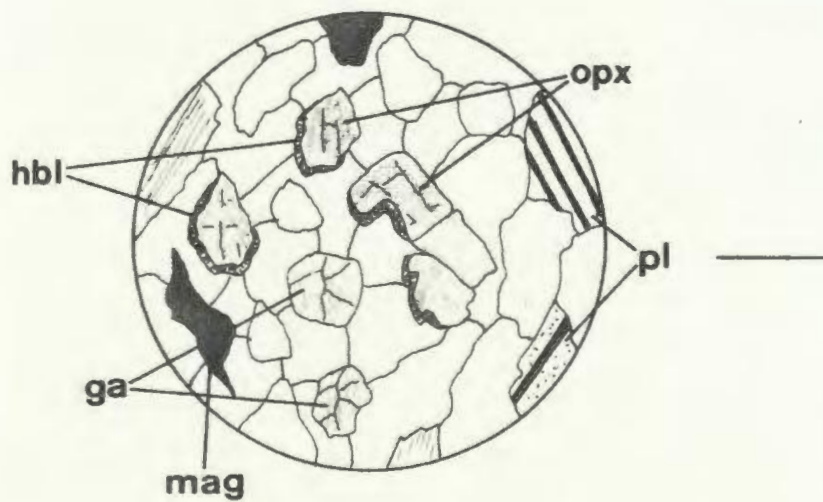
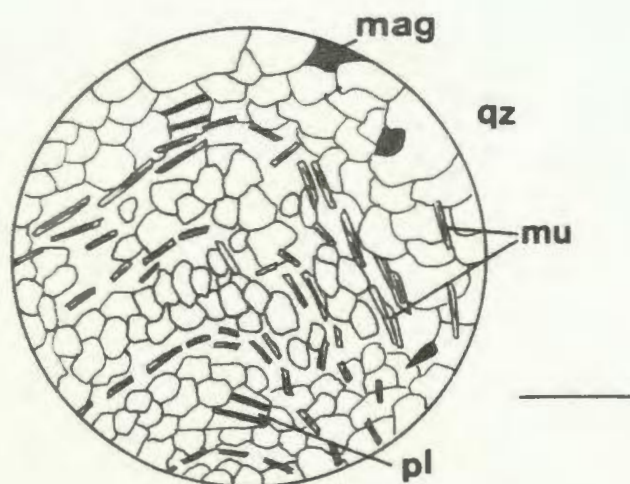
In the Lake Melville Terrane, the predominant assemblage in paragneiss is: sillimanite + garnet + K feldspar + biotite + melt. In contrast to the Groswater Bay Terrane, muscovite is generally absent, although some paragneiss zones in the Lake Melville Terrane are locally characterized by muscovite-bearing assemblages. In a few localities immediately south of the Rigolet thrust zone, prismatic sillimanite grains are observed overgrowing relict kyanite aggregates (Figure 18). On the basis of this observation, two interpretations can be proposed: (1) the overgrowth of kyanite by sillimanite is a result of decompression during late- or post Grenvillian uplift. (2) the overgrowth of kyanite by sillimanite is a Grenvillian metamorphic feature, which occurred prior to the replacement of kyanite by retrograde muscovite in the Groswater Bay Terrane during post-Grenvillian uplift, and thus the sillimanite + K feldspar assemblage is a Grenvillian feature developed prior to uplift. In view of previous discussions of the effect of the Grenvillian Orogeny

Figure 17: Crenulation of fabric defined by muscovite in Groswater Bay Terrane paragneiss (Sample CG81-756).

Figure 18: Overgrowth of kyanite by sillimanite in paragneiss, immediately south of the Rigolet thrust zone (Sample CG81-170B).

Figure 19: Retrograde hornblende rims on granoblastic orthopyroxene and clinopyroxene grains in Lake Melville Terrane mafic granulite (Sample VN84-431).

Scale bar - 2 mm



in eastern Labrador, the latter interpretation appears to be more reasonable. The overgrowth of sillimanite on kyanite in K feldspar bearing paragneisses in the Lake Melville Terrane, suggests either an increase in temperature or a decrease in pressure; which of these two possibilities occurred cannot be evaluated without additional information.

Garnet - Plagioclase - Opx - Cpx - Quartz

In the Groswater Bay Terrane, samples of metabasic rocks containing garnet + orthopyroxene + clinopyroxene assemblages, exhibit granoblastic textures in which all phases appear to be texturally stable. Microprobe analyses of several grains within any one thin section reveal a consistent composition, implying that chemical equilibrium was attained. In some samples, retrograde hornblende is present as thin fibrous rims surrounding granoblastic pyroxene grains (Figure 19) presumably a result of the breakdown of orthopyroxene + clinopyroxene in the presence of  $H_2O$ . In these samples, garnet, orthopyroxene and clinopyroxene exhibit serrated boundaries and embayed structures where in contact with hornblende. In addition, systematic microprobe analyses of pyroxenes within the same thin section reveals inconsistent compositions, implying disequilibrium relationships, although garnets yield reasonably consistent analyses. The development of hornblende in mafic rocks in the Groswater Bay Terrane is presumably the equivalent retrograde reaction to the formation of muscovite via the breakdown of kyanite observed in pelitic assemblages. Thus the formation of hornblende in mafic rocks

is interpreted to be a reflection of post-Grenvillian uplift and equilibrium whereas assemblages of garnet + opx + cpx are considered to be Grenvillian equilibria.

In the Lake Melville Terrane, similar textural and chemical relationships are observed in garnet + orthopyroxene + clinopyroxene assemblages, in which all phases appear to be in equilibrium (Figure 20). However, in contrast to the Groswater Bay Terrane, retrograde hornblende is not developed, with the exception of local retrogression in late shear zones. The lack of retrograde hornblende in mafic rocks from the Lake Melville Terrane correlates with the absence of muscovite in pelitic assemblages, supporting the interpretation that retrogression due to Grenvillian uplift in the Lake Melville Terrane was minimal.

In summary, microstructural and chemical relationships reveal: (1) in the Groswater Bay Terrane the kyanite + K feldspar and garnet + orthopyroxene + clinopyroxene assemblages in paragneiss and mafic rocks are interpreted to be Grenvillian equilibria. The development of retrograde muscovite via the breakdown of kyanite in paragneiss and the presence of hornblende as a result of pyroxene breakdown in mafic rocks are interpreted to be a result of post-Grenvillian retrogression and subsequent re-equilibration; (2) in the Lake Melville Terrane the sillimanite + K feldspar and garnet + orthopyroxene + clinopyroxene assemblages in paragneiss and mafic rocks represent Grenvillian metamorphism, but appear to have been minimally affected by Grenvillian uplift as evidenced by the lack of retrograde phases in either assemblage.

Geothermometry and geobarometry estimates obtained in this study

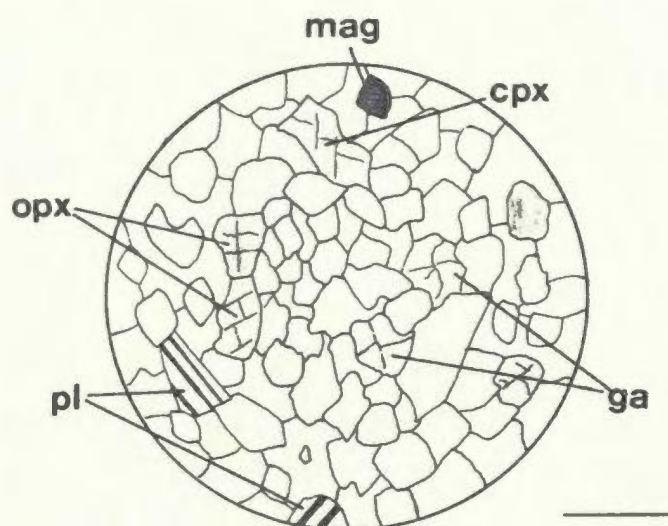


Figure 20: Granoblastic textures in garnet - orthopyroxene - clinopyroxene mafic granulite from the White Bear Arm Complex, Lake Melville Terrane (Sample VN84-229).

Scale bar - 2 mm

using kyanite + K feldspar and sillimanite + K feldspar assemblages in paragneiss and orthopyroxene + clinopyroxene + garnet + plagioclase + quartz assemblages in mafic rocks are thus interpreted to be Grenvillian metamorphic conditions. This interpretation supports the regional framework proposed for the Grenville Province in eastern Labrador, in which the major affect of the Grenvillian Orogeny was the overprinting and subsequent imbrication of contrastingly older crustal slices with pre-Grenvillian histories.



CHAPTER 5GEO THERMOMETRY-GEOBAROMETRY5.1 Introduction

One of the principal objectives of this study is to estimate metamorphic pressures and temperatures from the composition of co-existing minerals utilizing experimentally and empirically calibrated thermobarometric expressions. The purpose is two-fold: firstly to contribute to the understanding of metamorphic conditions in the Sandwich Bay area, eastern Labrador, in particular to determine the presence or absence of significant differences in the conditions of metamorphism between the Groswater Bay and Lake Melville Terranes; secondly, to investigate the consistencies of the calibrated geothermobarometers. Since several different methods have been employed, comparisons of independently calculated pressures and temperatures can be made with the aim of evaluating the merits of individual calibrations. The geothermobarometers employed are applicable to assemblages in pelitic and basic rocks. For pelitic gneisses, biotite - garnet and garnet - plagioclase -  $\text{Al}_2\text{SiO}_5$  - quartz assemblages were used. The following assemblages: orthopyroxene - clinopyroxene; garnet - clinopyroxene; garnet - orthopyroxene; garnet - clinopyroxene - plagioclase - quartz; and garnet - orthopyroxene - plagioclase - quartz, were used for basic rocks. These various methods have allowed the estimation of P-T conditions throughout the Sandwich Bay area.

Metamorphic pressures and temperatures have been estimated for 37 samples in the Sandwich Bay area. Appendix 2 shows sample localities.

## 5.2 Methods

For paragneiss lithologies, temperatures and pressures have been calculated on the basis of the Fe - Mg exchange between biotite and garnet mineral pairs, using the thermometers of Thompson (1976), Ferry and Spear (1978), Pigage and Greenwood (1982), Hodges and Spear (1982) and Indares and Martignole (1984), in conjunction with the garnet - plagioclase -  $\text{Al}_2\text{SiO}_5$  - quartz geobarometers of Ghent (1976), Ghent et al. (1979) and Newton and Haselton (1981).

For basic rocks temperatures and pressures were calculated using the orthopyroxene - clinopyroxene thermometers of Wood and Banno (1973) and Wells (1977), the garnet - clinopyroxene thermometers of Wells (1979) and Ellis and Green (1979) and the garnet - orthopyroxene thermometer of Sen and Bhattacharya (1984), in conjunction with the garnet - clinopyroxene - orthopyroxene - plagioclase - quartz barometers of Newton and Perkins (1982). A detailed discussion of the above geothermometers and geobarometers is presented in Appendix 5.

## 5.3 Geothermometry - Geobarometry Results

### 5.3.1 Calculation of Pressures and temperatures

Metamorphic temperature and pressure estimates were obtained from both pelitic and basic assemblages using the various mineral pairs discussed in the previous section. For each assemblage, temperature

dependent curves were generated from geothermometry calibrations by solving the expressions for two "model" pressures (8 and 10 kbar), and using the appropriate value of the distribution coefficient ( $K_D$ ) derived from compositional and thermodynamic data. Similarly, pressure dependent curves were generated from geobarometry calibrations by solving the barometric expressions for two separate temperatures (600°C and 800°C). The intersection of each thermometer and barometer in P-T space thus yields a unique P-T point. All P-T estimates are based on rim compositions of coexisting mineral phases, because cores may not be in equilibrium in all cases (see section 4.3.3). The procedures and methods used during microprobe analysis and acquisition of chemical data for each mineral assemblage are given in Appendix 6. Complete analyses are given in Appendix 8.5 and compositional parameters of the various mineral phases are given in Appendices 8.1 and 8.2.

The following section presents the results of the geothermobarometric calculations and assesses the reliability of each thermometer and barometer used in terms of treatment of non-ideal solutions in mineral phases, comparisons with other calibrations and distribution of P-T estimates with respect to experimentally derived pelitic and mafic reactions.

### 5.3.2 Geothermometry Results

#### 5.3.2.1 Garnet - Biotite

Temperature results from the five different thermometers are listed

in Table 1.

Estimates determined from the calibrations of Thompson (1976) and Ferry and Spear (1978) yield comparable temperatures ( $\pm 25^{\circ}\text{C}$ ) ranging from  $600^{\circ}\text{C}$  to  $770^{\circ}\text{C}$ . The generally good agreement between these two thermometers has been observed by other authors, notably Bohlen and Essene (1981), St Onge (1981), and Ghent et al. (1982). The Hodges and Spear (1982) thermometer, which explicitly accounts for the Ca and Mn content in garnet solution, yields a comparable temperature range of  $150^{\circ}\text{C} \pm 25^{\circ}\text{C}$ , but slightly higher estimates ranging from  $630^{\circ}\text{C}$  to  $850^{\circ}\text{C}$  than the Thompson and Ferry and Spear thermometers which do not specifically account for the effects of components other than Fe and Mg. The Indares and Martignole calibration yields estimates which are comparable to the Thompson and Ferry & Spear estimates for samples with low Mn garnets, but yields significantly higher temperatures for samples in which garnets contain more than 10 % spessartine component. The Ferry & Spear calibration with the corrections of Pigage and Greenwood (1982), yields somewhat anomalous results in which temperatures are in the order of  $100^{\circ}\text{C}$  to  $150^{\circ}\text{C}$  higher than estimates determined from any of the other thermometers, although, similar estimates are obtained from the Indares and Martignole calibration for Mn-rich garnets.

This discrepancy between the various thermometers, particularly between the Thompson, Ferry and Spear, Hodges and Spear and Indares and Martignole calibrations, appears to reflect how Mn substitution in the garnet solid solution is dealt with. The magnitude of the effects of non-ideality with respect to the spessartine component can be examined by considering the interaction parameters for a

Table 1 . Temperature estimates obtained from garnet-biotite thermometers in the Sandwich Bay area. The temperatures given represent temperatures of intersection of  $K_D$  of garnet-biotite with the  $K_D$  of the garnet-plagioclase- $Al_2SiO_5$  quartz barometer. Error range of estimates  $\pm 50^\circ C$ .

Sample #	T1	T2	T3	T4	T5
CG81-148	663	780	668	684	795
CG81-155	677	695	688	684	658
CG81-170B	751	765	712	739	805
CG81-239	679	711	793	686	843
CG81-299A	697	874	864	699	864
CG81-476	699	740	602	701	785
CG81-479	715	639	608	712	784
CG81-749A	726	663	765	720	812
CG81-756	596	614	663	617	740
GF81-16	641	667	822	657	783
GF81-18	601	630	771	626	828
GF81-23	661	684	814	672	920
GF81-141	748	764	592	737	779
GF81-235B	778	796	695	758	851
VAN84-12H	649	695	640	663	778
VAN84-12N	665	683	638	676	772
VAN84-16E	645	673	855	660	841
VAN84-34A	812	839	806	678	825
VAN84-35B	672	656	620	681	750
VAN84-36	743	777	784	753	837
VAN84-102	679	758	732	686	757
VAN84-150	756	770	742	742	764
VAN84-338	760	760	755	683	763
VO81-77A	755	792	805	742	821
VO81-518	670	692	620	685	723

T1-Ferry and Spear (1978)

T2-Ferry and Spear (1978) with Hodges and Spear (1982) corrections.

T3-Indares and Martignole (1984)

T4-Thompson (1976)

T5-Pigage and Greenwood (1982)

multi-component system. Newton and Haselton (1981) took account of the  $W_{\text{Ca-Mg}}$  binary, which was related to temperature by the expression:

$$W_{(\text{Ca-Mg})} = 3300 - 1.5T(\text{K})$$

Due to the lack of thermodynamic data the interactions involving Mn were neglected, resulting in the simplified expression

$$\ln(\gamma_{\text{Fe}}^{\text{gr}} / \gamma_{\text{Mg}}^{\text{gr}}) = -(3300 - 1.5T)X_{\text{Ca}}/RT$$

However, in a recent thermodynamic study of compositions of natural minerals, Ganguly and Saxena (1984) derived mixing parameters for other binaries in garnet solid solutions, and they suggested that the interaction or Margules parameters for mixing of Ca and Mn with Fe-Mg solutions were equal to 3000  $\pm$  500 cal/mole. The expression for the non-ideal mixing of Ca and Mn with the binary Fe-Mg system is therefore modified to:

$$RT \ln(\gamma_{\text{Fe}}^{\text{gr}} / \gamma_{\text{Mg}}^{\text{gr}}) = -3000(X_{\text{Ca}} + X_{\text{Mn}})$$

From the previous equations, it is clear that disregarding the effects of Ca and Mn in garnet-biotite thermometry results in an underestimation of temperatures. This is consistent with the data in Table 1, in which the temperature estimates by the method of Ferry and Spear (1978) are generally lower than those of other methods. However, Indares and Martignole (1984), in their discussion of this

problem, note that corrections for the effects of Ca and Mn in garnets (using their calibration), actually increase the discrepancy between temperatures obtained from Thompson's and Ferry and Spear's calibrations.

The anomalously high temperature estimates obtained from the Ferry and Spear calibration as modified by Pigage and Greenwood (1982) (which empirically account for Ca and Mn substitution in garnet) may suggest that its use should be restricted to a limited compositional range of garnet.

The Ferry and Spear (1978) thermometer as modified by Hodges and Spear (1982) is based on a consistent set of solution models which explicitly account for effects of addition of Ca and Mn in the garnet solid solution. A consistent range of temperatures is obtained from variable compositions (particularly samples with variable XCa and XMn in garnet), whereas the Indares & Martignole (1984) and Pigagé & Greenwood (1982) thermometers, which also account for addition of Ca and Mn, yield significantly different temperatures for variable garnet compositions. In addition, estimates obtained from the Hodges and Spear thermometer, compare reasonably well with the other thermometers. Thus on the basis of these results, the thermometer proposed by Hodges and Spear (1982) is most applicable to rocks examined in this study.

#### 5.3.2.2 Garnet - clinopyroxene - orthopyroxene

Temperatures were obtained from basic rocks by applying the two - pyroxene thermometers of Wood and Banno (1973) and Wells (1977), the

garnet - clinopyroxene thermometers of Ellis and Green (1979) and Dahl (1980) and the garnet - orthopyroxene thermometer of Sen and Battacharya (1984). Along with the garnet - clinopyroxene - orthopyroxene - plagioclase - quartz barometer of Newton and Perkins (1982), unique P-T estimates were obtained by graphical solution (Section 5.3.1).

Metamorphic temperatures obtained from basic rocks are listed in Table 2. The orthopyroxene - clinopyroxene thermometers of Wood and Banno (1973) and Wells (1977) (T2 and T3 in Table 2) yield results differing by only  $\pm 30^{\circ}\text{C}$ , which is well within the accuracy range of  $\pm 60^{\circ}\text{C}$  and  $\pm 70^{\circ}\text{C}$  respectively, suggested for both calibrations.

Comparison of temperatures obtained from the Ellis and Green (1977) and Dahl (1980) thermometers (T4 and T5 in Table 2), indicates a relatively large discrepancy (up to  $100^{\circ}\text{C}$ ) for some samples with the garnet - clinopyroxene thermometers. The calibration of Dahl (1980) yields the least consistent range of estimates spanning  $611^{\circ}\text{C}$  to  $916^{\circ}\text{C}$ . Estimates derived from the Ellis and Green (1979) thermometer yield a more reasonable range of  $710^{\circ}\text{C}$  to  $960^{\circ}\text{C}$ . According to Johnson et al. (1983) who tested various garnet - clinopyroxene thermometers in six separate granulite facies terranes, the Ellis and Green calibration yields the most satisfactory results whereas other garnet - clinopyroxene thermometers give highly erratic and generally unreasonable temperatures. The relatively consistent results obtained with the Ellis and Green thermometer are in accord with the above study and are considered to be the more reasonable temperature estimates for the garnet - clinopyroxene assemblages.



Table 2. Temperature estimates obtained from garnet-opx, garnet-cpx and opx-cpx thermometers in the Sandwich Bay area, solved graphically with the garnet-cpx-opx-plag-quartz barometers of Newton and Perkins (1982). Error range of estimates  $\pm 70^{\circ}\text{C}$ .

Sample #	T1	T2	T3	T4	T5
CG81-366	-	-	-	716	611
CG81-488A	-	-	-	756	718
CG81-641	635	765	743	712	626
CG81-811B	852	-	-	-	-
CG84-362	747	901	879	745	703
GF81-222	-	-	-	958	853
GF81-244A	1016	1058	1072	973	916
GF81-246A	746	862	845	797	743
VO81-89A	705	-	-	-	-
VO81-188	848	877	879	857	827
VN84-229	756	870	839	-	-
VN84-431	754	868	830	721	674
GF81-121	-	816	822	-	-
CG84-100	-	889	862	-	-
VN84-19	-	826	815	-	-
VN84-534	-	902	895	-	-

T1-Sen and Battacharya (1984) : garnet-opx

T2-Wells (1977) : opx-cpx

T3-Wood and Banno (1973) : opx-cpx

T4-Ellis and Green (1979) : garnet-cpx

T5-Dahl (1980) : garnet-cpx

The Sen and Bhattacharya (1984) garnet - orthopyroxene thermometer yields a wide range of temperatures (636°C to 1015°C), and in most cases agreement with other thermometers is poor, suggesting that it is of limited use in this study. Apart from samples CG81-811B and VO81-89A which contain only garnet - orthopyroxene, temperature estimates by other methods are preferred.

### 5.3.3 Geobarometry Results

#### 5.3.3.1 Garnet - plagioclase - $\text{Al}_2\text{SiO}_5$ - quartz

Various parameters necessary for geobarometric calculations using the garnet - plagioclase -  $\text{Al}_2\text{SiO}_5$  - quartz barometer are listed in Table 3. The complete mineral analyses are given in Appendix 8.5 and compositional parameters required for pressure calculations are given in Appendix 8.1. Using temperatures derived from garnet - biotite assemblages from the same sample, pressure estimates from the polybaric, polythermal expressions of Ghent (1976), Ghent et al. (1979) and Newton and Haselton (1981) are listed in Table 3.

Table 3 shows that the three geobarometers yield a wide range of pressures between 6 and 12 kbar; however, within sample variations are less than 1.5 kbar. The calibrations of Ghent (1976) and Ghent et al. (1979) incorporate only an approximation of the non-ideal component in garnet and plagioclase solutions, and in addition assume end-member volume change of phases. The Newton and Haselton (1981) calibration, however, explicitly defines and determines both the non-ideality of garnet and plagioclase solid solution and takes into

Table 3. Temperature and pressure estimates obtained from paragneiss using the garnet-biotite thermometer of Hodges and Spear (1982) and the garnet -  $\text{Al}_2\text{SiO}_5$  - plagioclase - quartz barometers of Newton and Haselton (1981) [P1], Ghent et al. (1979) [P2] and Ghent (1976) [P3]. Error range of pressure estimates  $\pm 1.5$  kbar

$a_{\text{gr}}$  = activity of grossular component in garnet

$a_{\text{an}}$  = activity of anorthite component in plagioclase

V = volume change ( $\text{cm}^3$ )

$\ln K = \ln[(a_{\text{an}})^3/(a_{\text{gr}})]$

$\log K_s = (X_{\text{gr}})^3/(X_{\text{an}})^3$

$\log kd = 3[\log(X_{\text{gr}} * Y_{\text{gr}})_{\text{ga}}] - 3[\log(X_{\text{an}} * Y_{\text{an}})_{\text{pl}}]$

A = aluminum silicate polymorph

S = Sillimanite

K = Kyanite: (K) = unstable

Sample #	Tl	a <sub>gr</sub>	a <sub>an</sub>	V	lnK	logKs	logKd	P1	P2	P3	A
CG81-148	780	.0469	.5249	56.9	7.24	2.80	3.15	5.9	5.7	5.9	S
CG81-155	695	.0481	.6355	56.2	7.74	3.02	3.36	7.5	7.3	7.8	S
CG81-170B	765	.0373	.5776	56.9	8.24	3.44	3.56	7.0	6.5	7.2	S/(K)
CG81-239	711	.0598	.3254	56.1	5.30	2.14	2.29	10.1	9.9	10.3	S
CG81-299A	874	.0496	.4678	66.7	4.70	2.38	2.41	11.7	11.4	11.3	K
CG81-476	740	.1061	.5408	54.6	4.88	1.98	2.41	9.2	8.9	9.2	S
CG81-479	639	.0622	.6375	56.0	6.98	2.89	3.03	6.1	5.2	6.3	S
CG81-749A	663	.0412	.3137	67.2	4.44	1.83	1.93	12.2	9.9	11.9	K
CG81-756	614	.0628	.5009	66.1	6.22	2.57	2.71	8.6	6.8	8.9	K
GF81-16	667	.0623	.3265	67.0	4.91	2.13	2.15	10.5	10.3	11.3	K
GF81-18	630	.0673	.4236	66.8	5.40	2.13	3.39	10.1	9.2	9.5	K
GF81-23	684	.0557	.3698	66.7	5.73	2.41	2.46	10.9	9.2	10.3	K
GF81-141	663	.0391	.5106	56.5	7.70	3.14	3.34	7.8	6.5	7.9	S
GF81-235B	796	.0421	.4314	56.0	6.97	2.86	3.03	9.6	7.4	9.2	S
VAN84-12H	695	.0591	.5324	56.1	7.43	2.99	3.14	7.3	5.9	5.7	S/(K)
VAN84-12N	683	.0418	.5221	55.8	7.55	3.07	3.29	7.1	6.8	7.4	S
VAN84-16E	673	.0639	.2897	67.2	4.53	1.97	1.96	12.5	10.1	12.1	K
VAN84-34A	839	.0361	.4394	56.6	7.41	3.16	3.24	9.0	8.5	9.2	S
VAN84-35B	656	.0552	.5724	56.4	5.53	2.58	2.39	7.1	6.9	7.1	S
VAN84-36	777	.0499	.5230	56.2	7.05	2.99	3.06	9.0	7.5	8.7	S
VAN84-102	758	.0398	.5724	56.9	5.84	2.78	2.70	7.8	7.3	7.8	S
VAN84-150	770	.0321	.5502	57.1	6.28	2.76	2.85	8.7	8.3	8.5	S
VAN84-338	760	.0318	.5796	57.1	6.21	2.76	2.69	8.5	7.3	7.2	S
V081-77A	792	.1032	.2798	66.8	4.52	1.16	1.29	12.9	11.8	13.0	K
V081-518	692	.0468	.3368	56.8	5.90	2.45	2.57	5.3	7.0	7.2	S

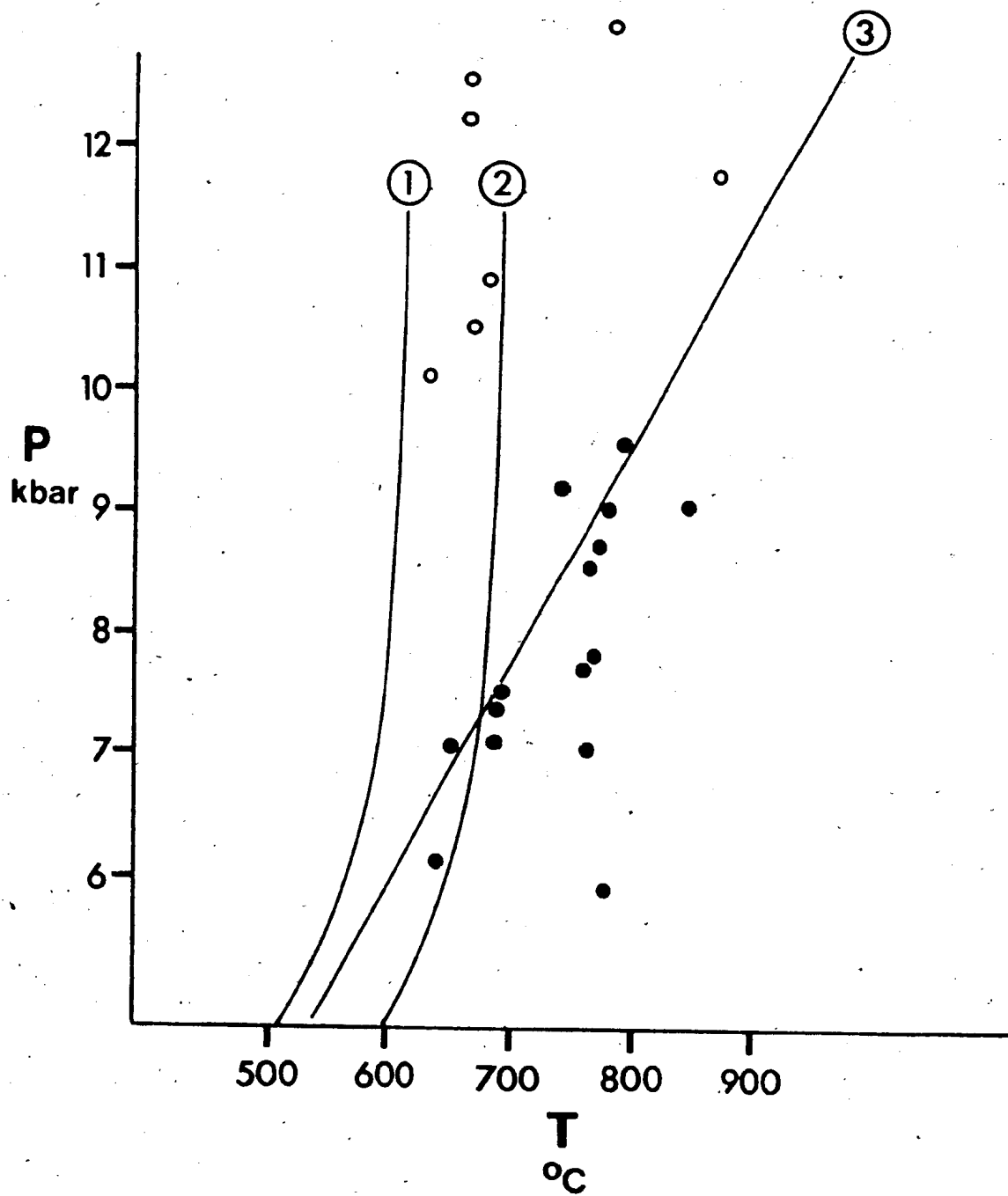
account the volume change with composition of phases (this is particularly significant for garnet which shows excess molar volume in the compositional range encountered in most pelitic rocks). Taking this into account the Newton and Haselton (1981) calibration is preferred.

To assess the validity of temperatures and pressures obtained from paragneiss assemblages, estimates were plotted on a P-T grid along with appropriate reactions for each terrane. Figure 21 shows P-T estimates obtained from paragneiss assemblages along with the kyanite - sillimanite and  $\text{Al}_2\text{SiO}_5 + \text{K feldspar} + \text{melt}$  reactions. This diagram reveals that all Groswater Bay paragneiss containing kyanite + K feldspar + melt plot within the kyanite field. However, the majority of estimates plot to the left of the kyanite K feldspar + melt reaction. Bearing in mind that this reaction is arbitrarily plotted at  $a\text{H}_2\text{O} = 0.5$  in Figure 21, the distribution suggests that the assumption of  $a\text{H}_2\text{O} = 0.5$  may not be valid in all rocks. In Figure 21, the kyanite + K feldspar + melt reaction is also plotted at  $a\text{H}_2\text{O} = 0.3$ , which is consistent with the distribution of P-T points. With the exception of two samples, all sillimanite + K feldspar + melt bearing paragneiss (Lake Melville Terrane) plot in the sillimanite field. The two samples which contain relict kyanite in addition to sillimanite are indicated in Figure 21; one plots very close to the kyanite - sillimanite transition, the other lies well within the sillimanite field. In addition, all but two samples are consistent with the position of the sillimanite + K feldspar + melt curve as plotted at  $a\text{H}_2\text{O} = 0.5$ . Allowing for slight  $a\text{H}_2\text{O}$  variations, the P-T estimates obtained from paragneiss assemblages are in good agreement

Figure 21. Plot of P-T estimates obtained from paragneiss assemblages together with the  $\text{Al}_2\text{SiO}_5$  + K feldspar + melt curve for  $a\text{H}_2\text{O} = 0.5$  (1) and 0.3 (2), (after Kerrick, 1972) and the kyanite - sillimanite boundary (3) (after Holdaway, 1971).

( O ) Groswater Bay Terrane paragneiss.

( ● ) Lake Melville Terrane paragneiss.



with the petrogenetic grid for paragneiss in the study area.

#### 5.3.3.2 Garnet - plagioclase - orthopyroxene - clinopyroxene - quartz

Metamorphic pressures for basic rocks were determined by applying the orthopyroxene - clinopyroxene - plagioclase - quartz barometers of Newton and Perkins (1982) in conjunction with the thermometers of Wells (1977), Ellis and Green (1979) and Sen and Bhattacharya (1984). The results are listed in Table 4. The pressure estimates obtained with the garnet - clinopyroxene - plagioclase - quartz barometer in combination with the Ellis and Green thermometer range from 6.4 to 12.1 kbar. These two extreme values, however, are anomalous, the remainder of estimates show a narrow range of 8.4 to 10.6 kbar. Pressures obtained from combining the temperature estimates of Wells (1977) with the same barometer yield similar results ranging from 9.4 to 10.8 kbar, excluding two extreme values of 7 and 12.4 kbar. Similar estimates are obtained when combining the Sen and Bhattacharya temperatures with the garnet - orthopyroxene - plagioclase - quartz barometer (8.4 to 11.5 kbar). Figure 22 shows a petrogenetic grid with reactions appropriate to mafic assemblages (after Wells, 1979) along with calculated P-T estimates. Although the positions of these reactions are somewhat arbitrary (since  $a_{H_2O}$  is unknown), the distribution of calculated pressures and temperatures may be used to partially constrain the P-T range of mafic equilibria within the study area. The erratic distribution of P-T estimates with respect to mafic stability fields suggests that  $a_{H_2O}$  in mafic



Table 4 . Temperature and pressure estimates obtained from garnet-cpx, garnet-opx and opx-cpx thermometers with the opx-cpx thermometers with the opx-cpx-plagioclase-quartz barometer. Error range of T estimates  $\pm 70^{\circ}\text{C}$ , of pressure estimates  $\pm 1.5$  kbar.

Sample #	T1	T2	T3	P1	P2	P3
CG81-366	716	-	-	10.6	-	-
CG81-488A	756	-	-	8.5	-	-
CG81-641	712	635	765	12.1	11.4	12.4
CG81-811B	-	852	-	-	10.7	-
CG84-362	745	747	901	8.7	9.3	9.7
GF81-222	958	-	-	-	10.6	-
GF81-244A	973	1016	1058	10.2	10.5	10.9
GF81-246A	797	746	862	10.4	9.1	10.8
VO81-89A	-	705	-	-	10.6	-
VO81-188	857	848	877	9.2	11.5	9.4
VN81-229	870	-	-	9.6	-	-
VN81-431	721	754	868	6.4	8.4	7.0

T1= Ellis and Green : garnet-cpx (1979)

T2= Sen and Battacharya :garnet-opx (1984)

T3= Wells : opx-cpx (1977)

P1= Perkins and Newton (1982)(cpx-garnet-plag) with T1

P2= Perkins and Newton (1982)(opx-garnet-plag) with T2

P3= Perkins and Newton (1982)(cpx-garnet-plag) with T3

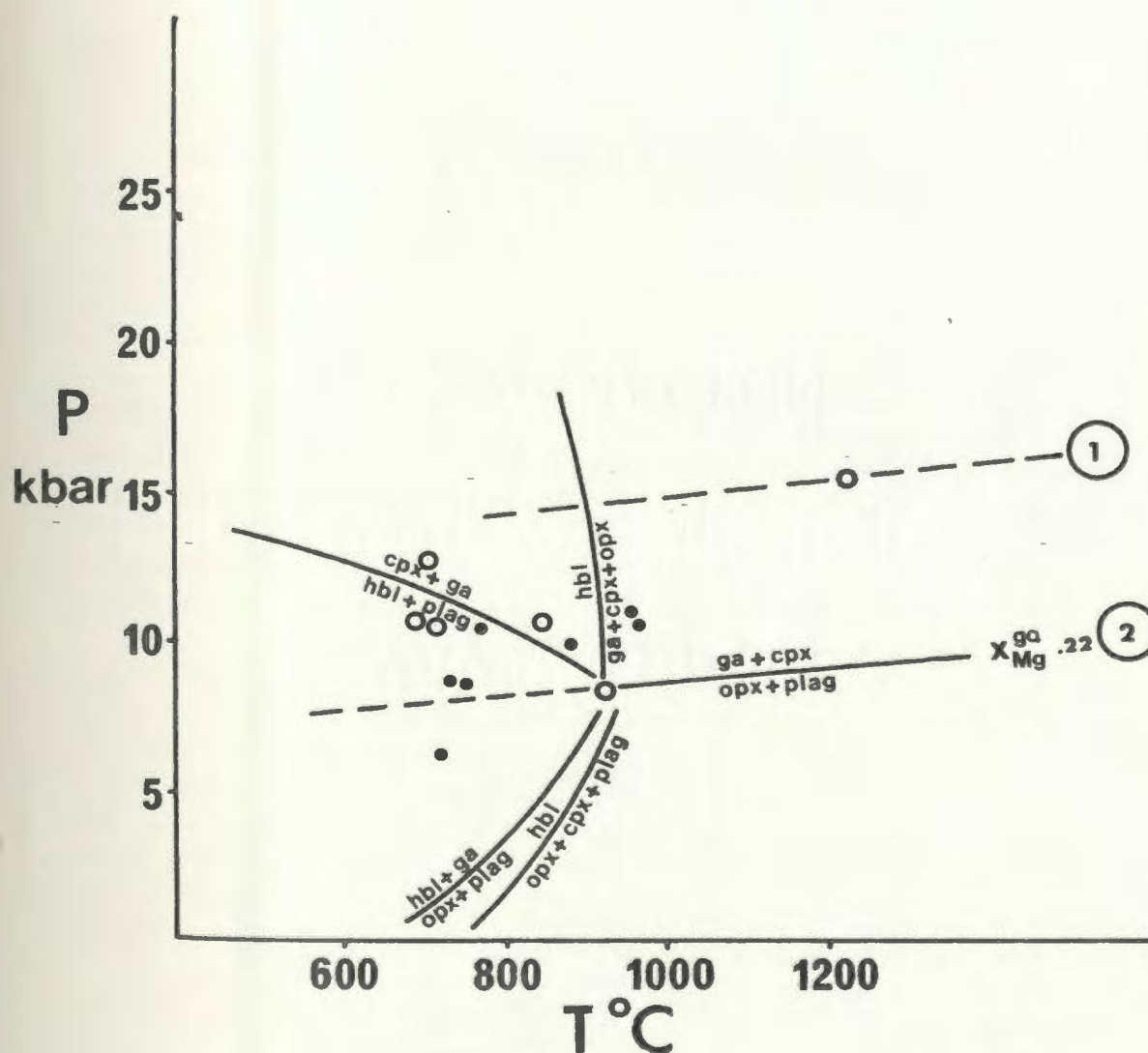


Figure 22. Plot of P-T estimates obtained from mafic assemblages compared with reactions in the CMAS system. Invariant point for  $a_{H_2O} = 0.5$  after Wells (1979) and  $X_{Mg} = 0.22$  after Glassley and Sorensen (1980).

( ○ ) Groswater Bay Terrane estimates.

( • ) Lake Melville Terrane estimates.

assemblages in the study area is quite variable as shown by the wide spread across several reaction boundaries for samples which contain only one assemblage. This distribution implies that  $a_{H_2O}$  may range from as low as 0.1 in the Groswater Bay Terrane and as high as 0.5 in the Lake Melville Terrane.

#### 5.3.4 Comparison of P-T results from basic rocks and paragneiss

Geothermobarometry results from paragneiss and mafic rocks are in reasonable agreement, and also with mineral equilibria as determined qualitatively with the petrogenetic grid. For the pelites, pressure estimates for the Groswater Bay Terrane are consistently higher than those for the Lake Melville Terrane (10-13 kbar and 6-9.5 kbar, respectively), with the temperature range (650°C-900°C) being approximately similar in both cases (though average temperature in the Lake Melville Terrane is higher than in the Groswater Bay Terrane). For mafic rocks, pressure and temperature estimates for the two terranes overlap somewhat (Groswater Bay Terrane: 8 - 12 kbar / 700 - 850°C and Lake Melville Terrane: 6 - 10 kbar / 750 - 950°C.)

#### 5.4 Interpretation of Geothermobarometry Results

To develop a consistent interpretation of the geothermobarometry data, the P-T estimates are assessed in three separate ways. Firstly, the regional distribution of P-T estimates obtained from garnet - biotite - plagioclase -  $\text{Al}_2\text{SiO}_5$  - quartz equilibria in paragneisses are independently assessed; secondly, P-T estimates derived from garnet - clinopyroxene - orthopyroxene - plagioclase - quartz assemblages in basic rocks are considered; and lastly, an interpretation of all data with respect to the regional tectono-metamorphic framework is made as an attempt to construct equilibrium P-T paths for each terrane. Estimates obtained from basic rocks are initially interpreted separately from those derived from paragneiss assemblages since the results of the different equilibria may not be directly correlatable.

##### 5.4.1 Garnet-biotite-plagioclase- $\text{Al}_2\text{SiO}_5$ -quartz

The regional distribution of pressure and temperature estimates obtained from paragneiss assemblages is shown in a locality map of the study area in Figures 23 and 24. In the Groswater Bay Terrane, there is a general increase in temperature from west to east. In the Cape Porcupine area, 6 temperatures estimates are very consistent ranging from  $614^\circ\text{C}$  to  $684^\circ\text{C}$ . Two higher estimates of  $792^\circ\text{C}$  and  $875^\circ\text{C}$  are located further to the south east in the Curlew Harbour area.

Temperatures obtained from paragneisses in the Lake Melville Terrane show a similar range of  $639^\circ\text{C}$  to  $839^\circ\text{C}$ . However, the majority of estimates lie within the range of  $700^\circ\text{C}$  to  $780^\circ\text{C}$ , which suggests

Figure 23. Distribution of temperature estimates in the Sandwich Bay area.

- (▲) estimates obtained from the garnet-biotite thermometer of Hodges and Spear (1982).
- (+) estimates obtained from the garnet - cpx thermometer of Ellis and Green (1979).

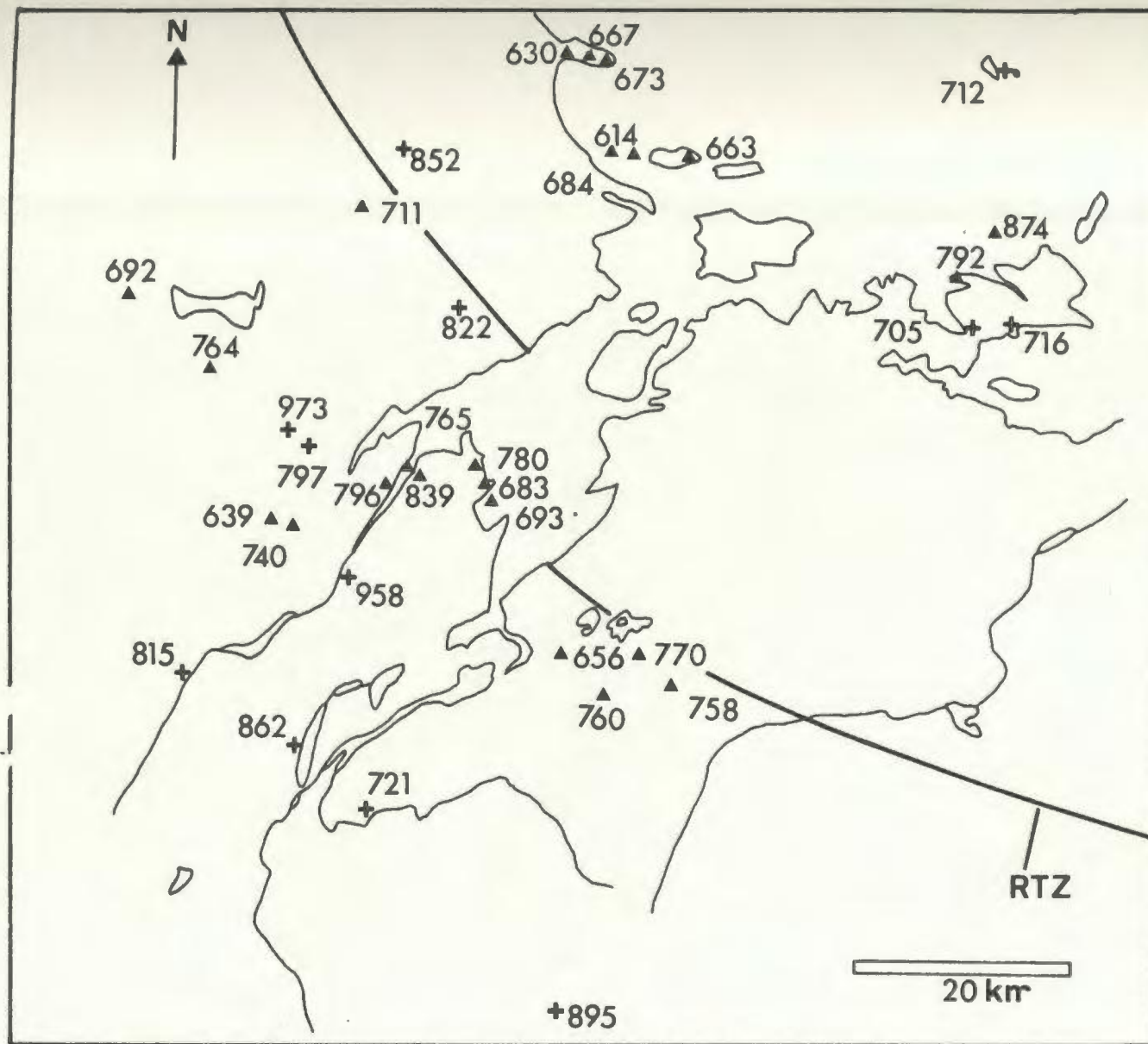
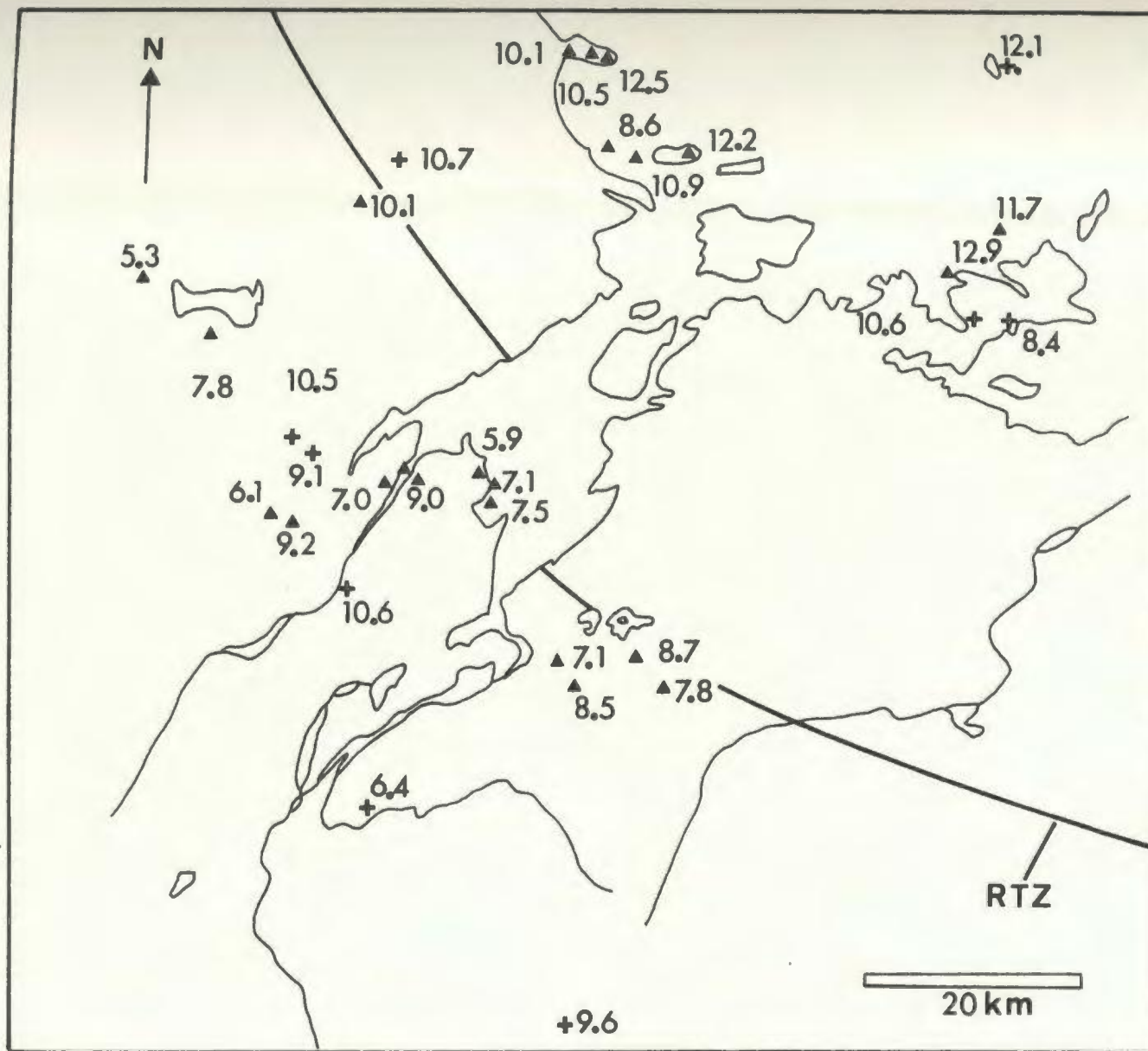


Figure 24. Distribution of pressure-estimates in the Sandwich Bay area.

- ( ▲ ) estimates obtained from the garnet-plagioclase -  $\text{Al}_2\text{SiO}_5$ -quartz barometer of Newton and Haselton (1982)
- ( + ) estimates obtained from the garnet - cpx-plagioclase barometer of Newton and Perkins (1982).





that the thermal gradient within the Lake Melville Terrane is relatively shallow.

A more significant contrast in the metamorphic conditions determined from paragneiss assemblages is shown in Figure 24, in which it can be seen that consistently higher pressures prevail in the Groswater Bay Terrane (8.6 to 12.9 kbar) than the Lake Melville Terrane (6.4 to 10.6 kbar).

#### 5.4.2 Garnet-plagioclase-orthopyroxene-clinopyroxene-quartz

Temperatures and pressures obtained from basic assemblages using the garnet - clinopyroxene and garnet - orthopyroxene thermometers of Ellis and Green (1979) and Sen and Bhattacharya (1984) and the garnet - clinopyroxene - orthopyroxene - plagioclase - quartz barometer of Newton and Perkins (1982) are shown in Figures 23 and 24.

In the Lake Melville Terrane, estimates are rather variable, with temperatures ranging from 721°C to 973°C, and pressure estimates ranging from 6.4 to 10.6 Kbar. In the Groswater Bay Terrane, temperatures range from 705°C to 852°C. However, the latter value, which occurs in the west, is obtained from orthopyroxene - garnet assemblages, whereas the remainder of estimates derived from clinopyroxene - garnet assemblages yield a more consistent range of 705°C to 716°C. Pressures in the Groswater Bay Terrane vary from 8.4 to 12.9 kbar. Figure 24 reveals that pressure estimates in basic

rocks are considerably lower than those in paragneiss near Curlew Harbour whereas the inverse is true in the Lake Melville Terrane. Temperature estimates in basic rocks generally are slightly higher than those in adjacent paragneiss.

#### 5.4.3 Regional Interpretation of Geothermobarometry Data

Figure 25, which represents a compilation of all geothermometry - geobarometry data on a P-T diagram, reveals a clear contrast in metamorphic conditions between the Groswater Bay and Lake Melville Terranes. Temperature estimates, ranging from about 630°C to 980°C, are obtained from both terranes, suggesting a similar thermal gradient across the Rigolet thrust zone. The most obvious distinction in metamorphic conditions is the pressure gradient between the two terranes (9 to 12 kbar for the Groswater Bay-Terrane and 6 to 10 kbar in the Lake Melville Terrane). The results of both temperature and pressure estimates should be viewed in the context of the mineral assemblages described earlier, which suggest that granulite facies metamorphism prevailed in the Lake Melville Terrane as opposed to upper amphibolite facies conditions in the Groswater Bay Terrane.

A major effect of the Grenvillian Orogeny in eastern Labrador was the juxtaposition of lower crustal rocks against higher crustal assemblages along major regional thrusts (i.e. upper amphibolite to granulite facies rocks against middle to upper amphibolite facies rocks). The crustal blocks bounded by these thrusts (i.e. the Groswater Bay and Lake Melville Terranes) are interpreted to be

Figure 25. Plot of P-T estimates obtained from paragneiss and mafic assemblages.

Groswater Bay Terrane

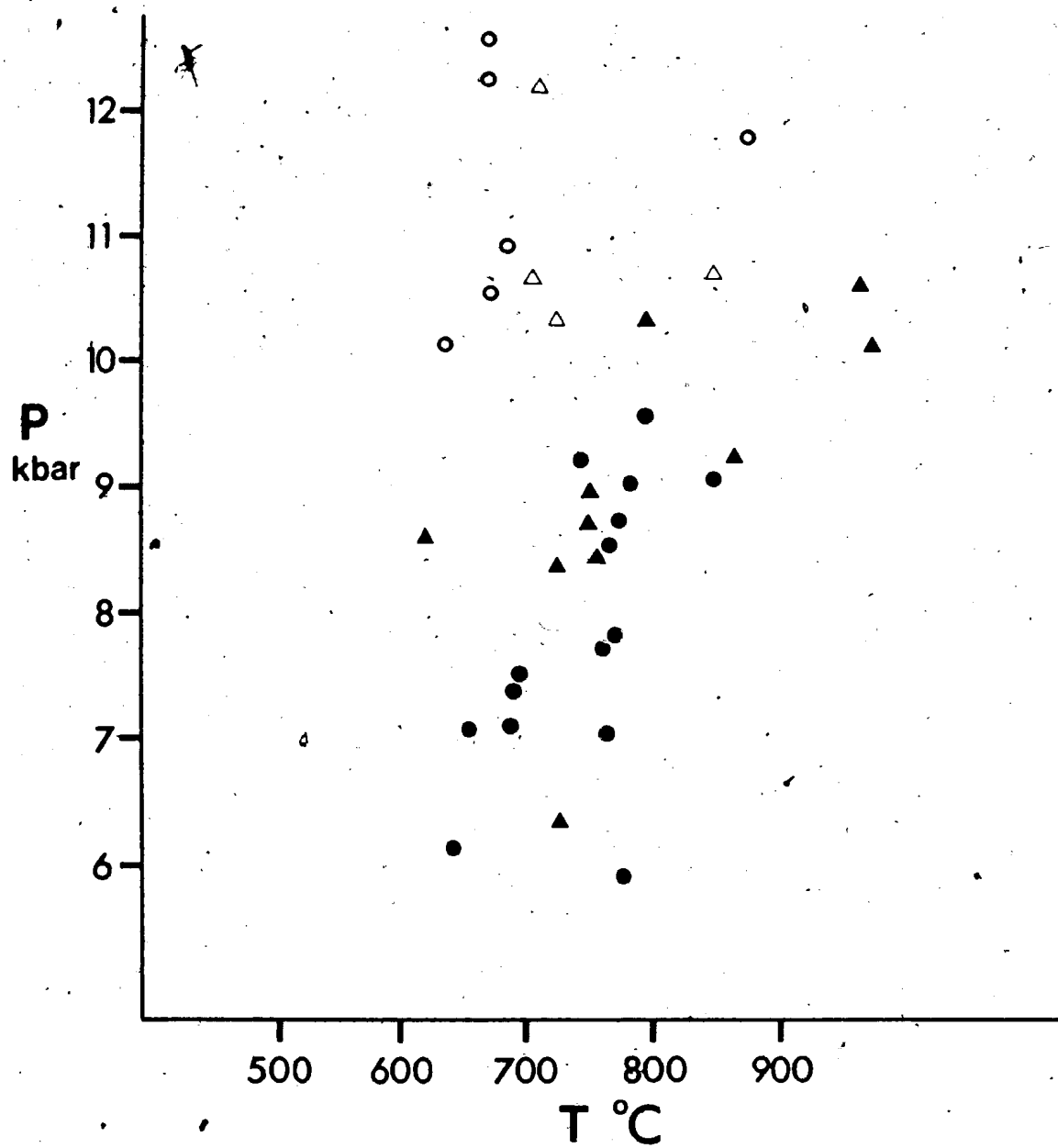
( ○ ) garnet-biotite-plagioclase-kyanite-quartz

( △ ) garnet-clinopyroxene-plagioclase-quartz

Lake Melville Terrane

( ● ) garnet-biotite-plagioclase-sillimanite-quartz

( ▲ ) garnet-clinopyroxene-plagioclase-quartz



deep-seated equivalents to rocks which occur to the north of the Grenville Province, in the Makkóvik Province (Gower and Ryan, 1986).

This interpretation is partially supported by the results of this study in which the quantitative metamorphic estimates obtained from the geothermobarometers in both the Groswater Bay and Lake Melville Terranes are interpreted to record Grenvillian conditions (Section 4.3.3). Following the regional tectonic framework, the distinctive contrast in metamorphic conditions, particularly pressures between the two terranes, appears to be largely a result of the positioning of the terranes within a major imbricate thrust stack during the Grenvillian Orogeny. However, two problems arise: (1) in the regional structural framework it was proposed that the Groswater Bay and Lake Melville Terranes represent part of an imbricate stack derived from intermediate and deep crustal levels, respectively. However, in contrast, the geothermobarometry estimates imply that the Groswater Bay Terrane was derived from deeper crustal levels (25 to 30 km) than the intermediate depths (18 to 25 km) for the Lake Melville Terrane; (2) since the estimates obtained from both terranes are interpreted to be a signature of the same metamorphic event (i.e. the Grenvillian orogeny), then it becomes crucial to explain the large temperature and pressure variations between the two terranes. These two problems will now be discussed separately.

The first problem involves the discrepancy between the regional tectonic framework, which suggests the juxtaposition of a deep level terrane (Lake Melville Terrane) against a higher level terrane (Groswater Bay Terrane), and the geothermobarometry results which in contrast imply that the Groswater Bay Terrane was derived from deeper

crustal levels than the Lake Melville Terrane. Four possible explanations for this discrepancy are discussed below;

(1) one interpretation to explain the pressure contrast is that the net transfer barometers may record post-emplacement conditions of the Groswater Bay and Lake Melville Terranes. Thus the pressures recorded in both terranes would reflect the positions of the nappes after emplacement, and not the positions that they were derived from. This would imply that the more deeply derived Lake Melville Terrane was emplaced as a "hot" nappe, on top of the relatively "cold", intermediate level Groswater Bay Terrane. Thus if the Lake Melville Terrane remained hotter, for a sufficient period of time (i.e. at lower pressure than maximum burial) then the net transfer barometers could continue to re-equilibrate after emplacement, and may even have continued to re-equilibrate during subsequent erosion and uplift. Thus the pressures recorded in the Lake Melville Terrane (6 to 10 kbar) probably do not represent the original depth of exhumation but rather the depth it attained following emplacement. Similarly, if barometers in the Groswater Bay Terrane, re-equilibrated following thrusting then the additional crustal thickness due to the overriding Lake Melville Terrane would result in burial of the Groswater Bay Terrane which would subsequently record higher pressures than the Lake Melville Terrane.

(2) an alternative viewpoint is that the contrasting pressures may be a result of an original difference in crustal thickness between the Groswater Bay Terrane and the Lake Melville Terrane dating from early Grenvillian metamorphism. This could indicate differential crustal thickening prior to or during Grenvillian metamorphism. The

differences in crustal thickness may have been enhanced by syn- or post-metamorphic erosion and could have persisted until the termination of the Grenvillian Orogeny. Wells (1979) suggested that erosion during metamorphism reduces differences in pressures between areas where there is initial difference in crustal thickness so that the difference recorded by the exposed mineral assemblage is less than the primary difference. Thus, in this case there would have been a minimum difference of 10 km between the Groswater Bay and Lake Melville Terranes.

(3) A third explanation, which would assume that pressures in both terranes reflect their positions prior to emplacement, is based on studies of pressure - temperature - time paths discussed by England and Thompson (1984) and Thompson and England (1984). Figure 26, (figure 5a in England and Thompson, 1984) shows temperature - time paths constructed for rocks buried at variable depths. Subsequent to burial by overthrusting of a 50 km thrust sheet, rocks experienced 20 Ma of isobaric heating and were then eroded and uplifted 50 km in the following 200 Ma. Using these curves England and Thompson (1984) propose that depending on the closure temperature for a particular system, and assuming that relevant minerals grow below (and never pass above) the closure conditions, it is possible for shallowly buried rocks to record higher pressures than rocks which were deeply buried. For example, the composition of 1 cm grains grown during prograde metamorphism on path C could reflect pressures in the depth range of 50 km to 35 km, while a mineral with the same size growing on paths C to A would record burial depths on the order of about 30 km. Therefore depending on the initial depths of burial

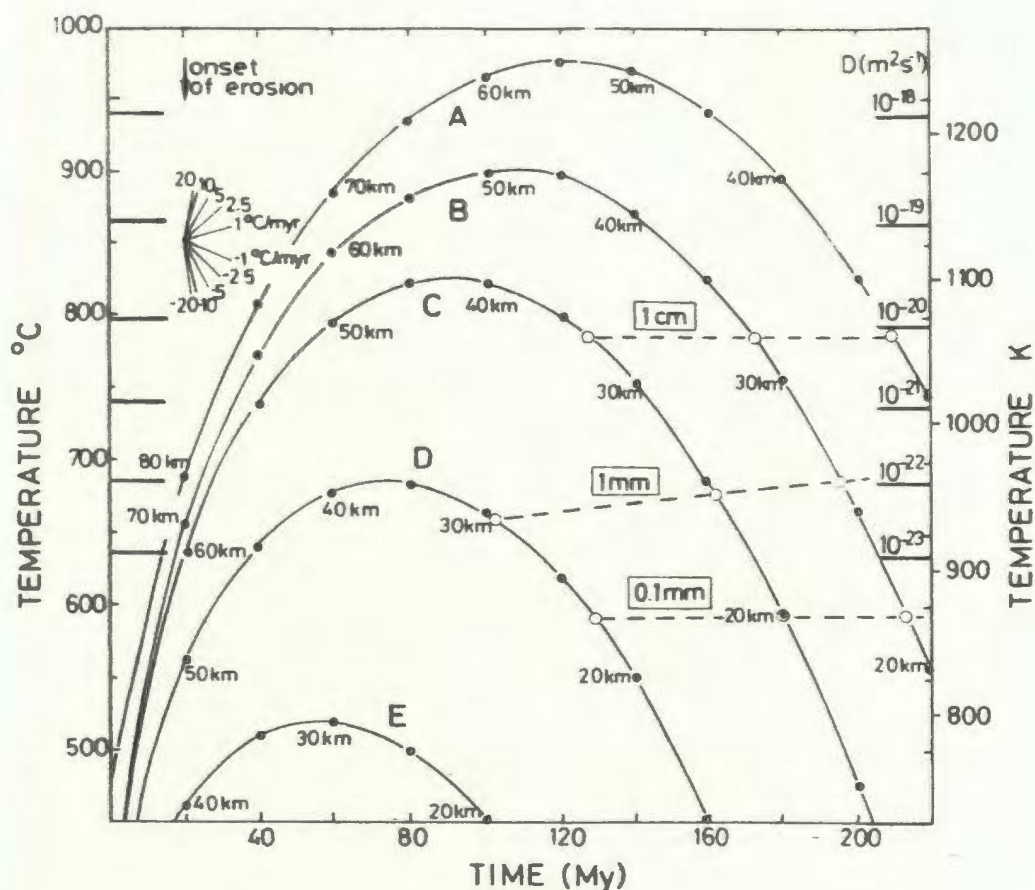


Figure 26. Temperature-time paths of rocks buried at variable depths after Thompson and England (1984). Paths are shown for rocks buried at 80 km (A), 70 km (B), 60 km (C), 50 km (D) and 40 km (E). Shown on the right hand axis are the coefficients of diffusivity of Fe and Mg in garnet and closure temperatures for grains of radii 1 cm, 1 mm and 0.1 mm, both calculated from diffusion equations of Dodson (1973, 1979). Solid circles on the curves are at 20 Ma intervals and the depths of exhumation are marked every 40 Ma.



of the Groswater Bay and Lake Melville Terranes, and assuming that the garnet - biotite - plagioclase - quartz and garnet - opx - cpx - plagioclase - quartz assemblages did not pass above the closure temperatures for these equilibria, it would seem reasonable that the shallow-level Groswater Bay Terrane may record higher pressures than those recorded by the deep-level Lake Melville Terrane.

(4) a more generalized explanation is that the regional kinematic framework is variable along the length of the Rigolet thrust zone. Thus, structural relationships between the eastern Groswater Bay and Lake Melville Terranes are not comparable with relationships further to the west. Gower et al. (1985) noted that east of the Double Mer White Hills region, the Rigolet thrust zone was predominantly a strike-slip fault with only a minor thrust component (see Figure 6), and that east of Sandwich Bay the structural significance of the extension of the Rigolet thrust zone was at present uncertain. In view of this, the "inverse" tectonic framework within the study area, based on the results of geothermobarometry estimates, suggests that the contrast in pressures between the Groswater Bay and Lake Melville Terranes may not be a result of the respective positioning in an imbricate thrust stack, as is proposed for the terranes further to the west.

The former problem of large temperature and pressure variations within each terrane may be somewhat resolved by considering four possible causes: (1) the presence of significant temperature and pressure gradients within the Groswater Bay and Lake Melville Terranes; (2) different closure conditions of the various geothermometers and geobarometers; (3) error propagation in

calibrated geothermobarometry expressions; and (4) re-equilibration of mineral components during regional uplift and cooling.

(1) In the Groswater Bay Terrane the large range of geothermobarometry estimates may be a reflection of significant metamorphic gradients. The consistent temperatures obtained in the Cape Porcupine area ranging from  $614^{\circ}\text{C}$  to  $673^{\circ}\text{C}$  (Figure 23) implies a relatively low temperature zone. Further to the east, slightly higher estimates of  $705^{\circ}\text{C}$  to  $874^{\circ}\text{C}$  suggest an increase in the thermal gradient. However, the somewhat erratic pressure distribution, in particular for adjacent sample localities, suggests that a systematic pressure gradient is not present. In the Lake Melville Terrane, some of the apparent anomalous temperature and pressure estimates may be a result of local thermal highs adjacent to large intrusive bodies. However, the rather erratic distribution of the estimates suggests that this is not the major cause of the large P-T variation.

(2) When applying geothermometers and geobarometers together, the sensitivity of the two general types of reactions: exchange reactions (for temperature) and net transfer reactions (for pressure) to changes in P-T conditions, must be considered. The assumption made when applying both exchange and net transfer reactions to geothermobarometric studies in metamorphic terranes is that both types of reactions closed and thus record at the same P and T conditions. Ellis and Green (1985) studied various exchange and net transfer reaction thermobarometers in mafic granulites from Enderby Land, Antarctica and concluded that closure temperatures for re-equilibration are lower for transfer reactions than for exchange reactions. The results in Figure 25, may similarly be interpreted to

imply that re-equilibration conditions for different mineral equilibria are different. In general, mafic assemblages in both terranes yield higher metamorphic conditions than those recorded by paragneiss assemblages. This distribution suggests that closure conditions for opx-cpx-plagioclase assemblages in mafic rocks are higher than the closure conditions for garnet-plagioclase-biotite assemblages. Although different closure conditions may explain the variable range of estimates obtained from mafic and paragneiss assemblages, they do not explain the variation between estimates obtained from the same assemblage.

(3) Large discrepancies in calculated estimates may be a result of the propagation of errors associated with the calibration of geothermobarometers. In general, errors in the determination of thermodynamic parameters of end-member equilibria, in addition to analytical uncertainty, result in errors on the order of  $\pm 50^{\circ}\text{C}$  and  $\pm 70^{\circ}\text{C}$  (Ferry and Spear, 1978) for garnet - biotite and pyroxene thermometers (Ellis and Green, 1979), respectively. Errors arising from the calibration of garnet - plagioclase -  $\text{Al}_2\text{SiO}_5$  - quartz and garnet - plagioclase - orthopyroxene - clinopyroxene - quartz barometers are on the order of 1 to 1.5 kbar (Newton and Haselton, 1981 and Newton and Perkins, 1982). However, since these formulation errors associated with thermobarometers would apply to estimates in both terranes, then any inaccuracies of the pressures and temperatures would be relative and thus would not explain the large variation in recorded pressures and temperatures between the two terranes.

(4) Many applications of element partitioning geothermometers and

geobarometers have been aimed at estimating "peak" metamorphic pressures and temperatures. However, many thermobarometers are susceptible to retrograde re-equilibration during uplift and subsequent cooling (Bohlen and Essene, 1980). Hodges and Royden (1984) suggested that if different samples from a single metamorphic terrane equilibrated at different times during uplift then empirically derived P-T estimates would reflect this as a range of pressure and temperature estimates in P-T space (P-T-t path). Thus the apparent anomalous "spread" of estimates in both terranes may be a reflection of variable equilibration conditions during uplift and subsequent cooling. To further examine this possibility, an attempt is made in this study to construct equilibrium P-T curves for both the Groswater Bay and Lake Melville Terranes on the basis of geothermometry and geobarometry estimates.

#### 5.4.4 Equilibrium P-T Paths

On the basis of the distribution of geothermobarometry estimates, two separate equilibrium P-T paths have been constructed. An assumption made is that the highest pressure and temperature estimates recorded in both terranes represent peak metamorphic conditions during the Grenvillian Orogeny. The P-T estimates in both the Groswater Bay and Lake Melville Terranes define trends in P-T space, and it is interpreted that the paths in Figure 25 reflect a portion of the P-T trajectory assumed by the Sandwich Bay area during uplift. This interpretation is based on the data presented and can be defended on the following grounds:

(1) the variation in pressures and temperatures is probably not due to metamorphic gradients within each terrane, nor to inaccuracies in the calibrations used (Section 5.4.3);

(2) there is no evidence that the scatter in P-T estimates reflects disequilibrium in the majority of samples, as discussed in Section 4.3.3;

(3) graphical analyses of phase equilibria in both the Groswater Bay and Lake Melville Terranes (Figure 27a and 27b) strongly suggest that paragneiss samples did not finally equilibrate under uniform pressure and temperature, a conclusion which is consistent with the P-T variation recorded in both terranes;

(4) calculated pressures and temperatures are in excellent agreement with experimentally determined stability fields (Section 5.3.4);

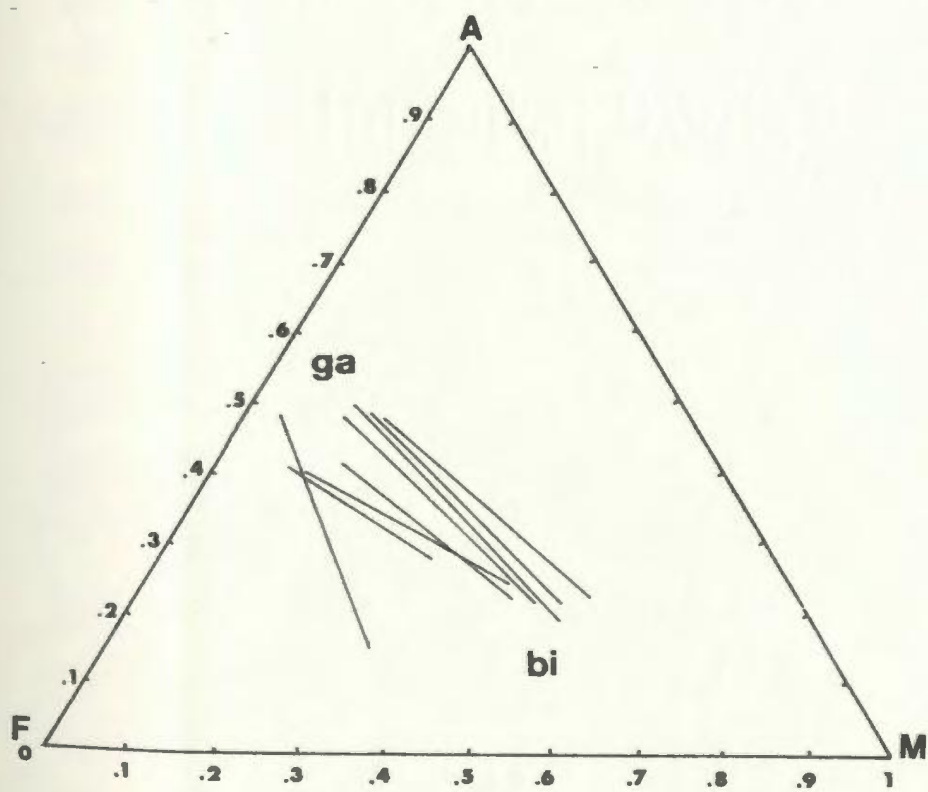
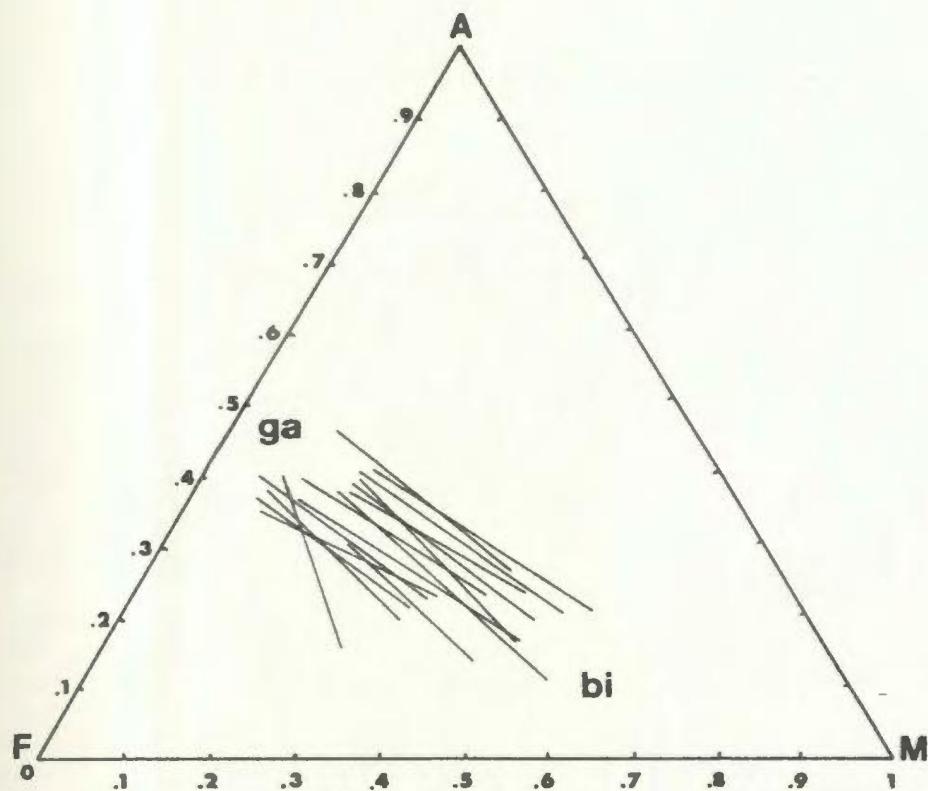
(5) since there is evidence that subsequent to the metamorphic peak, the terranes were subjected to retrograde metamorphism during uplift (Section 4.3.3), the range of pressure and temperature estimates in both terranes may be a result of different samples equilibrating at different times during metamorphic uplift.

On the basis of these observations it is suggested that the range of P-T estimates exhibited by the samples is a reflection of similar equilibria "blocking" at different times and/or temperatures and pressures during Grenvillian uplift and cooling.

To keep a consistent data set, only paragneiss samples, containing the assemblage garnet + biotite + kyanite/sillimanite + plagioclase were applied. The omission of mafic equilibria in this construction prevents any inconsistencies which may arise from differences in

Figure 27a: APM plot projected through K feldspar for  
garnet-biotite-sillimanite bearing paragneiss in the Lake Melville  
Terrane.

Figure 27b: APM plot projected through K feldspar for  
garnet-biotite-kyanite bearing paragneiss in the Groswater Bay  
Terrane.



blocking temperatures between paragneiss and mafic assemblages. In order to construct reasonable equilibrium P-T curves for each terrane, some of the more anomalous estimates have been omitted. The basis for omission is that the majority of samples which fall at the extremes of the P-T point clusters in Figure 25, exhibit the highest potential for textural disequilibrium. Whereas this is evidently a subjective criterion, the omission of "anomalous" samples in the construction of equilibrium P-T paths is nonetheless not entirely arbitrary.

On the basis of the criteria discussed above, Figure 28 shows the suggested equilibrium pressure-temperature paths for both the Groswater Bay and Lake Melville Terranes. The P-T curve constructed from the Groswater Bay Terrane samples demonstrates a nearly isothermal uplift path during which decompression from ca. 40 km to 30 km was accompanied by only ca. 100°C cooling. This steep portion of the P-T curve suggests that during early uplift, decompression was accompanied by only ca. 100°C cooling, and that major cooling of the Groswater Bay Terrane did not occur until the later stages of uplift (i.e. above about 30 km).

The wide range of pressure and temperature estimates in the Lake Melville Terrane prohibits the assignment of all of these estimates to one specific equilibrium P-T path. With the exception of one potential disequilibrium sample, all of the calculated pressure and temperature estimates are derived from samples which appear to be both texturally and chemically in equilibrium. Thus with the exception of one estimate, none of the pressures and temperatures can be discounted from a potential P-T path. A possible interpretation to



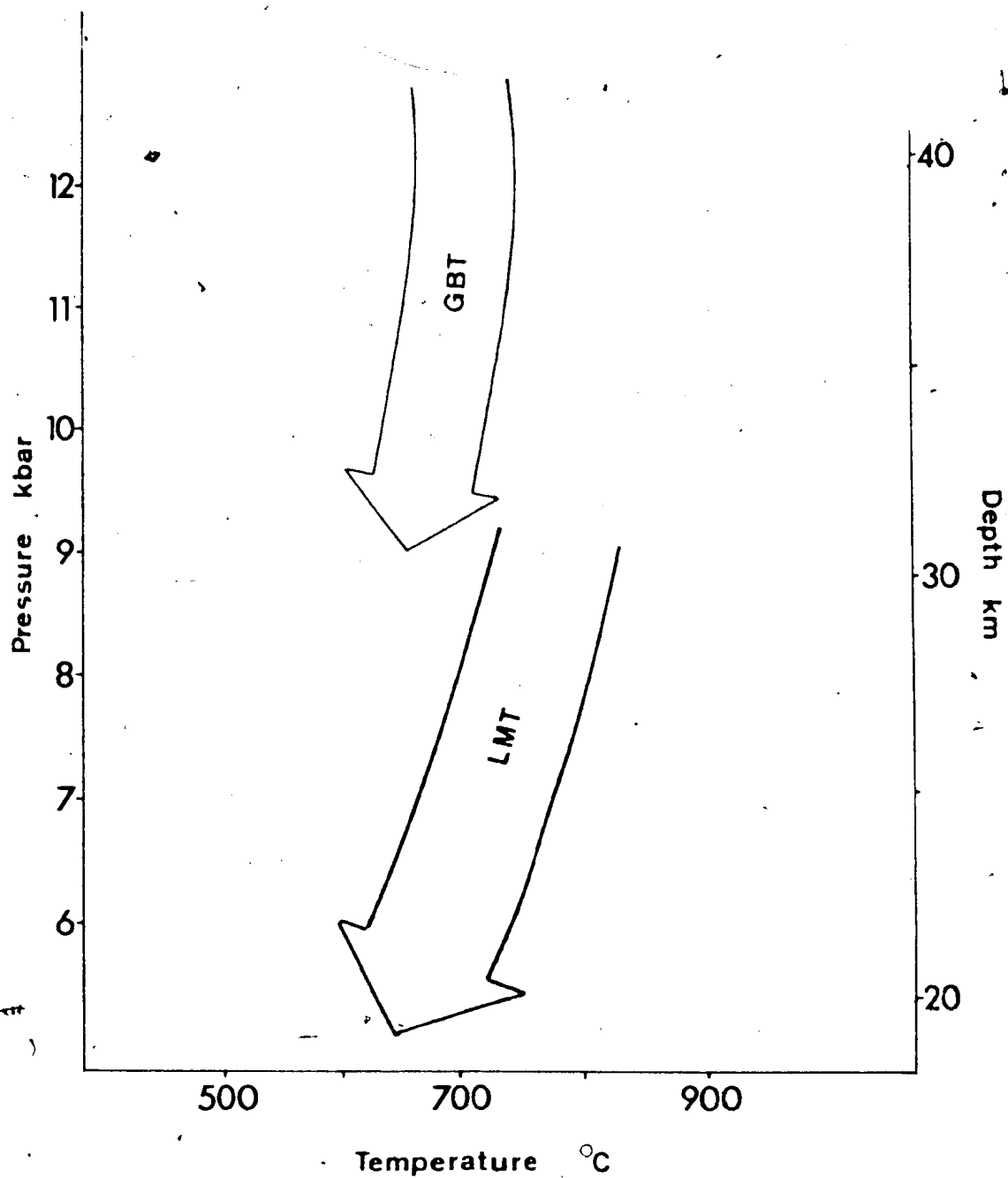


Figure 28. Equilibrium pressure-temperature paths for the Groswater Bay Terrane (GBT) and the Lake Melville Terrane (LMT).

consider is that a P-T "belt" may be constructed which encompasses the entire range of estimates, as shown in Figure 28. In this case a similar, near isothermal uplift trajectory is constructed, which suggests that ca. 4 kbar of decompression was accompanied by only about 100°C cooling, similar to the Groswater Bay Terrane. The lack of time constraints with respect to initiation and termination of uplift prevents any interpretation of possible uplift rates. However, although the uplift trajectories of the two terranes are highly speculative, the results demonstrate that the Grenvillian Orogeny resulted in significant crustal thickening. The near isothermal nature of the uplift paths implies that thickening of the crust occurred by thrusting as opposed to addition of magma in the lower crust.

In summary, the results of the geothermobarometry estimates reveal a distinct contrast in metamorphic conditions between the Groswater Bay and Lake Melville Terranes. Temperatures on the order of 630°C to 950°C in each terrane imply a negligible thermal gradient across the Rigolet thrust zone, whereas pressures on the order of 10-12 kbar and 6-10 kbar in the Groswater Bay and Lake Melville Terranes, respectively, suggest a sharp pressure gradient. However, the respective pressure ranges implying derivation from depths on the order of 28-35 km for the Groswater Bay Terrane and 18-28 km for the Lake Melville Terrane disagree with the presently accepted regional tectono-metamorphic framework which proposes that the Lake Melville Terrane represents a deep-seated allochthon which was juxtaposed against higher crustal assemblages in the Groswater Bay Terrane. This discrepancy suggests that P-T estimates recorded in the two terranes

reflect post-emplacement metamorphic conditions and not the depths from which they were derived. However, the effect of initial differences in crustal thicknesses of the two terranes prior to or during emplacement and the effect of metamorphic closure conditions on recorded pressures and temperatures for rocks buried at different crustal levels may also be partially responsible for the contrast in metamorphic pressures.

The range of temperatures and pressures within each terrane is interpreted to be predominantly a reflection of the re-equilibration of samples at different stages during Grenvillian uplift and subsequent cooling. The range of estimates thus represents a portion of the equilibrium P-T trajectory of the two terranes during uplift. The path from the Groswater Bay Terrane samples suggest near isothermal cooling, with only minor temperature change (ca.  $100^{\circ}\text{C}$ ) during uplift from approximately 40 km to 30 km. A similar P-T path constructed for the Lake Melville Terrane implies that decompression of ca. 4 kbar was accompanied by ca.  $100^{\circ}\text{C}$  cooling. These results imply that crustal thickening during the Grenvillian Orogeny occurred by thrusting as opposed to magma addition at lower crustal levels, which supports the regional structural framework of transport by regional thrusting of the Lake Melville Terrane over the Groswater Bay Terrane.

## CHAPTER 6

 $^{40}\text{Ar}/^{39}\text{Ar}$  DATING6.1 Introduction

The  $^{40}\text{Ar}/^{39}\text{Ar}$  dating technique is a recently developed variation based on the conventional K/Ar method. First described by Sigurgeirsson (1962) and more fully discussed by Merrihue and Turner (1966) and Mitchell (1968), the  $^{40}\text{Ar}/^{39}\text{Ar}$  method can overcome some of the limitations posed by the K/Ar method, since it is possible to distinguish between; (1) samples which have remained closed systems with respect to potassium and argon since initial closure; (2) samples which contain a component of extraneous non-atmospheric argon of  $^{40}\text{Ar}/^{39}\text{Ar}$  ratio in addition to radiogenic argon; and (3) samples which have undergone a post-crystallization thermal event and thus lost a component of their original argon. The additional capabilities of the  $^{40}\text{Ar}/^{39}\text{Ar}$  method are often very advantageous when dealing with metamorphic terranes with complex thermal histories.

The primary difference between K/Ar and  $^{40}\text{Ar}/^{39}\text{Ar}$  geochronology is that in the latter method, no direct chemical analysis of potassium is required. The amount of potassium is calculated indirectly from measurements of the amount of  $^{39}\text{Ar}$  which is produced from  $^{39}\text{K}$  by neutron activation. The ratio of the radiogenic  $^{40}\text{Ar}$  to neutron bombardment induced  $^{39}\text{Ar}$  is required for age determinations. This is of advantage because mass spectrometers can measure isotopic ratios very precisely, but absolute abundances are less easily determined.

However, the greatest potential of the  $^{40}\text{Ar}/^{39}\text{Ar}$  technique is

through the subsequent incremental (step-wise) heating method of treating irradiated samples. In this method, first described by Merrihue and Turner (1966) the sample is gradually heated through a number of temperature increments chosen by the operator, after each of which the argon is released into the mass spectrometer and analyzed isotopically for its  $^{40}\text{Ar}/^{39}\text{Ar}$  ratio, from which an age may be calculated. A series of ages, each corresponding to a different temperature fraction is thus generated for an individual sample. These incremental ages are plotted as a function of temperature (expressed as an accumulative percent of  $^{39}\text{Ar}$  released) giving an age spectrum for the sample. Such age spectra allow the evaluation of the behaviour of argon within the mineral samples and therefore permit a more thorough understanding of the significance of the results than can be obtained from conventional K/Ar dating.

## 6.2 Previous Geochronology

Previously reported radiometric dates in the Grenville Province of eastern Labrador are shown in Figures 29 and 30, after Gower and Ryan (1986). Figure 30 is a compilation of U-Pb, Rb-Sr and Nd-Sm ages which date pre-Grenvillian events, including Lower Proterozoic (1700 to 1900 Ma) ages in the Makkovik subprovince, Middle Proterozoic (1600 to 1650 Ma) ages which represent the newly defined Labradorian Orogeny and various post-orogenic plutons ranging from 1500 to 1270 Ma.

Figure 29 shows previous K-Ar and  $^{40}\text{Ar}/^{39}\text{Ar}$  dates which record pre-Grenvillian (Labradorian and Makkovikian) ages north of the

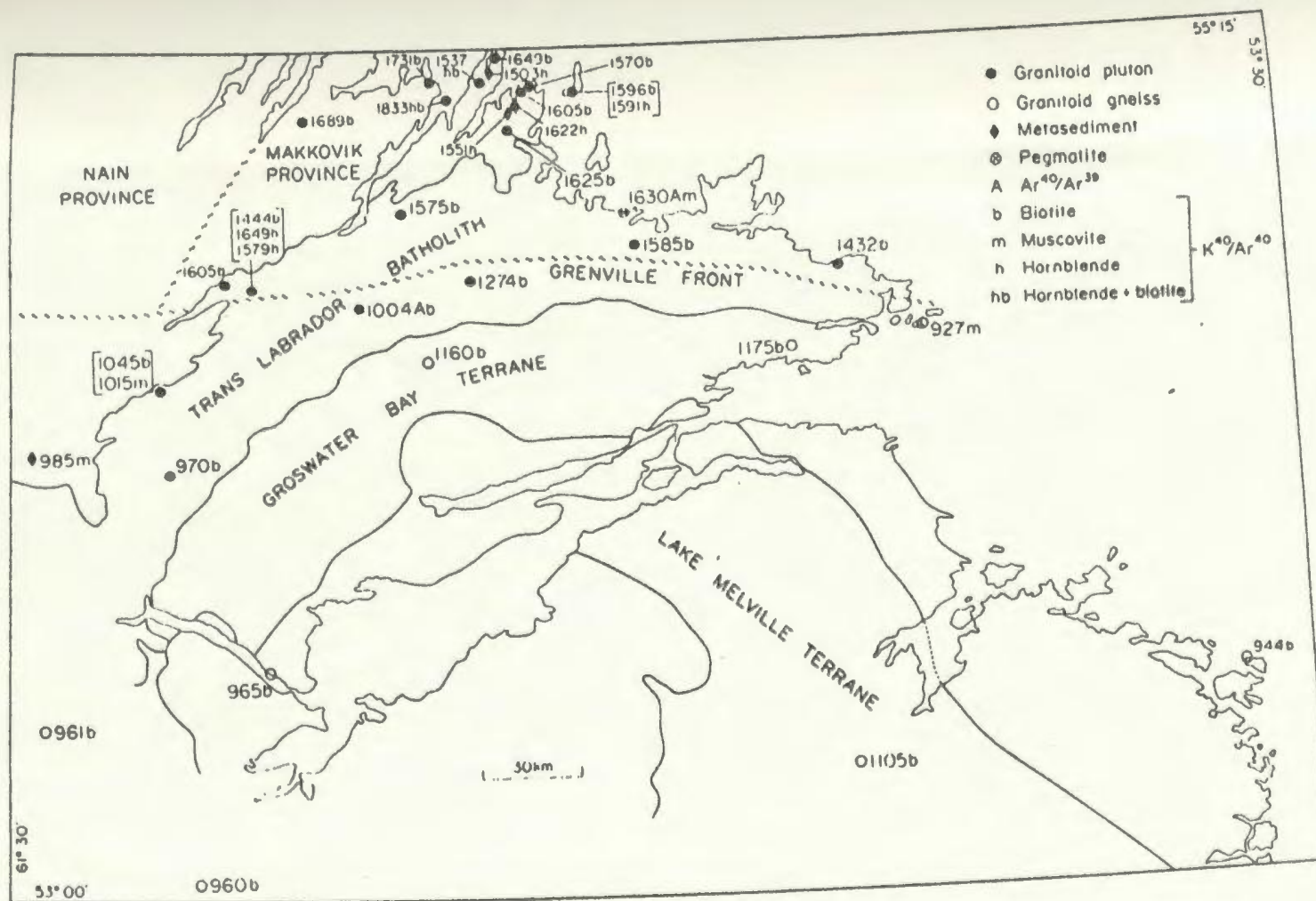


Figure 29.  $^{40}\text{Ar}/^{39}\text{Ar}$  and K/Ar dates in eastern Labrador, after Gower and Ryan (1986).

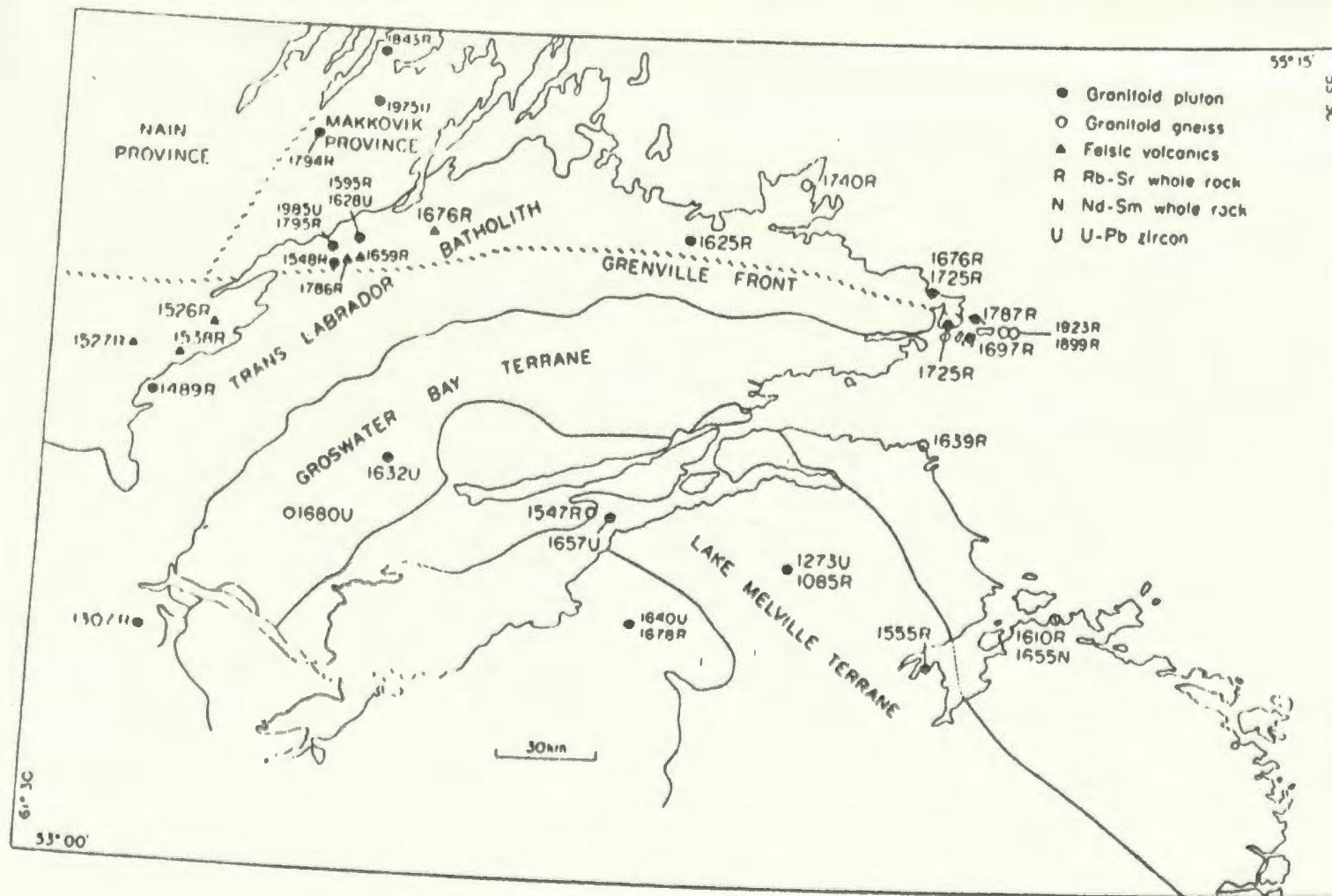


Figure 30. Rb/Sr, Nd/Sm and U/Pb dates in eastern Labrador, after Gower and Ryan (1986).

Grenville Front Zone. South of the Grenville Front, which marks the northern limit of  $950 \pm 75$  Ma K/Ar ages (Gower et al., 1982), ages ranging from 1200 to 950 Ma are recorded. Post-Grenvillian K-Ar ages of circa 550 Ma are recorded for lower Phanerozoic diabase dikes which are related to the development of the Sandwich Bay graben (Gower et al., 1983a, 1985 and 1986).

In the Smokey area (Figure 29) approximately 100 km to the north of the study area, K-Ar whole-rock ages of the Michael gabbro of 1348 Ma and 1325 Ma have been reported by Wanless et al. (1972, 1973), and are interpreted to date the intrusion of this unit by Enslie (1983).

U-Pb dates on zircon, titanite and monazite in the Groswater Bay and Lake Melville Terranes in eastern Labrador have recently been reported by Schärer et al. (1986). U/Pb zircon dates record similar 1600 to 1650 Ma concordant ages for both the Groswater Bay and Lake Melville Terranes, indicating that both have experienced Labradorian plutonism and metamorphism. However, these authors show that analyses of titanite and monazite yield ages of 940 to 970 Ma in the Groswater Bay Terrane and 1026 to 1038 Ma in the Lake Melville Terrane (concordant with U/Pb zircon lower intercepts on concordia.) The implication of these ages is that the culmination of Grenvillian anatexis and metamorphism in the Groswater Bay Terrane was attained approximately 60 Ma later than in the Lake Melville Terrane.

Within the study area, two K-Ar analyses of biotite from the Groswater Bay and Lake Melville Terranes yield ages of 944 Ma and 1105 Ma, respectively (Wanless et al., 1970). The age from the Groswater Bay Terrane may date closure of the biotite lattice to argon during post-Grenvillian uplift and cooling. The K/Ar age from



the Lake Melville Terrane, however, is not compatible with the interpretation of the onset of the culmination of Grenvillian metamorphism at circa 1030 Ma. Since the latter age is not in accord with available U/Pb ages, which are considered more reliable, both K/Ar ages should be interpreted with caution.

### 6.3 $^{40}\text{Ar}/^{39}\text{Ar}$ Problem

In recent years, radiometric age dating in polyorogenic terranes has proved to be an invaluable analytical tool in determining the timing of metamorphic events. With the advent of U/Pb, Nd/Sm and other dating techniques, it has become possible in some cases to determine not only the age of the last metamorphic episode, but also to "see through" that event to earlier stages of a rock's history. With respect to  $^{40}\text{Ar}/^{39}\text{Ar}$  dating, the following events in a rock's history may in favourable cases be determined: (1) the absolute timing of a metamorphic event, which could only be determined if uplift was very rapid; (2) the timing of post-metamorphic uplift and cooling; (3) distinction between those samples which contain extraneous argon components and those which do not; and (4) the recognition of thermally overprinted samples which have been partially degassed as a result of geologic reheating.

Application of the  $^{40}\text{Ar}/^{39}\text{Ar}$  method in eastern Labrador was intended to answer the following question: is there a difference in the Grenvillian metamorphic imprint between the Groswater Bay and Lake Melville Terranes? With the distinction of the two lithotectonic terranes in eastern Labrador, which exhibit contrasting

- lithologic, structural and metamorphic characteristics in addition to a prolonged tectonometamorphic history, there is clearly an opportunity to apply and evaluate the potential of the  $^{40}\text{Ar}/^{39}\text{Ar}$  method in a polyorogenic terrane.

Seven hornblende-bearing samples were collected from the Sandwich Bay area in eastern Labrador; three from the Groswater Bay Terrane and four from the Lake Melville Terrane (Table 5)

#### 6.4 $^{40}\text{Ar}/^{39}\text{Ar}$ Results

##### 6.4.1 Introduction

$^{40}\text{Ar}$ - $^{39}\text{Ar}$  incremental release ages have been determined for seven hornblende concentrates separated from rocks collected from the Groswater Bay and Lake Melville Terranes. Results of analyses are presented in Table 6 and shown as age spectra in Figure 31. The majority of samples analyzed, record internally discordant age spectra, generally with anomalous ages recorded in the low temperature fractions. As a result, several of the total gas ages are meaningless. However, plateau ages can be calculated for some of the spectra. A plateau age is defined as the apparent age recorded from that portion of a spectrum in which contiguous gas fractions (together constituting more than 50% of all the gas evolved from a sample) have apparent ages which are not different at a two sigma level of uncertainty (Fleck et al., 1977). Plateau data were averaged by calculating a weighted mean (with respect to the % of gas released), in which each datum was weighted by the the inverse of its variance. Where the variance is expressed as:

Table 5. Lithologies used in  $^{40}\text{Ar}/^{39}\text{Ar}$  analyses.Groswater Bay Terrane

- VAN84-17D: deformed fine-grained amphibolite dike which intrudes well banded tonalitic gneiss, Double Islands.
- VAN84-18A: well banded hornblende - biotite quartz diorite gneiss, Hare Harbour.
- VAN84-14B: fine-grained amphibolite dike which intrudes hornblende - biotite quartz diorite orthogneiss, East Arm, Sandwich Bay

Lake Melville Terrane

- VAN84-32A: medium grained hornblende - biotite quartz diorite orthogneiss, south end of Sandwich Bay.
- VAN84-23B: fine-grained amphibolite dike which intrudes migmatitic biotite - hornblende granodiorite to quartz diorite orthogneiss, upper Eagle River.
- VAN84-22B: fine-grained amphibolite enclave within fine-grained biotite - hornblende granodiorite orthogneiss, Second Choice Lake.
- VAN84-21A: fine-grained biotite - hornblende granodiorite orthogneiss, west of Camel Lake.

Table 6.  $^{40}\text{Ar}/^{39}\text{Ar}$  Analytical Data

TEMP(°C)	mv Ar39	% Ar39	$^{40}\text{Ar}/^{39}\text{Ar}$	AGE (Ma)	% ATMOS.	$^{37}\text{Ar}/^{39}\text{Ar}$	% I.I.C.
<u>VAN84-17D</u>							
350-850	10.6	2	1815.3	3287 +/-12	11.4	2.1	.1
850-900	5.7	1	579.9	1733 +/-15	14.8	6.2	.4
900-950	74.7	14.2	369.1	1268 +/- 3	3.2	4.4	.3
950-980	76.6	14.5	359.3	1243 +/- 2	2.2	3.9	.3
980-1010	132.2	25.1	353.7	1229 +/- 5	4.9	3.8	.3
1010-1040	175	33.2	365.3	1258 +/- 5	5.1	3.7	.3
1040-1100	35	6.6	-	0 +/- 0	0	0	0
1100-1125	6.2	1.1	380.2	1295 +/-12	12.2	4.8	.4
1125-1180	1.8	1.8	389.2	1312 +/-22	21.9	5.1	.4

\*1337 +/- 6

\*\*1260 +/- 6

VAN84-18A

300-850	184.3	25	787.6	2100 +/- 5	2.7	.4	0
850-900	113.5	15.4	758.9	2054 +/- 5	2.2	1.7	.1
900-950	234.6	31.8	579.1	1731 +/- 3	1.2	2.4	.1
950-1000	153	20.8	529.1	1631 +/- 5	1.1	3	.2
1000-1030	28.2	3.8	519.2	1610 +/- 5	3.4	3.4	.2
1030-1060	12.3	1.6	494.8	1559 +/- 5	7.4	4.3	.3
1060-1110	6.1	.8	466.3	1496 +/- 9	15.5	5.2	.4
1110-1160	3.5	.4	455.5	1472 +/-12	36.1	8.6	.6

\*1853 +/-12

VAN84-14B

200-850	5.6	2.3	273.6	1012 +/-32	74.2	4.3	.3
850-900	4.9	2	400.8	1346 +/-12	34.8	4	.3
900-950	44.8	18.4	390.1	1319 +/- 2	3.9	4.1	.3
950-980	50.8	20.9	412.1	1373 +/- 3	2.5	4.4	.3
980-1010	69.4	28.5	427.3	1408 +/- 3	.9	4.5	.3
1010-1040	48.6	19.9	439.7	1437 +/- 2	1.6	4.6	.3
1040-1070	14.3	5.8	432.2	1420 +/-10	9.2	4.7	.3
1070-1100	3.5	1.4	415.4	1380 +/-28	27.5	5.4	.4
1100-1150	1	.4	-	0 +/- 0	0	0	0

\*1382 +/- 8

TEMP(°C)   mv Ar39   % Ar39    $^{40}\text{Ar}/^{39}\text{Ar}$    AGE (Ma)   % ATMOS   Ar37/Ar39   % I.I.C.

VAN84-23B

200-850	12	3	429.2	1412 +/-353	28	1.6	.1
850-900	6	1.5	341.6	1198 +/-135	25.6	1	0
900-950	18	4.5	344.5	1205 +/- 29	8.4	2.8	.2
950-980	32	8.1	321.4	1145 +/- 31	4.4	3.6	.3
980-1010	54.1	13.7	298.5	1083 +/- 2	2.4	3.8	.3
1010-1040	141	35.9	294.2	1071 +/- 4	4.1	3.8	.3
1040-1070	93.5	23.8	311.6	1119 +/- 10	2.3	3.8	.3
1070-1100	8.8	2.2	316.6	1132 +/- 24	13.3	3.9	.3
1100-1180	27	6.8	323.2	1150 +/- 22	6	4.1	.3

\*1116 +/- 50

\*\*1070 +/- 50

VAN84-22B

300-850	5.5	1.8	223.4	863 +/-20	66.1	2.8	.2
850-900	2.5	.8	270.7	1005 +/-40	55.6	2.5	.2
900-950	21.7	7.3	279.4	1030 +/- 2	7.7	3.7	.3
950-970	35	11.7	277.2	1023 +/- 2	4.2	4	.3
970-990	46.5	15.6	275.9	1019 +/- 2	2.6	4	.3
990-1010	71.3	24	277.5	1024 +/- 2	1.7	4	.3
1010-1030	69.2	23.3	277.6	1024 +/- 3	2.5	4	.3
1030-1050	20.3	6.8	277.1	1023 +/- 6	6.1	4	.3
1050-1100	13	4.4	278.5	1027 +/- 3	11.2	4.2	.3
1100-1150	11.6	3.9	279.0	1028 +/- 5	15.4	4.3	.3

\*1020 +/- 5

VAN84-32A

300-850	5.8	2	297.7	1080 +/-12	51.6	3.1	.2
850-900	3.3	1.1	343.0	1202 +/-31	49.9	4.5	.3
900-950	41	14.3	360.5	1247 +/- 2	3.9	3.6	.3
950-980	72	25.1	358.9	1243 +/- 3	1.5	3.6	.3
980-1000	70.8	24.7	359.5	1244 +/- 2	1.5	3.7	.3
1000-1020	66.4	23.1	360.7	1247 +/- 2	2.4	3.7	.3
1020-1040	9.2	3.2	363.6	1254 +/- 5	5.1	3.8	.3
1040-1060	4.6	1.6	363.1	1253 +/- 9	15.5	3.9	.3
1060-1130	13.2	4.6	360.2	1246 +/- 3	10.5	5.1	.4

\*1241 +/- 3

TEMP(°C)   mv Ar39   % Ar39    $^{40}\text{Ar}/^{39}\text{Ar}$    AGE (Ma)   % ATMOS.   Ar37/Ar39   % I.I.C

VAN84-21A

300-850	11.1	2.8	277.9	1025 +/- 8	42.9	1.3	.1
850-900	22.6	5.8	272.2	1009 +/- 3	15.2	2.9	.2
900-950	168.6	43.6	261.6	978 +/- 2	2.3	3.3	.3
950-980	97.7	25.3	261.0	976 +/- 2	3.1	3.4	.3
980-1010	61.8	16	263.1	983 +/- 2	3.4	3.4	.3
1010-1040	13.9	3.6	264.8	987 +/- 3	7.7	3.5	.3
1040-1100	8.3	2.1	239.3	992 +/- 5	16.2	3.7	.3
1100-1150	2	.5	-	0 +/- 0	0	0	0

\*982 +/- 3

\*\*980 +/- 3

% ATMOS. - Atmospheric  $^{40}\text{Ar}$ .

% I.I.C. - Interfering Isotope Correction Factor  
Estimates at One Sigma Level.

mv Ar39 - millivolts of Ar39.

\* - Total Gas Age (Ma).

\*\* - Plateau Age (Ma) Based on 50% or more of total gas at a two sigma level.

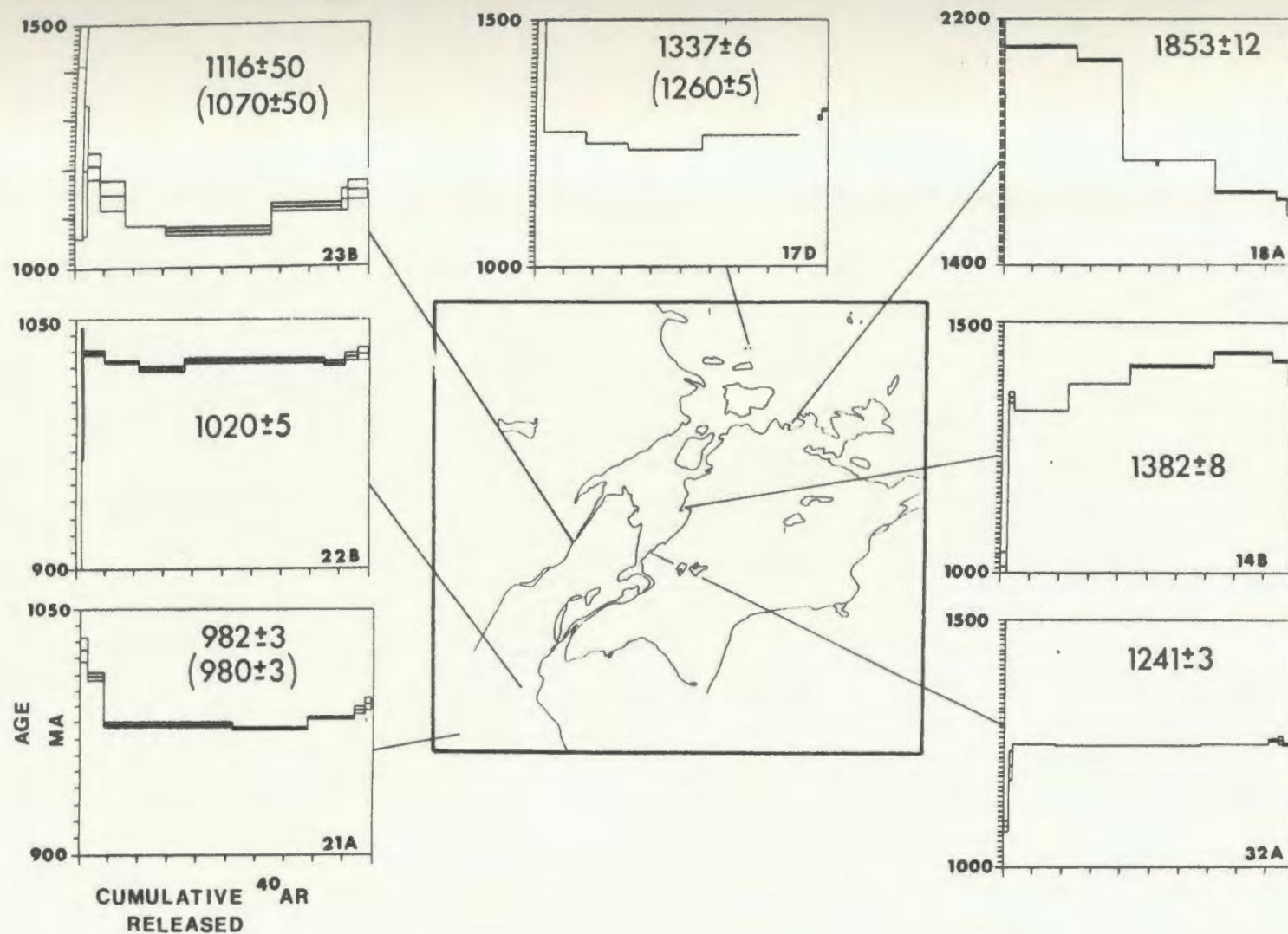


Figure 31. Distribution of  $^{40}\text{Ar}/^{39}\text{Ar}$  spectra in the Sandwich Bay area. Total gas ages without parentheses, plateau ages with parentheses.



$$\sum_{i=1}^n (X_i - \bar{X})^2 = (X_i - \bar{X})^2 / (n-1)$$

where  $X_i$  = increment age

$\bar{X}$  = average mean

$n$  = number of ages used in mean calculation.

The weighted mean is preferred since it takes into consideration the quantity of gas evolved in each increment. (Dalrymple and Lanphere, 1974). The plateau ages are taken to be the best approximation of the time of cooling through the argon closure temperature for hornblende. For the slow cooling rates generally encountered in regional metamorphic terranes the closure temperature for hornblende is 480°C to 500°C (Harrison 1981).

In this section an attempt is made to interpret the  $^{40}\text{Ar}/^{39}\text{Ar}$  results in terms of the presence of excess argon components and the timing of resetting episodes.

#### 6.4.2 $^{40}\text{Ar}/^{39}\text{Ar}$ Spectra in the Groswater Bay Terrane

Two samples of amphibolite dike and one sample of a hornblende bearing orthogneiss collected from the Groswater Bay Terrane were dated. All samples record a discordant age spectra. Since each sample exhibits a different type of age spectrum, they will now be considered individually.

VAN84-17D was collected from a relatively undeformed amphibolite dike, which intrudes strongly deformed, well banded orthogneiss. A hornblende concentrate prepared from this sample yields a discordant



age spectrum in which an anomalously high age is recorded in the low temperature increment (350°C-850°C) with a slightly saddle-shaped spectrum in intermediate temperature increments (Figure 31). The high age recorded in the first heating increment is the "classic" signature of excess (non-radiogenic) argon and suggests the presence of loosely bounded excess  $^{40}\text{Ar}$  located in hornblende sites with relatively low activation energies, since the excess components are liberated at low experimental temperatures. The rapid and systematic age decrease in the low temperature increments implies that the excess  $^{40}\text{Ar}$  components are mainly concentrated in the margins of hornblende grains and that the ratio of excess / radiogenic  $^{40}\text{Ar}$  decreases rapidly to insignificant levels in the grain interior. Harrison and McDougall (1981) considered that this type of profile developed when excess argon components diffused from an intergranular vapour phase into hornblende crystals after they had cooled below intercrystalline retention temperatures. Since excess argon is interpreted to be present, the total gas age of  $1337 \pm 6$  Ma recorded by the spectrum is geologically meaningless. However, since 80% of the gas evolved from the sample record, apparent ages which are not different at a two sigma level of uncertainty, a relatively well defined plateau age of  $1260 \pm 5$  Ma is interpreted. The wide saddle-shaped spectrum recorded in the intermediate temperature fractions suggests that the system has experienced a partial gas loss as a result of a thermal resetting event at about 1260 Ma.

VAN84-18A, was collected from a moderately foliated hornblende - biotite quartz diorite. A hornblende concentrate prepared from this sample displays a very discordant  $^{40}\text{Ar}/^{39}\text{Ar}$  age spectrum (Figure 31),

which records a systematic decrease in age throughout the entire heating analyses. Similar patterns of discordance in hornblende age spectra have been interpreted by Dallmeyer (1975) and Harrison and McDougall (1981), who considered that the systematic age decrease at higher temperatures reflects the presence of excess  $^{40}\text{Ar}$  components relative to radiogenic  $^{40}\text{Ar}$  in both grain margins and interiors. The total gas age of  $1853 \pm 12$  Ma, for VAN84-18A is therefore considered to be a result of radiogenic and non-radiogenic argon and thus geologically meaningless. In addition, the highly discordant spectrum prevents any interpretation of crystallization or post-crystallization events.

VAN84-14B was collected from a moderately deformed amphibolite dike which intrudes the Earl Island quartz diorite unit (Gower et al., 1981, 1984). This sample yields a discordant spectrum which records a total gas age of  $1382 \pm 8$  Ma. The low temperature increment ( $200^\circ\text{C}$ - $850^\circ\text{C}$ ) records an age of 1012 Ma. Ages systematically increase in the intermediate temperature increments and appear to level out to about 1400 Ma in the high temperature fractions (Figure 31). The regular increase in apparent age from low to high temperature fractions may be interpreted as a result of a thermal overprint, in which the outer part of the grains (i.e. early release increments) are more strongly affected than the more tightly bound gas in the grain interiors. The low temperature fraction age may be a reflection of a Grenvillian overprint at 1012 Ma, with the increasing ages in the intermediate fractions suggesting a decrease in the Grenvillian thermal overprint. The apparent levelling off of the spectrum at about 1400 Ma may indicate that the high temperature

fractions of gas were not affected by Grenvillian overprinting and that this age approaches the time of crystallization of hornblende in this rock or the time at which hornblende cooled through the blocking temperature.

#### 6.4.3 $^{40}\text{Ar}/^{39}\text{Ar}$ Spectra in the Lake Melville Terrane

The four samples collected from the Lake Melville Terrane yield more consistent results than those from the Groswater Bay Terrane. Three of the samples (VAN84-21A, 22B and 32A) record very well defined age spectra, yielding total gas ages ranging from 982 to 1241 Ma; the fourth (VAN84-23B) has a disturbed spectrum but yields a total gas age in the same range (Figure 31).

VAN84-23B was collected from a concordant amphibolite dike, which intrudes a well-banded migmatitic granodiorite orthogneiss. The sample yields a discordant age spectrum in which an anomalously old age of  $1412 \pm 353$  Ma is recorded in the low temperature increment (200-850°C), and a saddle-shaped pattern is displayed in the intermediate fractions. The systematic decrease in ages in the low temperature fractions implies the presence of excess argon components in the grain margins with less significant levels in the grain interiors. The saddle-shaped spectrum is interpreted to record a partial loss of radiogenic  $^{40}\text{Ar}$  as a result of a post crystallization event. The plateau defined by 70 % of the total gas in the intermediate fractions suggests a closure of the argon in hornblende at ca. 1070 Ma (Figure 31).

VAN84-22B, which was collected from an amphibolite enclave within

a granodiorite orthogneiss, records a well defined age spectrum yielding a total gas age of 1020 Ma. An anomalously low age of 860 Ma is recorded in the low temperature increment (300-850°C); however, this fraction represents only 2 % of the total gas liberated. The remaining gas released records an essentially undisturbed spectrum and the 1020 Ma age is interpreted to represent the "true age" at which the hornblende lattice began to retain radiogenic argon (i.e. at a temperature of approximately 500°C).

A similar spectrum is displayed by VAN84-32A, which was collected from a moderately deformed quartz diorite, in which the low temperature fraction (300°C-850°C) yields an age of 1080 +/- 12 Ma, representing only 2% of the total gas released, thus no significance can be placed on this age. With the exception of this increment, a very well defined, undisturbed age spectrum is recorded, yielding a plateau age of 1241 +/- 3 Ma. This age is similarly interpreted to represent the true age of argon retention in the hornblende lattice.

VAN84-21A, which was collected from a strongly foliated granodiorite gneiss, records a reasonably well defined plateau, with the development of a shallow "saddle" in the intermediate temperature fractions. This pattern is interpreted to be the result of a combination of excess argon along the grain margin (i.e. low temperature increments) and a partial gas loss due to a thermal resetting, resulting in the saddle-shaped spectrum. However, the excess argon accounts for less than 10 % of the total gas released, and therefore a concordant plateau defined by 80 % of the total gas is recorded. The similarity of the total gas age (982 Ma) and the plateau age (980 Ma) coupled with the shallow saddle-shaped spectrum

in the intermediate fractions, suggests a retention of radiogenic argon in hornblende took place at ca. 980 Ma.

## 6.5 Interpretation of $^{40}\text{Ar}/^{39}\text{Ar}$ Results

### 6.5.1 Introduction

The main purpose of the  $^{40}\text{Ar}/^{39}\text{Ar}$  analyses was to attempt a determination of the extent of Grenvillian metamorphic effects in the Sandwich Bay area, in addition to an interpretation of the uplift and subsequent cooling histories of the Groswater Bay and Lake Melville Terranes. Of the seven hornblende concentrates analyzed, samples from the Groswater Bay Terrane yield the most discordant age spectra, interpreted to be due to a combination of excess argon components in hornblende and to a variable thermal overprint. Sample VAN84-17D, however yields a plateau (80% of total gas) age of 1260  $\pm$  5 Ma, suggesting a resetting of the argon system at this time.

In the Lake Melville Terrane the well defined plateaux displayed by 32A and 22B, record essentially undisturbed spectra, yielding plateau ages of 1241  $\pm$  3 Ma and 1020  $\pm$  5 Ma respectively.

Slightly discordant, saddle shaped spectra recorded by samples 23B and 21A suggest some subsequent gas loss after the main closure of the system yielding plateau ages of 1070 Ma and 980 Ma respectively.

In the following section the geological implications of the  $^{40}\text{Ar}/^{39}\text{Ar}$  dates in each terrane are discussed in order to assess the ages with respect to significance and timing of metamorphic and post-metamorphic events.

### 6.5.2 $^{40}\text{Ar}/^{39}\text{Ar}$ Ages in the Groswater Bay Terrane

The geological significance of the  $^{40}\text{Ar}/^{39}\text{Ar}$  results in the Groswater Bay Terrane is not immediately apparent.

Sample VAN84-18A is interpreted to contain a substantial excess argon component, whereas the spectrum in sample VAN84-14B has been disturbed by a post-closure thermal event. In both cases the total gas ages are considered to be geologically meaningless. It is unclear whether any significance should be attached to the ages derived from the highest temperature gas fractions, which in some circumstances may be used as an indication of the time of initial closure of the crystal lattice to argon. Although the spectrum in sample VAN84-17D is also discordant, a plateau defined by 80 % of the total gas in the intermediate temperature fractions, yields an age of  $1260 \pm 6$  Ma. However, the "saddle-shape" of the spectrum again indicates a post-closure thermal disturbance.

U-Pb dates on zircon, titanite and monazite, reported by Schärer et al. (1986) suggest that the two widespread thermal events which affected the Groswater Bay Terrane were the Labradorian Orogeny at about 1650 Ma and the subsequent Grenvillian Orogeny at 970 Ma. Since the discordant spectra recorded by 18A and 14B, are interpreted to be a reflection of excess argon components, a correlation with either of these two events is deemed impossible. However, sample VAN84-17D, which yielded a plateau age of  $1260 \pm 6$  Ma was collected from the same amphibolite dike dated by U/Pb methods by Schärer et al. (1986). Their sample (CG-172E), when regressed with the  $978 \pm 4$  Ma titanite

age obtained from a granodiorite to tonalite gneiss host rock, yielded an upper intercept age of  $1426 \pm 6$  Ma, interpreted to date emplacement of the gabbro. At present the implication of the of the 1260 Ma age is not understood, since it does not correspond with either of the dates obtained from U/Pb analyses. Although no other major event (thermal or cooling) on the order of 1260 Ma has previously been established, Gower and Ryan (1986) noted emplacement of the upper North River quartz syenite at 1273 Ma (Figure 29). The relationship, if any between these ages is at present unknown.

#### 6.5.3 $^{40}\text{Ar}/^{39}\text{Ar}$ Ages in the Lake Melville Terrane

Samples from the Lake Melville Terrane generally yield more internally concordant spectra than those from the Groswater Bay Terrane. Sample VAN84-32A, collected from the northern margin of the Lake Melville Terrane, displays a very well-defined total gas plateau age of  $1241 \pm 3$  Ma. The similarity of this date to the plateau age of 1260 Ma recorded by VAN84-17D in the Groswater Bay Terrane is intriguing. Furthermore, a plateau age of  $1240 \pm 17$  Ma has recently been obtained from a mafic dike in the Mealy Mountains Terrane to the west of the study area (P. Reynolds, personal communication, 1986). The similarity of these three ages suggests the existence of a widespread resetting of the argon system at about 1240 to 1260 Ma. The implications of these pre-Grenvillian ages within the study area are at present not understood. However, they suggest that these rocks remained above  $500^\circ\text{C}$ , (or cooled and were reheated above  $500^\circ\text{C}$ ), until about 1240 to 1260 Ma, and subsequently cooled below the gas

retention temperature to close the argon system in hornblende. Furthermore they imply that these rocks were not heated above 500°C during the Grenvillian Orogeny, which is in conflict with the interpretation of Grenvillian metamorphism at upper amphibolite to granulite facies.

An alternative, although intuitively less reasonable, interpretation for the pre-Grenvillian ages recorded by  $^{40}\text{Ar}/^{39}\text{Ar}$  plateaux, is that all gas fractions liberated from the samples contain the same proportion of excess  $^{40}\text{Ar}$  relative to radiogenic  $^{40}\text{Ar}$ . Pankhurst et al. (1973) and Roddick et al. (1980) have reported internally concordant  $^{40}\text{Ar}/^{39}\text{Ar}$  biotite age spectra from samples known to contain excess argon components. Pankhurst et al. suggested that the concordant spectra resulted from homogenization of excess and radiogenic  $^{40}\text{Ar}$  components during irradiation. They argued however, that both components were indistinguishable before irradiation. These factors suggest that detection of the distribution of excess and radiogenic argon components is not possible through  $^{40}\text{Ar}/^{39}\text{Ar}$  analysis in the study area. Thus the acquisition of excess argon in samples from the Groswater Bay Terrane and northern Lake Melville Terrane samples has not been resolved, and it remains a possible explanation for the pre-Grenvillian plateau ages.

Samples VAN84-22B, 23B and 21A from the Lake Melville Terrane yield  $^{40}\text{Ar}/^{39}\text{Ar}$  spectra which are relatively well defined with only a minor component (< 5%) of excess argon in low temperature fractions. Plateau ages determined from the spectra of these samples record ages of 1070  $\pm$  50 Ma, 1020  $\pm$  5 Ma and 980  $\pm$  4 Ma respectively, which although broadly "Grenvillian" are nevertheless distinctly different.



The error range of  $\pm 50$  Ma for the 1070 Ma age suggests that this age is in "broad" agreement with the 1030 Ma age suggested for culmination of Grenvillian metamorphism in the Lake Melville Terrane, and may represent very rapid uplift following Grenvillian thermal overprinting. Although an alternative viewpoint is that the age represents thermal heating during the Grenvillian Orogeny. However, the large error range limits the implications of this age.

The relatively well-defined plateau ages recorded by 22B and 21A imply complete Grenvillian resetting and in addition these ages are younger than the 1030 Ma age suggested for culmination of Grenvillian metamorphism in the Lake Melville Terrane (Scharer et al., 1986).

Thus the 1020 Ma and 980 Ma ages are interpreted to record post-Grenvillian uplift and subsequent cooling through the retention temperature of hornblende.

A tentative interpretation of the Grenvillian cooling history of the Groswater Bay and Lake Melville Terranes, based on the  $^{40}\text{Ar}/^{39}\text{Ar}$  ages determined in this study along with U-Pb ages of Scharer et al. may be proposed for the Sandwich Bay area.

Since  $^{40}\text{Ar}/^{39}\text{Ar}$  ages recorded by 18A and 14B are a reflection of excess argon components, no inference of Grenvillian cooling can be assessed. The relatively well defined plateau age recorded by 17D suggests the Groswater Bay Terrane may have been partially reheated and subsequently cooled through the retention temperature of hornblende at about 1260 Ma. The data of Scharer et al. suggest that Grenvillian anatexis and metamorphism culminated at about 970 Ma in the Groswater Bay Terrane.

In the Lake Melville Terrane, the very well defined total gas age

of  $1241 \pm 3$  Ma suggests that the northern Lake Melville Terrane may have been affected by the same thermal overprint recorded by VAN84-17D in the Groswater Bay Terrane. Schärer et al. propose that Grenvillian metamorphism in the Lake Melville Terrane culminated between 1026 and 1038 Ma.

The implications of the 1260 to 1240 Ma ages are at present not fully understood. As mentioned above, these ages do not correspond with any major thermal or cooling event in eastern Labrador. Although the ages are tentatively interpreted to date thermal resetting of the argon at this time, the present data do not provide an explanation to suggest why these pre-Grenvillian ages were not reset during anatexis at ca. 970 Ma and 1030 Ma in the Groswater Bay and Lake Melville Terranes, respectively. However, the "preservation" of these ages may tentatively suggest that the effects of the rate and timing of heating in the two terranes may have been quite variable during the Grenvillian Orogeny.

The data from this study suggest that post-Grenvillian uplift and subsequent cooling through the retention temperature required for hornblende in the Lake Melville Terrane was attained immediately following Grenvillian metamorphism and anatexis at ca. 1030 Ma and continued until ca. 980 Ma, which is in accord with the data of Schärer et al. However, the ages from this study imply that the rates of uplift and cooling were variable throughout the Lake Melville Terrane.

#### 6.5.4 Implications for Geothermobarometry

These results support the interpretation proposed in Section 4.4.3, in which it has been suggested that geothermometry and geobarometry estimates reflect the Grenvillian Orogeny. The ages recorded by samples in the Lake Melville Terrane imply that these rocks were heated above 500°C during the Grenvillian Orogeny.

Equilibration and resetting temperatures of several of the mineral phases and mineral pairs used in the geothermobarometry calculations have been studied by various authors. Tracey et al. (1976), note that garnets which are heated to temperatures near or above the sillimanite + K feldspar isograd (approximately 650°C) are homogenized by volume diffusion which obliterates any pre-existing compositional zoning. Lasaga et al. (1977) suggested that the temperatures of cation exchange of Fe and Mg between biotite and garnet range from 700°C down to 500°C. Plagioclase and alkali feldspar homogenization is reported by Bohlen and Essene (1982) to occur at temperatures of approximately 500°C. Essene (1981) notes that the cation exchange in pyroxenes on the M1 and M2 structural sites occurs rapidly above 600°C so that all information about prior states (i.e. higher temperatures) is lost.

Thus equilibration (or resetting) temperatures of several of the mineral phases used in the geothermobarometry analyses are in the range of that required to reset the "argon clock" in hornblende, so it appears likely that the thermometry and barometry assemblages were similarly reset during Grenvillian metamorphism (i.e.  $T > 500^{\circ}\text{C}$ ).

However, evidence of a 1260 to 1240 Ma thermal event, implied by two samples from the study area in addition to ages recorded in the Mealy Mountains (P.H.R Reynolds, personal comm., 1986) suggests that this event was not effaced in parts of both the Groswater Bay and Lake Melville Terranes during the Grenvillian Orogeny.

#### 6.5.5 Origin of Extraneous Argon Components

Excess argon components in hornblende appear to be present to some degree in the majority of samples analyzed in the study area. Sample VAN84-18A records a strongly discordant spectrum in which incremental dates systematically decrease during analyses, suggesting that excess argon components are inhomogeneously distributed throughout the hornblende grains. Sample VAN84-14B, however, displays a less discordant spectrum in which incremental ages increase during the low and intermediate temperature fractions with an apparent levelling-out of the spectrum in the high temperature fractions. This suggests that excess argon components may only be present in the marginal zones of the hornblende, and the core zones may contain only negligible amounts. In samples 17D, 23B, 22B and 21A relatively small amounts of excess argon are present, on the order of 5 to 10%, implied by the anomalous ages recorded in only the the lowest temperature fraction(s). The very well defined total gas spectrum displayed by VAN84-32A suggests that the excess components are not present.

The source of the extraneous argon is not directly known. However, Dallmeyer and Rivers (1983), who recognized extraneous argon components in biotite and hornblende in gneisses across the

Grenvillian metamorphic gradient in western Labrador, note that structural imbrication during the Grenvillian Orogeny, was accomplished while the allochthons were maintained at elevated temperatures. They suggested that evolved  $^{40}\text{Ar}$  migrated upward during post-metamorphic cooling, thus producing large and variable  $^{40}\text{Ar}/^{36}\text{Ar}$  ratios within the intergranular vapour phase, which subsequently infiltrated biotite and hornblende lattices in structurally higher (cooler) levels of the nappe stack. A similar interpretation may be applicable to the excess argon components observed in the Sandwich Bay area. Following the model of Dallmeyer and Rivers, and noting that the effects of excess argon are most noticable in the Groswater Bay Terrane, it is possible that the Aphebian or Archean gneissic basement, which is inferred to underly the lithotectonic terranes in eastern Labrador (Gower and Owen, 1984) evolved radiogenic  $^{40}\text{Ar}$  during Grenvillian uplift and imbrication. This evolved argon may have migrated upward thus producing variable  $^{40}\text{Ar}/^{36}\text{Ar}$  ratios within the intergranular phase. However, since no direct evidence of this basement has yet been found in the region, the interpretation for the origin of excess argon proposed here is highly speculative.

In summary,  $^{40}\text{Ar}/^{39}\text{Ar}$  ages recorded by samples VAN84-14B and 18A are interpreted to be a result of the presence of large quantities of excess  $^{40}\text{Ar}$  components in hornblende. The strongly discordant spectra displayed by VAN84-18A and 14B are the "classic" signature of large excess argon components. The spectra of VAN84-17D and 32A are tentatively interpreted to represent a thermal disturbance at 1260 to 1240 Ma, which is displayed as a complete resetting by the very well defined plateau of 32A and as a partial resetting which is "masked"

by minor excess argon components in 17D. The implications of a 1260 to 1240 Ma thermal event in the Grenville Province, which is evidenced by these age spectra in addition to similar ages obtained in the Mealy Mountains is at present not understood and additional age dating appears to be required before any interpretation of such an event could be established. However, tentatively the record of these well-defined pre-Grenvillian ages suggests that thermal reworking during the Grenvillian Orogen may have been variable in the Groswater Bay and Lake Melville Terranes. Ages from the southern Lake Melville Terrane suggest that post-Grenvillian uplift and subsequent cooling ranged from immediately following Grenvillian metamorphism at ca. 1030 Ma until ca. 980 Ma.

The origin of excess argon components in some of the analyzed samples is interpreted to be a result of evolution and migration of  $^{40}\text{Ar}$  from the inferred gneissic basement during Grenvillian uplift and imbrication.

## CHAPTER 7

### SUMMARY AND CONCLUSIONS

Recent improvements in understanding of Grenvillian geology in Labrador have largely been a result of the distinction between the effects of pre-Grenvillian and Grenvillian orogenic events. Previous studies involved with the analysis of Grenvillian features, in particular metamorphic and structural relationships, were largely speculative.

This study which focusses on the interpretation of the metamorphic conditions in relation to the Grenvillian and pre-Grenvillian Orogenies in eastern Labrador, has involved principally; (1) the determination of quantitative metamorphic P-T conditions on the basis of co-existing mineral assemblages and element partitioning between experimentally and empirically calibrated mineral equilibria; and (2)  $^{40}\text{Ar}/^{39}\text{Ar}$  radiometric dating of hornblende concentrates with an attempt at interpreting the extent of Grenvillian effects and the metamorphic cooling history.

The marked contrast in lithologic association, structural style and metamorphic grade between two recently defined lithotectonic terranes in eastern Labrador has been used as a basis to distinguish these terranes as parautochthonous and allochthonous units.

The northern terrane, Groswater Bay Terrane, is characterized by granodioritic to tonalitic orthogneiss, diorite to quartz diorite, K feldspar megacrystic and non-megacrystic granodiorite, pyroxene-bearing granitoids, various mafic lithologies and minor

semi-pelitic paragneiss. The southern terrane, the Lake Melville Terrane, is underlain by semi-pelitic paragneiss and associated supracrustal rocks, K feldspar megacrystic granitoids, hornblende and pyroxene-bearing granitoids, layered mafic intrusions and granodiorite orthogneiss.

The structural evolution of these two terranes centers on the effects of Grenvillian metamorphism and tectonism on pre-Grenvillian features. A major effect of the Grenvillian Orogeny in eastern Labrador was to uplift and slice contrastingly older crustal blocks with pre-Grenvillian histories into thrust-bounded units. Structures in the Groswater Bay Terrane define a relatively simple north-west to east-west regional trend in which Labradorian fabrics have been variably reworked by Grenvillian deformation. In some areas NNE trending fabrics, interpreted to be a relict Labradorian feature, have been preserved in a structurally unmodified region whereas elsewhere Grenvillian fabrics predominate. In the Lake Melville Terrane, a more complex structural pattern is developed in which pre-existing (Labradorian) fabrics have been strongly reworked by Grenvillian folding.

The Groswater Bay Terrane, is characterized by the development of upper amphibolite facies metamorphic mineral assemblages of kyanite + garnet + biotite + muscovite + plagioclase + K feldspar + quartz + magnetite in pelitic rocks. Basic lithologies commonly contain garnet + orthopyroxene + clinopyroxene. A later post-Grenvillian lowest amphibolite facies overprint of muscovite + quartz and hornblende + chlorite + epidote assemblages is developed in paragneiss and mafic rocks, respectively.



In the Lake Melville Terrane, paragneisses are characterized by upper amphibolite to granulite facies assemblages of sillimanite + garnet + biotite + cordierite. Sapphirine + osumilite + orthopyroxene assemblages are developed in contact metamorphic zones. Granitoid and orthogneisses are characterized by biotite + garnet + hornblende + orthopyroxene assemblages. Garnet + orthopyroxene + clinopyroxene + (hornblende) assemblages are present in mafic lithologies.

Temperatures obtained from garnet - biotite, clinopyroxene - orthopyroxene, clinopyroxene - garnet and orthopyroxene - garnet thermometers yield estimates of 615°C to 874°C in the Groswater Bay Terrane and 639°C to 973°C in the Lake Melville Terrane. Pressures derived from garnet - plagioclase -  $\text{Al}_2\text{SiO}_5$  - quartz, garnet - clinopyroxene - plagioclase - quartz and garnet - orthopyroxene - plagioclase - quartz barometers are in the range of 9 to 12 kbar for the Groswater Bay Terrane and 6 to 10 kbar for the Lake Melville Terrane, implying derivation from depths on the order of 30 to 35 km and 18 to 25 km, respectively. These estimates, on the basis of microstructural and chemical relationships in mineral assemblages, are interpreted to be a reflection of Grenvillian metamorphism. The pressure estimates are in disagreement with the regional tectonic framework proposed for the Grenville Province in eastern Labrador in which the Lake Melville Terrane represents an exhumed deep level allochthon which was transported northward over a higher crustal level parautochthonous unit, the Groswater Bay Terrane. Geothermobarometry estimates suggests that the Groswater Bay Terrane was derived from deeper crustal levels than the Lake Melville Terrane.

The most likely explanation for this apparent "reversal" of the regional tectonic framework as well as the distinct contrast in metamorphic pressures between the two terranes is that the relatively "low" pressures recorded in the granulite facies Lake Melville Terrane, reflect a later (i.e. lower pressure) re-equilibration of barometers than in the Groswater Bay Terrane. If the Lake Melville Terrane was emplaced as a "hot" nappe than net transfer barometers may have been able to re-equilibrate after thrust emplacement and in fact to continue re-equilibrating during subsequent uplift, thus recording lower pressures than the maximum pressures attained at lower crustal depths prior to emplacement. Similarly, if barometers in the Groswater Bay Terrane reflect re-equilibration after emplacement, than the relatively higher pressures record crustal thickening due to the overriding Lake Melville Terrane.

On the basis of the geothermobarometry results, equilibrium pressure-temperature paths have been constructed for the two terranes. These curves are interpreted to represent a portion of the re-equilibration path followed by both the Groswater Bay and Lake Melville terranes during Grenvillian uplift.

The P-T path for the Groswater Bay Terrane, implies that uplift was nearly isothermal, and that decompression was accompanied by minimal cooling during the early stages. A similar P-T path is interpreted from the Lake Melville Terrane, suggesting that decompression and cooling in the Lake Melville Terrane followed a similar path to that of the Groswater Bay Terrane.

These results imply that crustal thickening during the Grenvillian Orogeny occurred by thrusting as opposed to magma addition at lower

crustal levels, which supports the regional structural framework of transport by regional thrusting of the Lake Melville Terrane over the Groswater Bay Terrane.

$^{40}\text{Ar}/^{39}\text{Ar}$  incremental release dating of hornblende concentrates from the Groswater Bay and Lake Melville Terranes yielded variable results in which ages range from pre- to post-Grenvillian. Total gas ages obtained from discordant age spectra in the Groswater Bay Terrane are interpreted to be a result of significant components of excess  $^{40}\text{Ar}$ . A plateau age of  $1260 \pm 12$  Ma recorded by one sample from the Groswater Bay Terrane and a well-defined total gas age of  $1241 \pm 3$  Ma obtained from the northern Lake Melville Terrane implies a resetting of the argon system in these samples at ca. 1250 Ma. However, this age does not correlate with any previously known event (thermal or cooling) in the Grenville Province. In addition, if the blocking temperature of hornblende is ca.  $500^\circ\text{C}$ , it is not clear why older Ar is retained in some samples if the regional metamorphic temperature estimates have a minimum of  $615^\circ\text{C}$ . The significance of these ages is at present not understood, although the presence of these ages suggests that thermal reworking during the Grenvillian Orogeny may have been quite variable.

Samples from the southern Lake Melville Terrane display relatively well-defined age spectra yielding plateau ages of 1070, 1020 and 980 Ma. These ages are interpreted to represent post-Grenvillian uplift and subsequent cooling following anatexis and metamorphism at ca. 1030 Ma. Although the first age is in excess of 1030 Ma, the large error of  $\pm 50$  Ma, suggests that it is within "broad agreement" with this age and is thus interpreted to represent very rapid uplift

following Grenvillian anatexis and metamorphism. The southern most samples which yield the 1020 and 980 Ma are interpreted to result from slower post-Grenvillian uplift and cooling through the retention temperature required for argon in the hornblende lattice.

Although a tentative interpretation of the extent and timing of the post-Grenvillian uplift and cooling history in the Sandwich Bay area is proposed here, it is apparent the incorporation of additional  $^{40}\text{Ar}/^{39}\text{Ar}$  dates on both hornblende and biotite is required in order to more fully elucidate the timing of Grenvillian thermal and cooling events.

These features indicate that the Grenville Province within the study area has undergone an extensive metamorphic and structural evolution involving uplift and subsequent imbrication of pre-Grenvillian crust during the Grenvillian Orogeny. The implications of the tectonic framework and estimation of metamorphic P-T conditions, together with the recent identification of allochthons in west and central Labrador provides evidence of significant crustal thickening during the Grenvillian Orogeny. Such features have long been recognized as being a major component of Phanerozoic orogenies and recently appear to be applied to evolutionary plate tectonic models of Precambrian orogenic belts.

## REFERENCES

- Alexander, E.C., Jr., Michelson, G.M., and Lamphere, M.A. (1978): MMhb-1: A new  $^{40}\text{Ar}/^{39}\text{Ar}$  dating standard, in Zartman, R.E., ed., Fourth International Conference on Geochronology, Cosmochronology, and Isotope Geology. U.S. Geol. Surv. Open-File Report 78-701, 6-8.
- Banno, S. (1970): Classification of eclogites in terms of physical conditions of their origin. *Phys. Earth Planet. Interiors*, 3, 405-421.
- Banno, S. and Matsui, Y. (1965): Eclogite types and partition of Mg, Fe and Mn between clinopyroxene and garnet. *Proc. Japan Acad.*, 41, 716-721.
- Bohlen, S.R. and Essene, E.J. (1980): Evaluation of coexisting garnet - biotite, garnet - clinopyroxene and other Fe-Mg exchange thermometers in Adirondack granulites: Summary. *Geol. Soc. Amer. Bull.*, 91, 107-109.
- Bohlen, S.R. and Essene, E.J. (1980): Evaluation of coexisting garnet - biotite, garnet - clinopyroxene and other Fe-Mg exchange thermometers in Adirondack granulites: *Geol. Soc. Am. Bull. Part II*, 91, 685-719.
- Cressey, G., Schmid, R., and Wood, B.J. (1978): Thermodynamic properties of almandine-grossular garnet solid solution. *Contrib. Mineral. Petrol.*, 67, 397-404.
- Dahl, P.S. (1980): The thermal-compositional dependence of  $\text{Fe}^{2+}$ -Mg distribution between coexisting garnet and pyroxene: applications to geothermometry. *Am. Mineral.* 65, 852-866.
- Dallmeyer, R.D. and Rivers, T. (1983): Recognition of extraneous argon components through incremental-release  $^{40}\text{Ar}/^{39}\text{Ar}$  analysis of biotite and hornblende across the Grenvillian metamorphic gradient in southwestern Labrador. *Geochim. Cosmochim. Acta*, 47, 413-428.
- Dalrymple, G.B. and Lamphere, M.A. (1974):  $^{40}\text{Ar}/^{39}\text{Ar}$  age spectra of some terrestrial samples. *Geochim. Cosmochim. Acta*, 38, 715-738.
- Dodson, M.H. (1973): Closure temperatures in cooling geochronological and petrological systems. *Contrib. Mineral. Petrol.*, 40, 259-274.
- Dodson, M.H. (1979): Theory of cooling ages. in Jager, E. et al., eds., *Lectures in isotope geology*. New York, Springer-Verlag, 194-202.
- Ellis, D.J. and Green, D.H. (1979): An experimental study of the effect of Ca upon garnet - clinopyroxene exchange equilibria. *Contrib. Mineral. Petrol.*, 71, 13-22.

Ellis, D.J. and Green, D.H. (1985): Garnet forming reactions in mafic granulites from Enderby Land, Antarctica - Implications for geothermometry and geobarometry. *Jour. Petrol.*, 26, 633-662.

Esslie, R.F. (1983): The coronitic Micheal gabbros, Labrador: assessment of Grenvillian metamorphism in northeastern Grenville Province. in *Current Research, Part A. Geol. Surv. Can. Paper 83-1A*, 139-145.

England, P.C. and Thompson, A.B. (1984): Pressure-temperature-time paths of regional metamorphism I. Heat transfer during the evolution of regions of thickened continental crust. *Jour. of Petrol.*, Vol. 25, Part 4, 894-928.

Essene, E.J. and Fyfe, W.S. (1967): Omphacite in Californian metamorphic rocks. *Contrib. Mineral. Petrol.*, 15, 1-23.

Ferry, J.M. and Spear, F.S. (1978): Experimental calibration of the partitioning of Fe and Mg between biotite and garnet. *Contrib. Mineral. Petrol.*, 66, 113-117.

Fleck, R.J., Sutter, J.F. and Elliot, D.H. (1977): Interpretation of discordant  $^{40}\text{Ar}/^{39}\text{Ar}$  age spectra of Mesozoic tholeiites from Antarctica. *Geochimica et Cosmochimica Acta*, 41, 15-32.

Froese, E. (1973): The oxidation of almandine and iron cordierite. *Can. Mineral.*, 11, 991-1002.

Ganguly, J. (1976): The energetics of natural garnet solid solution II. Mixing of the calcium silicate end-members. *Contrib. Mineral. Petrol.*, 55, 81-90.

Ganguly, J. and Kennedy, G.C. (1974): The energetics of natural garnet solid solution. I. Mixing of the aluminosilicate end-members. *Contrib. Mineral. Petrol.*, 48, 137-148.

Ganguly, J. and Saxena, S. (1984): Mixing properties of aluminosilicate garnets: constraints from natural and experimental data, and applications to geothermobarometry. *Am. Mineral.*, 69, 88-97.

Ghent, E.D. (1976): Plagioclase - garnet -  $\text{Al}_2\text{SiO}_5$  - quartz: a potential geobarometer-geothermometer. *Am. Mineral.*, 61, 710-714.

Ghent, E.D., Knitter, C.C., Raeside, R.P., and Stout, M.Z. (1982): Geothermometry and geobarometry of pelitic rocks, upper kyanite and sillimanite zones, Mica Creek area, British Columbia. *Can. Mineral.*, 20, 295-305.

Ghent, E.D, Robbins, D.B., and Stout, M.Z. (1979): Geothermometry, geobarometry, and fluid compositions of metamorphosed calc-silicates and pelites, Mica Creek, British Columbia. *Amer. Mineral.*, 64, 874-885.

Glassley, W.E. and Sorensen, K. (1980): Constant P-T amphibolite to granulite facies transition in Agto (West Greenland) metadolerites: Implications and applications. *Jour. Petrol.*, Vol.21, Part.1, 69-105.

Goldman, D.S. and Albee, A.L. (1977): Correlation of Mg/Fe partitioning between garnet and biotite with  $^{18}O/^{16}O$  partitioning between quartz and magnetite. *Am. Jour. Sci.*, 277, 750-767.

Goldsmith, J.R. (1980): The melting and breakdown of reactions of anorthite at high pressures and temperatures. *Am. Mineral.*, 65, 272-284.

Gower, C.F. (1981): The geology of the Benedict Mountains, Labrador (13J northeast and 13I northwest). Newfoundland Department of Mines and Energy, Mineral Development Division., Report 81-3, 26p.

Gower, C.F., Noel, N., and Gillespie, R.T. (1983): Groswater Bay 1:100,000 Map Sheet. Department of Mines and Energy, Mineral Development Division, Map 83-43.

Gower, C.F., Noel, N. and van Nostrand, T. (1985): Geology of the Paradise River region, Grenville Province, eastern Labrador; in *Current Research, Part B, Geol. Surv. Can. Paper 85-1B*, 547-560.

Gower, C.F., Owen, V., and Finn, G. (1982): The geology of the Cartwright region, Labrador, in *Current Research, Newfoundland Department of Mines and Energy, Mineral Development Division, Report 82-1*, 122-130.

Gower, C.F. and Owen, V. (1984) Pre-Grenvillian and Grenvillian lithotectonic regions in eastern Labrador - Correlations with the Sveconorwegian orogenic belt in Sweden. *Can. Jour. Earth Sci.*, 21, 678-693.

Gower, C.F., Ryan, A.B., Bailey, D.G., and Thomas, A. (1980): The position of the Grenville Front in eastern and central Labrador., *Can. Jour. Earth Sci.* 17, 784-788.

Gower, C.F. and Ryan, B. (1986): Proterozoic evolution of the Grenville Province and adjacent Makkovik Province in eastern-central Labrador. in *Geol. Assoc. Can. Spec. Paper . The Grenville Province*, ed. by J.M. Moore et al.; p 281-296.

- Gower, C.F., van Nostrand, T., McRoberts, G., Crisby, L. and Prevec, S. (1986): Geology of the Sand Hill River - Bateau Map Region, Grenville Province, eastern Labrador. in Current Research, Newfoundland Department of Mines and Energy, Mineral Development Division, Report 86-1, 340-344.
- Greene, B.A. (1972): Geological Map of Labrador, Newfoundland Department of Mines, Agriculture and Resources, Mineral Development Division.
- Harrison, T.M. (1981): The diffusion of  $^{40}\text{Ar}$  in hornblende. *Contrib. Mineral. Petrol.*, 78, 324-331.
- Harrison, T.M. and McDougall, I. (1981): Excess  $^{40}\text{Ar}$  in metamorphic rocks from Broken Hill, New South Wales: implications for  $^{40}\text{Ar}/^{39}\text{Ar}$  age spectra and the thermal history of the region. *Earth Planet. Sci. Lett.*, 55, 123-149.
- Hariya, Y. and Kennedy, G.C. (1968): Equilibrium study of anorthite under high pressure and high temperature. *Am. J. Sci.*, 266, 193-203.
- Hays, J.F. (1967): Lime-alumina-silica. *Carnegie Inst. Wash. Yearb.*, 65, 234-239.
- Hodges, K.V. and Royden, L. (1984): Geologic thermobarometry of retrograded metamorphic rocks: an indication of the uplift trajectory of a portion of the northern Scandinavian Caledonides. *Jour. Geophys. Res.*, 89, 7077-7090.
- Hodges, K.V., and Spear, F.S. (1982): Geothermometry, geobarometry and the  $\text{Al}_2\text{SiO}_5$  triple point at Mt. Moosilauke, New Hampshire. *Amer. Mineral.*, 67, 1118-1134.
- Holdaway, M.J. (1971): Stability of andalusite and the aluminosilicate phase diagram. *Am. Jour. Sci.*, 271, 97-131.
- Holdaway, M.J. and Lee, S.M. (1977): Fe-Mg cordierite stability in high grade pelitic rocks based on experimental, theoretical and natural observations. *Contrib. Mineral. Petrol.*, 63, 175-198.
- Hormann, P.K., Raith, M., Raase, P., Ackermann, D., Seifert, F. (1980): The granulite complex of Finnish Lapland. *Geol. Soc. Finl. Bull.*, 308, 1-95.
- Indares, A. and Martignole, J. (1984): Evolution of P-T conditions during a high grade metamorphic event in the Maniwaki area. *Can. Jour. Earth Sci.*, 21, 853-863.
- Johnson, C.A., Bohlen, S.R., and Essene, E.J. (1983): An evaluation of garnet-clinopyroxene geothermometry in granulites. *Contrib. Mineral. Petrol.*, 84, 191-198.



- Kerrick, D.M. (1972): Experimental determination of muscovite + quartz stability with  $\text{PH}_2\text{O} < \text{Ptotal}$ . *Am. Jour. Sci.*, 272, 946-958.
- Kerrick, D.M. and Darken, L.S. (1975): Statistical thermodynamic models for ideal oxide and silicate solid solution, with applications to plagioclase. *Geochim. Cosmochim. Acta*, 39, 1431-1442.
- Kretz, R. (1959): Chemical study of garnet, biotite and hornblende from gneisses of S.W. Quebec, with emphasis on distribution of elements in coexisting minerals. *J. Geol.*, 67, 371-402.
- Kretz, R. (1961): Some applications of thermodynamics to coexisting minerals of variable composition. Examples: orthopyroxene-clinopyroxene and orthopyroxene-garnet. *Jour. Geol.*, 69, 361-387.
- Kretz, R. (1964): Analysis of equilibrium in garnet-biotite-sillimanite gneisses from Quebec. *J. Petrol.*, 5, 1-20.
- Lasaga, A.C., Richardson, S.M. and Holland, H.C. (1977): Mathematics of cation diffusion and exchange between silicate minerals during retrograde metamorphism. In Saxena, S.K. and S. Bhattacharji, Eds., *Energetics of Geological Processes*, 353-388, Springer-Verlag, Berlin.
- Lindsley, D.H. (1983): Pyroxene Thermometry. *Am. Mineral.*, 68, 477-493.
- Merrill, C. and Turner, G. (1966): Potassium-argon dating by activation with fast neutrons. *Jour. Geophys. Res.*, 71, 2852-2857.
- Mitchell, J.G. (1968): The argon-40/argon-39 method for potassium-argon age determination. *Geochim. Cosmochim. Acta*, 32, 781-790.
- Mysen, B.O. and Heier, K.S. (1972): Petrogenesis of eclogite in high grade metamorphic gneisses, exemplified by the Hareidland Eclogite, Western Norway. *Contrib. Mineral. Petrol.*, 36, 73-94.
- Newton, R.C. (1972): An experimental determination of the high pressure stability limits of magnesian cordierite under wet and dry conditions. *Jour. Geol.*, 80, 398-420.
- Newton, R.C., Charlu, T.V., and Kleppa, O.J. (1974): A calorimetric investigation of the stability of anhydrous magnesium cordierite with application to granulite facies metamorphism. *Contrib. Mineral. Petrol.*, 44, 295-311.
- Newton, R.C., Charlu, T.V., and Kleppa, O.J. (1980): Thermochemistry of the high structural state plagioclases. *Geochim. Cosmochim. Acta*, 44, 933-941.

- Newton, R.C. and Haselton, M.T. (1981): Thermodynamics of the garnet-plagioclase- $\text{Al}_2\text{SiO}_5$ -quartz geobarometer. in *Thermodynamics of Minerals and Melts*. Springer-Verlag, 131-147.
- Newton, R.C. and Perkins, D. III (1982): Thermodynamic calibration of geobarometers based on the assemblages garnet - plagioclase - orthopyroxene - (clinopyroxene) - quartz. *Am. Mineral.*, 67, 203-222.
- O'Neill, H.C. and Wood, B.J. (1979): An experimental study of Fe-Mg partitioning between garnet and olivine and its calibration as a geothermometer. *Contrib. Mineral. Petrol.*, 70, 59-70.
- Owen, V., Gower, C.F. and Finn, G. (1983): Table Bay 1:100,000 Map Sheet. Mineral Development Division, Newfoundland Department of Mines and Energy, Map 83-46.
- Owen, V. (1985): Tectonometamorphic Evolution of the Grenville Front Zone, Smokey Archipelago, Labrador. Ph.D Thesis, Memorial University of Nfld., 382 pp.
- Pankhurst, R.J., Moorbath, S. Rex, D.C. and Turner, G. (1973): Mineral age pattern in ca. 3700 m.y. old rock from west Greenland. *Earth Planet. Sci. Lett.*, 20, 157-170.
- Perkins, D. III, and Newton, R.C. (1982): Charnockite geobarometers based on coexisting garnet-pyroxene-plagioclase-quartz. *Nature*, 292, 144-146.
- Pigage, L.C. and Greenwood, H.J. (1982): Internally consistent estimates of pressure and temperature: the staurolite problem. *Am. Jour. Sci.*, 282, 943-969.
- Reynolds, P.H., Kublick, E.E. and Muecke, G.K. (1973): Potassium argon dating of slates from the Meguma Group, Nova Scotia. *Can. Jour. Earth Sci.*, 10, 1059.
- Rivers, T. (1983a): Progressive metamorphism of pelitic and quartzofeldspathic rocks in the Grenville Province of western Labrador-Tectonic implications of bathozone 6 assemblages. *Can. Jour. Earth Sci.*, 20, 1791-1804.
- Rivers, T. and Nunn, G.A.G. (1985): A reassessment of the Grenvillian Orogeny in western Labrador. NATO ASI Series C, V.158, p. 163-174.
- Rivers, T. and Chown, E.H. (1986): The Grenvillian orogeny in eastern Quebec and western Labrador-definition, identification and tectonometamorphic relationships of autochthonous, parautochthonous and allochthonous terranes. in *The Grenville Province*, Geol. Assoc. Can. Spec. Paper 31, ed. by J.M Moore et al., p. 31-50.

- Roddick, J.C., Cliff, R.A. and Rex, D.C. (1980): The evolution of excess argon in alpine biotites -  $^{40}\text{Ar}/^{39}\text{Ar}$  analysis. *Earth Planet. Sci. Lett.*, 12, 208-214.
- Saxena, S.K. (1969): Silicate solid-solutions and geothermometry: distribution of Fe and Mg between coexisting garnet and biotite. *Contrib. Mineral. Petrol.*, 22, 259-276.
- Schärer, U., Krogh, T.E. and Gower, C.F. (1986): Age and evolution of the Grenville Province in eastern Labrador from U/Pb systematics in accessory minerals. *Contrib. Mineral. Petrol.*, 94, 438-451.
- Schmidt, R., Cressey, G. and Wood, B. J. (1978): Experimental determination of univariant equilibria using divariant solid solution assemblages. *Am. Mineral.*, 63, 511-515.
- Sen, S.K. and Bhattacharya, A. (1984): An orthopyroxene - garnet thermometer and its applications to the Madras charnokites. *Contrib. Mineral. Petrol.*, 88, 64-71.
- Signatureirsson, T. (1962): Dating recent basalt by the potassium-argon method. *Rep. Phys. Lab. Univ. Iceland*, 9 p.
- Steiger, R.H. and Jäger, E. (1977): Subcommittee on geochronology: convention on the use of decay constants in geo- and cosmochemistry. *Earth Planet. Sci. Lett.*, 36, 359-362.
- St-Onge, M.R. (1981): Metamorphic conditions of the low-pressure internal zone of north-central Wopmay Orogen, Northwest Territories, Canada [Ph.D. thesis], Kingston, Ontario, Queens University, 240 p.
- Thomas, A., Nunn, G.A.G. and Wardle, R.J. (1985): A 1650 Ma orogenic belt within the Grenville Province of northeastern Canada. In Tobl, A.C. and Touret, J.L.R., eds., *The Deep Proterozoic Crust in the North Atlantic Provinces*, NATO Advanced Science Institute Series, ser. C, v. 158, 151-161.
- Thompson, A.B. (1974): Calculation of muscovite-paragonite-alkali feldspar relations. *Contrib. Mineral. Petrol.*, 44, 173-194.
- Thompson, A.B. (1976): Mineral reactions in pelitic rocks: II. Calculations of some P-T-X (Fe-Mg) phase relations. *Am. J. Sci.*, 276, 425-454.
- Thompson, A.B. and Algor, J.R. (1977): Model systems for anatexis of pelitic rocks. I. Theory of melting reactions in the system  $\text{KAlO}_2\text{-NaAlO}_2\text{-Al}_2\text{O}_3\text{-SiO}_2\text{-H}_2\text{O}$ . *Contrib. Mineral. Petrol.*, 63, 247-269.

- Thompson, A.B. and England, P.C. (1984): Pressure-temperature-time paths of regional metamorphism II. Their inference and interpretation using mineral assemblages in metamorphic rocks. *Jour. Petrol.* 25, Part 4, p. 929-955.
- Tracy, R.J., Robinson, P. and Thompson, A.B. (1976): Garnet composition and zoning in the determination of temperature and pressure of metamorphism, central Massachusetts. *Am. Mineral.*, 61, 762-775.
- Wanless, R.K., Stevens, R.D. and Loveridge, W.D. (1970): Anomalous parent-daughter isotopic relationships in rocks adjacent to the Grenville Front near Chibougamau, Quebec. *Ecolog. Geol. Helv.*, 63, 345-364.
- Wanless, R.K., Stevens, R.D., Lachance, G.R. and Delabio, R.N. (1972): Age determinations and geological studies. K-Ar isotopic ages, Report 10; *Geol. Surv. Can. Paper* 71-2.
- Wanless, R.K., Stevens, R.D., Lachance, G.R. and Delabio, R.N. (1973): Age determinations and geological studies. Report 11, *Geol. Surv. Can. Paper* 73-2.
- Weaver, B.L., Tarney, J., Windley, B.F., Sugavanam, E.B. and Venkata Rao, V. (1978): Madras granulites: Geochemistry and P-T conditions of crystallization. In *Archean Geochemistry*, (B.F. Windley and M. Naqvi, eds.), 177-204.
- Wells, P.R.A. (1977): Pyroxene thermometry in simple and complex systems. *Contrib. Mineral. Petrol.*, 62, 129-139.
- Wells, P.R.A. (1979): Chemical and thermal evolution of Archean sialic crust, southern west Greenland. *Jour. Petrol.*, 20 (2), 187-226.
- Wood, B.J. (1974): The solubility of alumina in orthopyroxene coexisting with garnet. *Contrib. Mineral. Petrol.*, 46, 1-15.
- Wood, B.J. and Banno, S. (1973): Garnet-orthopyroxene and orthopyroxene-clinopyroxene relationships in simple and complex systems. *Contrib. Mineral. Petrol.*, 42, 109-124.
- Wynne-Edwards, H.R. (1972): The Grenville Province. In *Variations in Tectonic Styles in Canada*. Price, R.A and Douglas, R.J.W. (eds). *Geol. Assoc. Can. Spec. Paper* 11, 263-334.

APPENDIX 1PETROGRAPHYParagneissGroswater Bay Terrane

Paragneisses in the Groswater Bay Terrane are characterized by the assemblage: kyanite + biotite + garnet + muscovite + plagioclase + K feldspar + quartz + opaque (magnetite). Kyanite generally forms fine-grained aggregates which locally are pseudomorphed by retrograde muscovite. In some samples both kyanite and muscovite appear to co-exist, with no evidence for retrogression. Grain size varies from 0.1 to 0.75 mm, for relict kyanite and retrograde muscovite. Secondary muscovites are generally larger in grain size ranging up to 3 mm in size.

In some areas, the main fabric, defined by muscovite, is crenulated, resulting in the development of a secondary foliation axial planar to the crenulations.

Garnets are characteristically subidioblastic, mauve to pink in color and are usually specked with fine magnetite inclusions. Grain size of garnets vary from 0.5 to 4 mm. Alteration is evident by the development of chlorite along boundaries and within fractures, usually associated with the breakdown of kyanite to muscovite.

Biotite occurs both as fine-grained inclusions within the larger garnet porphyroblasts, and as fine - to medium grained subidioblastic laths which define the dominant gneissic fabric. The latter biotites are typically pre-garnet growth, although one sample exhibits

post-garnet biotite growth. Local alteration to chlorite along cleavage planes and grain boundaries occurs.

K feldspar occurs as polygonal recrystallized grains both in the restite and leucosome components. Grain size ranges from 0.5 to 2 mm in the leucosome and 0.3 to 1.0 mm in the restite. In retrogressed assemblages, K feldspar is locally replaced by secondary muscovite.

Plagioclase, is generally fine-grained (0.5-2 mm) and strongly recrystallized with the development of straight boundaries and triple-point textures.

Quartz occurs as 0.5 to 2.5 mm polygonal grains along with plagioclase and K feldspar in the leucosome component.

#### Lake Melville Terrane

Paragneisses in the Lake Melville Terrane exhibit a more variable mineralogy compared to those in the Groswater Bay Terrane.

Sillimanite + K feldspar + biotite + garnet + plagioclase + quartz + opaque (magnetite) is the typical assemblage but cordierite + sapphirine + hypersthene + sillimanite assemblages occur in anhydrous, granulite facies paragneiss.

Sillimanite is present both as medium grained prismatic grains and as fine to very fine grained fibrolitic aggregates. Three samples immediately south of the Rigolet thrust zone exhibit relict kyanite grains pseudomorphed by later prismatic sillimanite.

Garnets in psammitic gneiss are characteristically mauve in color in hand specimen, in pelitic and semi-pelitic gneiss the color ranges from colorless to light pink. Grain size varies from fine-grained

idioblastic phases, ranging from 0.5 to 2 mm, to large porphyroblasts up to 5 mm in diameter. Locally alteration to chlorite occurs, specifically where gneisses are associated with fault zones.

Biotite ranges from light to reddish brown in color and varies from very fine-grained (< 0.3 mm) up to 1.0 cm. Chloritization occurs in zones of faulting and thrusting. Biotite forms a major component in restite layers and less significant in leucosome, possibly as a xenocrystic phase.

Cordierite occurs as porphyroblasts up to 4 mm in size and is characterized by abundant inclusions of sillimanite, biotite and magnetite.

K feldspar occurs both as fine polygonal grains in restite layers along with sillimanite, biotite, garnet and magnetite and as fine to medium grained polygonal aggregates in the leucosome component.

The leucosome phases quartz, plagioclase and K feldspar occur predominantly as strongly recrystallized subgrains with well developed equilibrium textures. Relict porphyroclasts of these phases are common and generally exhibit serrate grain boundaries with mortar texture development.

#### Mineral Assemblages in Paragneiss Samples

##### Groswater Bay Terrane

CG81-749B gar+bio+kyn+musc+plag+ksp+qtz+zir+tour+sph+mag.

CG81-756 bio+gar+kyn+plag+ksp+qtz+chl+mag.

GF81-16 gar+bio+kyn+musc+chl+plag+ksp+qtz+mag.

GF81-18 gar+bio+kyn+musc+chl+plag+ksp+qtz+mag.

GF81-23 gar+bio+kyn+(musc)+plag+ksp+qtz+mag.

VO81-77A bio+gar+kyn+(musc)+plag+ksp+qtz+mag.

VAN84-16E gar+bio+kyn+musc+ksp+qtz+plag+mag

#### Lake Melville Terrane

VAN84-12N gar+bio+sill+plag+ksp+qtz+mag.

VAN84-12H gar+bio+sill+(chl)+plag+ksp+qtz+mag.

VAN84-34A gar+bio+sill+plag+ksp+qtz+mag.

VAN84-36 gar+bio+sill+(musc)+plag+ksp+qtz.

VN84-35B gar+bio+sill+plag+ksp+qtz+mag.

VN84-102 gar+bio+sill+plag+ksp+qtz+mag.

VN84-150 gar+bio+sill+plag+ksp+qtz+mag.

VN84-338 gar+bio+sill+plag+ksp+qtz+mag.

CG81-148 gar+bio+sill+plag+ksp+qtz+mag.

CG81-155 gar+bio+sill+plag+ksp+qtz+mag.

CG81-170B gar+bio+sill+[kyn]+[cord]+plag+ksp+qtz+mag.

CG81-239 gar+bio+sill+[kyn]+plag+ksp+qtz

CG81-285 gar+bio+sill+opx+plag+ksp+qtz+mag.

CG81-476 bio+gar+sill+plag+ksp+qtz+zir+mag.

CG81-479 bio+gar+sill+plag+ksp+qtz+mag.

GF81-141 gar+bio+sill+plag+ksp+qtz+mag+sph.

GF81-235B gar+bio+sill+plag+ksp+qtz+mag.

VO81-518 bio+gar+sill+plag+ksp+qtz+mag.

[ ] - metastable phases

( ) - retrograde phases



### Mafic rocks

#### Groswater Bay Terrane

Mafic rocks and associated lithologies in the GBT are characterized by garnet + clinopyroxene + orthopyroxene assemblages. Amphibole (hornblende) locally occurs as retrograde subidioblastic porphyroblasts as well as thin coronas around cpx and opx grains. Garnet is generally fine-grained (0.2 to 1mm) with xenoblastic grain shapes. Cpx and opx commonly exhibit moderate to strong recrystallization textures although large relict crystals partially altered to hornblende do occur. Plagioclase and quartz occur both as relict porphyroclasts and moderately recrystallized subgrains in the matrix. Opaque minerals generally occur as small (0.2mm) xenoblastic grains associated with orthopyroxene and clinopyroxene.

#### Lake Melville Terrane

In the Lake Melville Terrane clinopyroxene + orthopyroxene + garnet assemblages are predominant. Cpx and opx grains are generally strongly recrystallized to fine subgrains with well developed equilibrium textures. Garnets occur as porphyroblasts up to 3 mm as well as recrystallized subgrains associated with cpx and opx. Hornblende is a relatively minor mafic phase which occurs predominantly as fine recrystallized grains and as thin alteration rims around cpx and opx. Plagioclase and quartz occur as relict porphyroclasts and as fine subgrains. Opaque phases occur as fine

xenoblastic grains commonly as inclusions within orthopyroxene and clinopyroxene.

### Mineral Assemblages in Mafic Lithologies

#### Groswater Bay Terrane

VO81-89A opx+gar+(hbl)+bio+plag+qtz.

CG81-366 cpx+(hbl)+gar+bio+plag+qtz.

CG81-641 opx+cpx+gar+plag+qtz.

CG81-811B opx+gar+(hbl)+bio+plag+qtz.

#### Lake Melville Terrane

CG84-362 opx+cpx+gar+(hbl)+plag+qtz+mag.

CG84-100 opx+cpx+(hbl)+plag+qtz+mag.

CG81-488A cpx+gar+hbl+plag+qtz.

GF81-121 opx+cpx+hbl+bio+plag+qtz

GF81-222 gar+cpx+hbl+olv+plag+qtz.

GF81-244A gar+opx+cpx+plag+qtz.

GF81-246A gar+cpx+bio+plag+qtz.

VO81-188 opx+cpx+gar+hbl+plag+qtz.

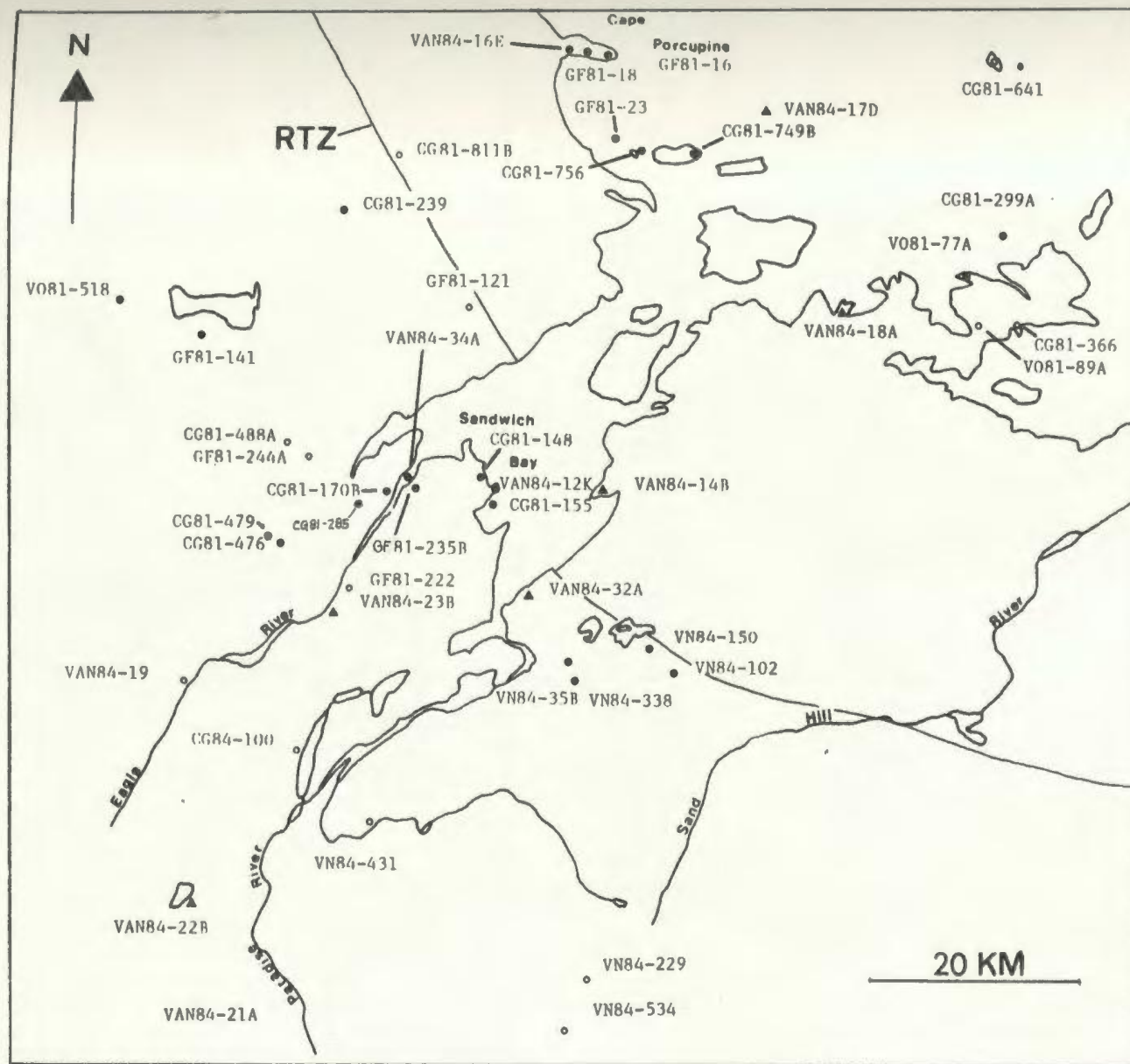
VAN84-19 opx+cpx+plag+ksp+qtz+hbl

VAN84-431 opx+cpx+gar+bio+plag+qtz

VN84-229 cpx+gar+plag+qtz+mag.

VN84-534 opx+cpx+plag+qtz+mag.

( ) - retrograde phases



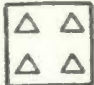
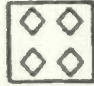


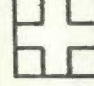

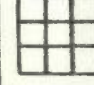
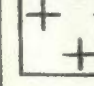


Appendix 2. Sample location map: ( • ) paragneiss samples

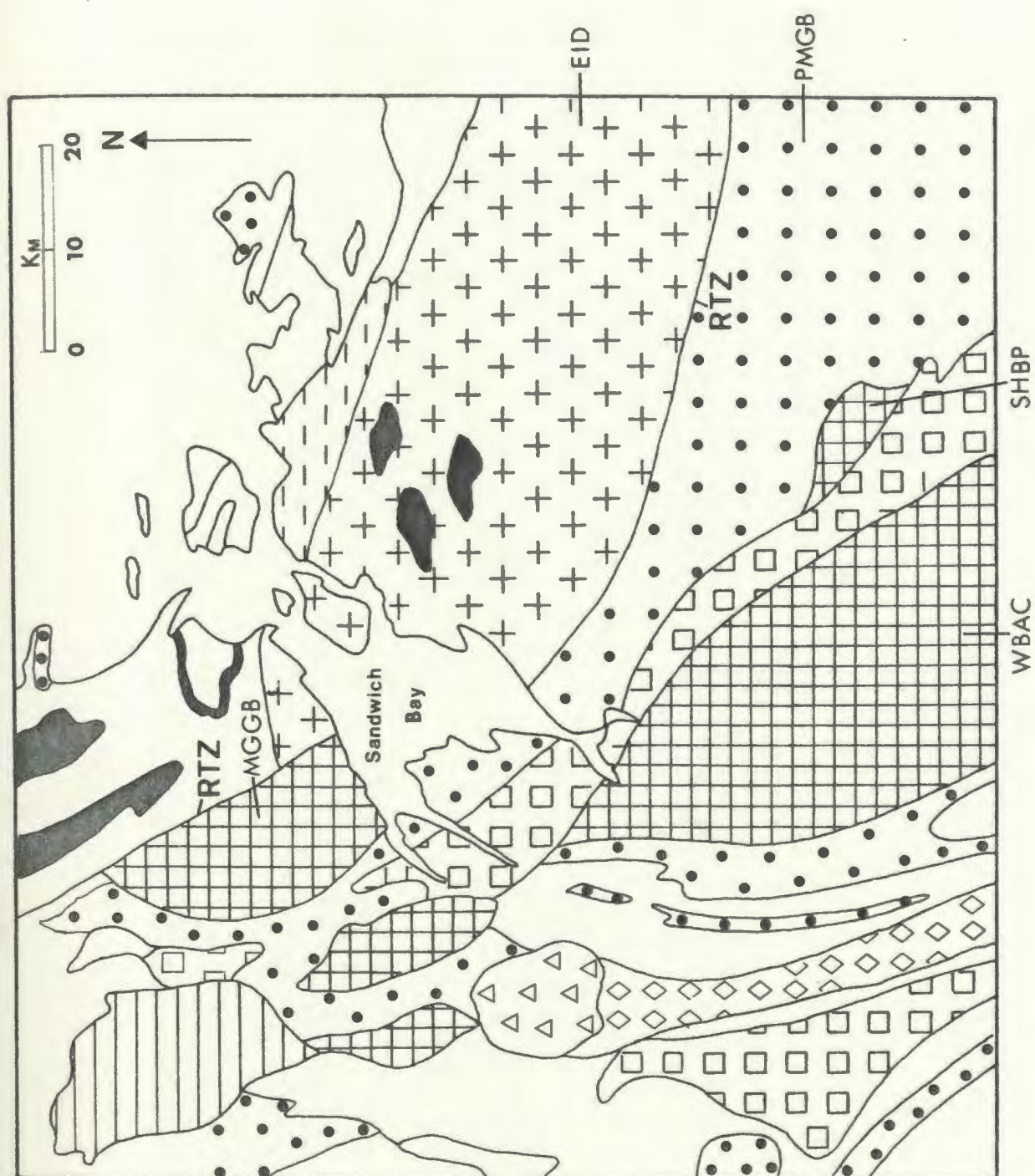
( ◦ ) mafic samples

( ▲ )  $^{40}\text{Ar}/^{39}\text{Ar}$  samples

Appendix 3. Geologic map of study area, after Gower and Owen, 1984;  
Gower et al., 1985, 1986).

EID - Earl Island Domain  
MGGB - Mount Gnat Granulite Belt  
PMGB - Paradise Metasedimentary Belt  
SHBP - Sand Hill Big Pond gabbro-norite  
WBAC - White Bear Arm Complex  
RTZ - Rigolet thrust zone

	Granite, Alkali Feldspar Granite
	Anorthosite, Leucogabbro
	Clinopyroxene Syenite, Monzonite, Granite
	Hornblende and Pyroxene Granodiorite to Syenite
	K Feldspar Megacrystic Granitoid Rocks
	Unassigned Metagabbro, Amphibolite, Mafic Granulite
	Gabbro, Troctolite, Anorthosite, Monzodiorite, Fine-Grained Leuconorite (Granulite Facies)
	Diorite to Quartz Monzonite
	Granodiorite to Tonalite Gneiss
	Pelitic and Psammitic Metasedimentary Gneiss



APPENDIX 4ACTIVITY-COMPOSITION RELATIONS

Activity-composition relationships for garnet, plagioclase, orthopyroxene and clinopyroxene solid solutions presented below were used in all thermobarometric calculations and can be referred to for the following discussion of geothermometers and geobarometers in Appendix A.4

## GARNET

$$\gamma_{py} = \exp ((3300 - 1.5T_K) * (X_{gr}^2 + X_{al}X_{gr} + X_{gr}X_{sp}) / RT_K)^3$$

$$\gamma_{gr} = \exp ((3300 - 1.5T_K) * (X_{py}^2 + X_{al}X_{py} + X_{py}X_{sp}) / RT_K)^3$$

$$a_{py} = (X_{py} * \gamma_{py})^3$$

$$a_{gr} = (X_{gr} * \gamma_{gr})^3$$

$X_{gr}$  = Ca/Fe+Mg+Ca+Mn in garnet

$X_{al}$  = Fe/Mg+Ca+Fe+Mn in garnet

$X_{py}$  = Mg/Fe+Ca+Mg+Mn in garnet

$X_{sp}$  = Mn/Mg+Fe+Mn+Ca in garnet

## PLAGIOCLASE

$$a_{an} = \exp[(X_{ab})^2 (2025 + 9442X_{an}) / RT_K]$$

$$a_{an} = (X_{an}(1+X_{an})^2 / 4 * \gamma_{an}$$

$$X_{an} = \text{Ca} / \text{Na} + \text{Ca} + \text{K in plagioclase}$$

$$X_{ab} = \text{Na} / \text{Ca} + \text{Na} + \text{K in plagioclase}$$

## PYROXENE

$$a_{en} = X_{Mg} * X_{Mg} \text{ in opx}$$

$$a_{di} = X_{Mg} * X_{Ca} \text{ in cpx}$$

$$X_{Mg} = \text{Mg} / \text{Mg} + \text{Fe}$$

$$X_{Ca} = \text{Ca} / \text{Ca} + \text{Fe} + \text{Mg}$$

## APPENDIX 5

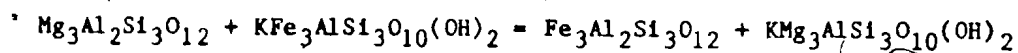
### GEO THERMOMETRY - GEOBAROMETRY METHODS

#### A.5.1 Exchange Thermometers

##### A.5.1.1 Garnet - Biotite

Experimental and theoretical calibrations imply that the Fe-Mg distribution between garnet and biotite, expressed as  $K_D = (Mg/Fe)_{ga} / (Mg/Fe)_{bi}$ , is a temperature sensitive equilibrium affected only to a slight degree by pressure (Saxena, 1969; Thompson 1976; Goldman and Albee 1977; Holdaway and Lee 1977; Ferry and Spear 1978). This expression of the distribution coefficient applies to solid solutions which are ideal. In natural rocks, however, the presence of other elements commonly results in a departure from ideality in both garnet and biotite solutions. In recent years, detailed thermochemical work has led to the derivation of activity - composition relationships in solid solutions, allowing geothermometry calibrations to approximate more closely the thermodynamics of natural systems (Pigge and Greenwood 1982; Hodges and Spear, 1982; Indares and Martignole, 1984 and Hodges and Royden, 1984).

The exchange reaction is:



Thompson's (1976) calibration is based on empirical derivation from independent temperature estimates of natural assemblages. He combined compositional data on AFM assemblages with available experimental and thermochemical data in order to provide a pressure-temperature



calibration of continuous reactions. The derived equilibrium expression is:

$$0 = 5444.2 - 3.100T(^{\circ}\text{K}) + .0465P(\text{bars}) + RT\ln K$$

where  $K = (\text{Fe/Mg})_{\text{garnet}} / (\text{Fe/Mg})_{\text{biotite}}$

Although the effects of non-ideality are not specifically accounted for in this model, since the calibration is based on natural assemblages the effects of additional components is probably minimized. Thompson notes a  $\pm 50^{\circ}\text{C}$  error with the use of the calibration.

The Ferry and Spear (1978) calibration is based on experimental work in the purely binary Fe-Mg system between synthetic annite-phlogopite and almandine-pyrope. The distribution of Mg and Fe, is therefore taken to be ideal. Their calibration is expressed as:

$$0 = 12454 - 4.662T(^{\circ}\text{K}) + .057P(\text{bars}) + RT(K)\ln K$$

where  $K = (\text{Fe/Mg})_{\text{garnet}} / (\text{Fe/Mg})_{\text{biotite}}$

The application of this calibration to natural systems is limited in that the compositions of natural garnet and biotite deviate significantly from the model binary Fe-Mg solutions. As a result of this restriction this calibration has been criticized in the literature, in particular for not taking into account the

substitution of Ca and Mn in the garnet structure, hence yielding systematically low temperatures. The authors state that the thermometer has a maximum practical resolution of approximately  $\pm 50^\circ\text{C}$ , which corresponds to the error in temperature that results when  $\pm 0.01$  errors in the determination of molar compositions of components in garnet and biotite are propagated through the equation.

Hodges and Spear (1982) presented an improved calibration in which a consistent set of solution models were derived. In their approach they applied the Ferry and Spear (1978) thermometer to garnet - biotite - plagioclase -  $\text{Al}_2\text{SiO}_5$  - quartz bearing assemblages near the  $\text{Al}_2\text{SiO}_5$  triple point, to derive activity - composition relationships to account for the non-ideality in garnet and plagioclase solid solutions. The results of their study concluded that only pyrope - grossular mixing in the quaternary garnet system is significantly non-ideal at triple point conditions. Applying the non-ideal solutions, the equilibrium constant for the garnet-biotite thermometer becomes:

$$K^* = \frac{[(X_{\text{py}})^3(X_{\text{ann}})^3] * [\gamma_{\text{py}}]^3}{[(X_{\text{ph}})^3(X_{\text{al}})^3] * [\gamma_{\text{al}}]^3}$$

where  $X_{\text{py}} = \text{Mg}/\text{Mg}+\text{Fe}+\text{Ca}+\text{Mn}$  and  $X_{\text{al}} = \text{Fe}/\text{Fe}+\text{Mg}+\text{Ca}+\text{Mn}$

$$\gamma_{py}^{ga} / \gamma_{al}^{ga} = \exp \left[ \frac{(3300 - 1.5T_k)(X_{gr}^2 + X_{al}X_{gr} + X_{gr}X_{sp} + X_{py}X_{gr})}{RT(^{\circ}K)} \right. \\ \left. + \frac{W_{MgMn}(X_{sp}^2 + X_{gr}X_{sp} + X_{al}X_{sp} + X_{py}X_{sp})}{RT(^{\circ}K)} \right]$$

and

$$X_{ann}^{bi} = Fe / (Fe + Mg + Ti + Al^{VI}) \text{ and } X_{ph}^{bi} = Mg / (Mg + Fe + Ti + Al^{VI})$$

where the term  $[(\gamma_{py}^{ga})^3 / (\gamma_{al}^{ga})^3]$  accounts for non-ideality in the garnet solid solution. Fe-Mg substitution in biotite is considered to be ideal, as in Ferry and Spear (1978).

The garnet-biotite calibration of Hodges and Spear (1982) is therefore:

$$0 = 12454 - 4.662T(^{\circ}K) + .057P(\text{bars}) + RT(^{\circ}K)\ln K^*$$

Although the assumptions in this calibration are acceptable in the range of the  $Al_2SiO_5$  triple point conditions, their validity at P-T conditions greatly removed from the triple point is unclear. The authors note an error of  $\pm 50^{\circ}C$  for temperatures calculated with the calibration, although this error would be reduced for internally consistent calculated pressures and temperatures.

Pigage and Greenwood (1982) derived a theoretical calibration of the garnet-biotite equilibrium that takes into account the effect of Ca and Mn on the garnet Fe-Mg binary solution used in the Ferry and

Spear calibration. The thermometer corrects for any Ca and Mn component in the garnet by using the interaction parameters proposed by Ganguly (1979). The calibration is expressed as:

$$T(^{\circ}\text{K}) = \frac{1586X_{\text{Ca}} + 1308X_{\text{Mn}} + 2089 + 0.00956P(\text{bars})}{.78198 - \ln K}$$

where  $K = (\text{Mg/Fe})_{\text{garnet}} / (\text{Mg/Fe})_{\text{biotite}}$

and

$$X_1 = 1 / \text{Mg} + \text{Fe} + \text{Ca} + \text{Mn}$$

Pigage and Greenwood suggest an accuracy of about  $\pm 50^{\circ}\text{C}$  for their thermometer.

Indares and Martignole (1985) proposed a more elaborate geothermometry expression based on the Ferry and Spear (1978) equation, which takes into account the non-ideality of both garnet and biotite solid solutions. The expression is derived from a combination of an experimental calibration of the ideal part of the exchange reaction between garnet and biotite and an empirical calibration of the deviation from the non-ideal model. The empirical calibration takes into account the interaction of Al and Ti in the biotite lattice and the effect of Ca in Fe-Mg garnets. The proposed thermometer is expressed as:

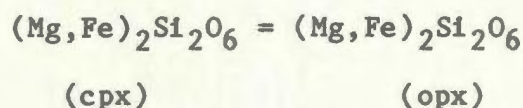
$$T(^{\circ}\text{K}) = \frac{12454 + 0.057P(\text{bars}) + 3(mX_{\text{Al}} + nX_{\text{Ti}}) - (W_{\text{Ca}} X_{\text{Ca}} + W_{\text{Mn}} X_{\text{Mn}})}{4.662 - 5.9616 \ln K_D}$$

where  $K_D = (\text{Fe/Mg})_{\text{garnet}} / (\text{Fe/Mg})_{\text{biotite}}$

and  $n$  and  $m$  are interaction parameters depending on the model adopted for the non-ideality in garnet. The thermometer is noted to be accurate to within  $\pm 50^\circ\text{C}$ .

#### A.5.1.2 Orthopyroxene - Clinopyroxene

Temperature variations of the position and shape of the solvus in the pyroxene quadrilateral have been employed by Wood and Banno (1973) and Wells (1977), based on the exchange reaction:



Wood and Banno's calibration is based on the approximation that the solubility of enstatite in diopside co-existing with orthopyroxene is an ideal solution. An empirical approach is taken to account for  $\text{Fe}^{2+}$  on the orthopyroxene - clinopyroxene miscibility gap in natural systems. The calibration is expressed as:

$$\frac{10202}{\ln(a_{\text{Mg}}^{\text{opx}} / a_{\text{Mg}}^{\text{cpx}}) - 7.65X_{\text{Fe}} - 3.88(X_{\text{Fe}}^{\text{opx}})^2 - 4.6}$$

where:

$$a_{\text{Mg}}^{\text{opx}} = X_{\text{Mg}}^{\text{opx}} * \gamma_{\text{Mg}}^{\text{opx}}$$

$$a_{\text{Mg}}^{\text{cpx}} = X_{\text{Mg}}^{\text{cpx}} * X_{\text{Ca}}^{\text{cpx}} * \gamma_{\text{MgCa}}^{\text{cpx}}$$

$$X_{\text{Fe}} = \text{Fe} / \text{Fe} + \text{Mg}$$

They state that there is a close agreement between calculated and observed temperatures ( $\pm 70^{\circ}\text{C}$ ) and in addition the calculated equilibration temperatures are independent of composition.

Wells's 1979 calibration is a semi-empirical formulation derived from available experimental data for the diopside - enstatite miscibility gap. The solubility of  $\text{Fe}^{2+}$  in the pyroxene solution has been calibrated empirically using experimental data for multicomponent pyroxenes. The derived equation which reproduces the miscibility gap over a wide range of temperatures is apparently applicable to aluminous pyroxenes with  $\text{Al}_2\text{O}_3$  up to 10 weight per cent. The equation is expressed as:

$$T = \frac{7341}{3.355 + 2.44X_{\text{Fe}} - \ln(a_{\text{Mg}}^{\text{cpx}} / a_{\text{Mg}}^{\text{opx}})}$$

Wells noted that providing the composition and equilibration conditions lie within the calibration range, his calibration should produce results which are accurate to within  $70^{\circ}\text{C}$ .

#### A.5.1.3 Garnet - Clinopyroxene

The temperature dependence of Mg-Fe exchange between garnet and clinopyroxene has long been recognized as a potential geothermometer. Several workers (Banno and Matsui 1965; Essene and Fyfe 1967; Banno 1970; Mysen and Heier 1972) noted the correlation between the distribution coefficient ( $K_D$ ) for the exchange reaction:



In recent years, additional studies have been conducted to evaluate the importance of various compositional parameters to  $K_D$  and to experimentally formulate garnet - clinopyroxene thermometers over a wide range of P-T-X conditions. Ellis and Green (1979) experimentally calibrated the effect of Ca on the distribution coefficient based on crystallization of garnet - clinopyroxene assemblages in the system  $\text{CaO} - \text{MgO} - \text{FeO} - \text{Al}_2\text{O}_3 - \text{SiO}_2$ . They noted that the effect of the Ca component is due to a combination of non-ideal Ca-Mg substitution between garnet and clinopyroxene. The expression they derived is:

$$T = \frac{[3104X_{\text{Fe}} + 3030 + 10.86P(\text{kbar})]}{\ln[(\text{Fe/Mg})_{\text{ga}} / (\text{Fe/Mg})_{\text{cpx}}] + 1.9034}$$

where  $X_{\text{Fe}} = \text{Fe} / \text{Fe} + \text{Mg}$  in cpx.

#### A.5.1.4 Garnet - Orthopyroxene

The exchange of Fe and Mg between garnet and orthopyroxene has been recently calibrated by Sen and Bhattacharya (1984) based on the reaction :



In this application, the orthopyroxene solution is taken to be



ideal in the temperature range for granulites and a ternary symmetrical solution has been adopted for garnet. Thermodynamic parameters for end-member solutions were taken from available data of Froese (1973) and O'Neill and Wood (1979). Taking the enthalpy, entropy and the volume data of Mg and Fe end-member components in garnet and orthopyroxene they obtained the expression:

$$T = \frac{2713 + 0.022P(\text{bars}) + 3300X_{\text{Ca}} + 195(X_{\text{Fe}} - X_{\text{Mg}})}{-1.9872 \ln K_D + 0.787 + 1.5X_{\text{Ca}}}$$

$$X_1 = 1/\text{Ca} + \text{Mg} + \text{Fe} + \text{Mn}$$

$$\text{where } K_D = [(X_{\text{Fe}}/X_{\text{Mg}})_{\text{opx}} / (X_{\text{Fe}}/X_{\text{Mg}})_{\text{ga}}]$$

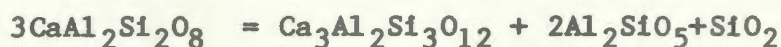
Comparison of Sen and Bhattacharya's thermometer with the garnet - clinopyroxene and clinopyroxene - orthopyroxene thermometers of Ellis and Green (1979) and Wood and Banno (1973) reveals a discrepancy of  $\pm 50^\circ\text{C}$ . Estimates determined from the garnet - orthopyroxene thermometers of Wells (1977) and Lindsley (1983) yield significantly lower temperatures. Sen and Bhattacharya (1984) state an accuracy of  $\pm 60^\circ\text{C}$  for their garnet - orthopyroxene thermometer.

#### A.5.2 Net Transfer Barometers

##### A.5.2.1 Garnet-Plagioclase- $\text{Al}_2\text{SiO}_5$ -Quartz

The equilibrium between grossular, anorthite,  $\text{Al}_2\text{SiO}_5$  and quartz for the net transfer reaction:





was first recognized as a potential geobarometer by Kretz (1959, 1964) and was studied experimentally by Hays (1967), Hariya and Kennedy (1968), Schmidt et al. (1978) and Goldsmith (1980). Recent calibrations proposed by Ghent (1976) as modified by Ghent et al. (1979) and Newton and Haselton (1981) have been applied in this study.

Ghent (1976) used equilibrium constant equations derived from experimental data on pure phases and an ideal solution model for garnet and plagioclase solid solutions, to define P-T curves calculated for different values of the distribution coefficient. He noted that the degree of non-ideality of grossular solid solution in garnet can be estimated from calculations using the activity coefficients of anorthite in plagioclase and the kyanite - sillimanite curve as a limiting case for kyanite and sillimanite - bearing assemblages. The equilibrium can be described by:

$$0 = \frac{-3272}{T(^{\circ}\text{K})} + 8.3969 - \frac{0.3448(P-1)}{T(^{\circ}\text{K})} + \log a_{\text{Ca}}^{\text{ga}} - 3 \log a_{\text{Ca}}^{\text{pl}} \text{ (kyanite)}$$

$$0 = \frac{-2551.4}{T(^{\circ}\text{K})} + 7.1711 - \frac{0.2842(P-1)}{T(^{\circ}\text{K})} + \log a_{\text{Ca}}^{\text{ga}} - 3 \log a_{\text{Ca}}^{\text{pl}} \text{ (sill)}$$

where

$$a_{\text{Ca}}^{\text{ga}} = (X_{\text{Ca}}^{\text{ga}})^3 * (\gamma_{\text{Ca}}^{\text{ga}})^3 \text{ and}$$

$$a_{\text{Ca}}^{\text{pl}} = (X_{\text{Ca}}^{\text{pl}}) * (\gamma_{\text{Ca}}^{\text{pl}})$$

$$X_{Ca}^{ga} = Ca / Ca+Mg+Fe+Mn$$

$$X_{Ca}^{pl} = Ca / Ca+Na+K$$

$$\gamma_{Ca}^{ga} = \exp[(3300-1.5T) * (X_{py} + X_{al}X_{py} + X_{py}X_{sp}) / RT]^3$$

$$\gamma_{Ca}^{pl} = \exp [(X_{ab}^2 (2025 + 9442X_{an}) / RT]$$

A revised version of the empirical calibration of Ghent (1976) was proposed by Ghent et al. (1979), in which an average value of the activity coefficient product  $K\gamma$  was obtained to correct for the values of  $a_{Ca}$  and  $a_{Ca}$ . Their estimate of  $K\gamma$  was based on selected samples which straddle the kyanite = sillimanite isograd, and values of the solids activity product,  $K_s$ , were obtained. Using these values of  $K_s$  and the position of the kyanite = sillimanite curve of Holdaway (1971) values of  $K\gamma$  for several P-T points on the isograd were obtained. Their results yielded an average log  $K_s$  value of -2.0 which led to an average log  $K\gamma$  value of -0.4. This average value can be added to the equilibrium equation of Ghent (1976) as an empirical correction to the values of the activities of grossular in garnet and anorthite in plagioclase.

Newton and Haselton (1981) applied recent solution and low temperature calorimetry in addition to experimental phase equilibrium data on garnet and plagioclase solid solution. The result was a more precise, experimental determination of the garnet - plagioclase -  $Al_2SiO_5$  - quartz assemblage, making possible a major improvement on non-ideal formulations.

If the temperature of crystallization of the assemblage is estimated independently, the pressure is given implicitly as a function of the temperature and the activities of the grossular

component in garnet and the anorthite component in plagioclase by:

$$\Delta G_A + RT \ln(a_{gr}^{ga} / a_{an}^{pl})^{3+P} \Delta V = 0$$

where  $G_A$  is expressed as:  $G_A = -P \Delta V_A$

and

$$a_{gr}^{ga} = \frac{X_{gr}^{ga} * \exp(3300-1.5T) * (X_{py} + X_{py}X_{al})^3}{RT(K)}$$

and

$$a_{an}^{pl} = X_{an}(1+X_{an})^2 * \exp \frac{(1-X_{an})^2}{(RT(^{\circ}K) * 2050+9392X_{an})}$$

The change in volume term ( $\Delta V$ ) is considered to be a very significant parameter since both the pyrope - grossular and almandine - grossular binary joins have large positive excess partial molal volumes near end-member grossular. In these compositional ranges, the partial molal volume of  $CaAl_{2/3}SiO_4$  will deviate considerably from the ideal molar volume. Therefore it is necessary to determine the partial molal volume of the grossular component for each compositional interval. Newton and Haselton (1981) show the partial molal volume relations for both the pyrope - grossular and almandine - grossular binary joins, after Cressey et al., (1978). Since the curves are nearly identical, the partial molal volumes of the grossular component in garnets may be determined directly from the figure.

Ganguly and Saxena (1984) revised the end member calculations for the garnet - plagioclase -  $Al_2SiO_5$  - quartz barometer proposed by Newton and Haselton (1981).



The calibrated geobarometer is expressed as:

$$0 = 13352 - 36.709T_K + \Delta V [P-1] + 1.9872T_K \ln (a_{gr}^{gr} / a_{an}^{pl})$$

(with kyanite)

and:

$$0 = 10055 - 31.101T_K + \Delta V [P-1] + 1.9872T_K \ln (a_{gr}^{gr} / a_{an}^{pl})$$

(with sill)

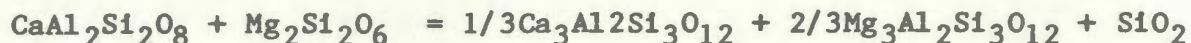
where  $\Delta V$  and  $P$  are expressed in cal/bar and kbar, respectively

#### A.5.2.2 Garnet-clinopyroxene-orthopyroxene-plagioclase-quartz

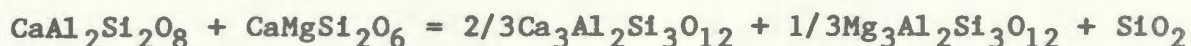
The reaction of garnet with pyroxene solid solutions was first calibrated from experimental phase equilibrium studies as a geobarometer by Wood and Banno (1973). Their calibration was based on the equilibrium of pyrope, enstatite and Mg-Tshermakite, which although was originally intended for application to garnet peridotites, has been widely applied to high grade crustal rocks (Weaver et al., 1978; Wells, 1979; Hormann et al., 1980). This calibration has some limitations due to inadequate experimental data for crustal ranges of pressure, temperature and mineral composition. In recent years, the improvement of activity - composition relations in both garnet and pyroxene solutions has resulted in the calibration of more widely applicable garnet - pyroxene geobarometers.

Newton and Perkins (1982) have calibrated two mineralogic geobarometers based on the assemblage garnet - plagioclase - pyroxene - quartz, which are applicable to granulite grade quartzofeldspathic

and basic lithologies. The equilibrium has been calibrated on the basis of the continuous reactions:



and



The calibrations have been derived almost entirely from thermodynamic quantities, in particular the enthalpy of solution and heat capacities. The activities of garnet solid-solution in the ternary system are adopted using the formulations of Ganguly and Kennedy (1974) and plagioclase activities were determined using the models of Kerrick and Darken (1975) and Newton et al. (1980). The pyroxene solution model assumes an ideal two-site mixing on the M1 and M2 structural sites in clinopyroxene and orthopyroxene (Wood and Banno 1973 and Wells 1979). The choice of temperature depends on mineralogic thermometry. Although this approach has inherent uncertainties, it turns out that the barometric indicators are quite insensitive to temperature uncertainties. The authors note that a temperature error of 100°C introduces pressure errors of only a few hundred bars. The calibrations are expressed as:

$$P(\text{bars}) = 3944 + 13.070T(\text{K}) + 3.50381\ln K_A$$

for orthopyroxene assemblages, where

$$K_A = (a_{\text{Ca}}^2 * a_{\text{Mg}})^{\text{ga}} / (a_{\text{Ca}}^{\text{pl}}) * (a_{\text{Mg}}^{\text{opx}})$$

and

$$P(\text{bars}) = 675 + 17.179T(\text{K}) + 3.59621\ln K_B$$

for clinopyroxene assemblages, where

$$K_B = (a_{Ca}^2 * a_{Mg})^{ga} / (a_{Ca}^{pl}) * (a_{CaMg}^{cpx})$$

where  $a_{Ca}^{ga} = X_{Ca}^{ga} * \gamma_{Ca}^{ga}$

$$a_{Mg}^{ga} = X_{Mg}^{ga} * \gamma_{Mg}^{ga}$$

$$a_{Ca}^{pl} = X_{Ca}^{pl} * \gamma_{Ca}^{pl}$$

$$a_{Mg}^{opx} = X_{Mg}^{M2} * X_{Mg}^{M1} \text{ in opx}$$

$$a_{CaMg} = X_{Ca}^{M2} * X_{Mg}^{M1} \text{ in cpx}$$

APPENDIX 6MICROPROBE ANALYTICAL PROCEDURE

All mineral analyses used in geothermobarometry calculations were conducted at the Department of Earth Sciences, Memorial University of Nfld, using a fully automated JEOL JXA-50A wavelength dispersive electron microprobe with Krisel control, equipped with three spectrometers and a Digital Equipment Corporation PDP-11 computer with teleprinter. The microprobe was operated with a beam current of 22 nanoamps and an accelerating voltage of 15 kv. Counts were made for 30 seconds or to a maximum of 60,000. Beam diameter was set for 1-2 micrometers. Bence-Albee corrections were employed in data reduction, and analyses were performed using a variety of calibration standards. The majority of analyses were calibrated with the "FCPX" clinopyroxene standard. This standard, among others, was analyzed routinely during operation of the microprobe. Since microprobe analyses are unable to distinguish ferric from ferrous iron, total iron in all analyses is expressed as FeO.

For each geothermometry - geobarometry assemblage, between 3 and 6 analyses of each mineral phase was performed to assess the compositional consistency of co-existing phases. Within each polished thin section, analyses were carried out both on mineral phases in contact as well as grains which were separated generally by 2 - 3 grains, to assess possible discrepancies due to local retrograde re-equilibration between minerals in contact. Each grain was analysed

an average of 4 times, generally performed as 2 core and 2 - 3 rim spot analyses. Point analyses were performed on mineral grains and mineral pairs which exhibited both textural and chemical equilibrium to minimize possible analyses of disequilibrium relationships. Analyses from each assemblage, using rim analyses, were utilized to compute P-T estimates for each sample



APPENDIX 7 $^{40}\text{Ar}/^{39}\text{Ar}$  RADIOMETRIC DATING PROCEDURE

$^{40}\text{Ar}/^{39}\text{Ar}$  radiometric dating analyses were carried out in the Department of Physics at Dalhousie University under the supervision of Dr. P. Reynolds and Mr. K. Taylor. Irradiations were performed in the McMaster University nuclear reactor. Samples were wrapped individually in aluminum foil and arranged in a vertical stack inside a cadmium shield with an aluminum irradiation canister. Interdispersed among the samples were 9 standards, either the laboratory standard NS 231/232 (Reynolds et. al., 1973) or the widely distributed hornblende standard MM Hb-1 (Alexander et.al., 1978). The J value appropriate for a given sample was interpolated from values obtained from the standards.

Samples were outgassed in a step-wise fashion in a quartz tube placed inside a Lindberg tube-type furnace, which is connected on-line to the mass spectrometer. Temperatures were precisely and accurately maintained by a thermocouple-controlled regulator. Heating steps were approximately 1 hour in duration. Extracted gases cleaned by means of a titanium "getter" operated at 600°C were subsequently analyzed by a substantially modified MS 10 mass spectrometer (operated in the static mode). Data acquisition and subsequent analyses were carried out automatically under the control of an Apple IIe computer. Decay and isotopic constants are those suggested by Steiger and Jager (1977). Corrections for interfering isotopes were

made on the basis of correction factors determined for the McMaster University reactor by York (personal communication to P.H.Reynolds, 1984).

APPENDIX 8.1. Compositional parameters of garnet-biotite and plagioclase rims in paragneiss.

Sample #	Mg/Mg+Fe	Garnet			Biotite Mg/Mg+Fe	Plagioclase	
		XCa	XMn	XFe		Xan	Xab
CG81-148	.1648	.0432	.1625	.6634	.4775	.3719	.6254
CG81-155	.2655	.0418	.1409	.6003	.6178	.4246	.5698
CG81-170B	.2919	.0323	.0464	.6523	.6009	.4537	.5410
CG81-239	.2301	.0517	.3275	.4778	.5717	.3835	.6129
CG81-299A	.1547	.0759	.2099	.5891	.4385	.3182	.6789
CG81-476	.1826	.0923	.0342	.7050	.5033	.4238	.5712
CG81-479	.3159	.0541	.0265	.7209	.5302	.4996	.5003
CG81-749A	.1661	.0661	.1576	.6472	.4435	.2656	.7213
CG81-756	.1809	.0546	.2253	.5898	.5544	.3913	.5998
GF81-16	.2662	.0593	.4161	.3837	.6426	.3045	.6846
GF81-18	.2144	.0639	.3743	.4412	.5983	.3287	.6698
GF81-23	.3199	.0522	.3644	.3967	.6863	.3312	.6709
GF81-141	.2014	.0345	.0093	.7635	.4903	.3855	.6102
GF81-235B	.1506	.0386	.0710	.7562	.3893	.4379	.5587
VAN84-12H	.1228	.0591	.1556	.6288	.4015	.3818	.6133
VAN84-12N	.1999	.0376	.1146	.6782	.5348	.3994	.5987
VAN84-16E	.2205	.0610	.4204	.3968	.5976	.2605	.7320
VAN84-34A	.2965	.0325	.1338	.5864	.5809	.3676	.6310
VAN84-35B	.3510	.0439	.0911	.5295	.6498	.3200	.6720
VAN84-36	.2927	.0421	.1802	.5499	.6115	.4194	.5710
VN84-102	.3014	.0134	.1433	.5890	.6569	.4145	.5745
VN84-150	.1437	.0242	.1698	.4270	.3867	.2020	.7898
VN84-338	.3316	.0236	.1733	.4263	.6942	.1963	.7984
VO81-77A	.2460	.0896	.1464	.4862	.5509	.2193	.7765
VO81-518	.1475	.0392	.0281	.7131	.4356	.2571	.7410

$$X_1(\text{garnet}) = 1/\text{Mg}+\text{Fe}+\text{Ca}+\text{Mn}$$

$$X_1(\text{plagioclase}) = 1/\text{Ca}+\text{Na}+\text{K}$$

APPENDIX 8.2 Compositional parameters of garnet - orthopyroxene - clinopyroxene and plagioclase in mafic rocks.

Sample #	Garnet				Opx		Cpx		Plagioclase	
	Xal	Xpy	Xgr	Xsp	XMg	XFe	XMg	XFe	Xan	Xab
CG81-366	.5398	.1637	.2703	.0262	-	-	.0153	.5928	.3021	.6823
CG81-488A	.6257	.1694	.1493	.0556	-	-	.0494	.5399	.3724	.6148
CG81-641	.6487	.0447	.2427	.0609	.0568	.4717	.0061	.2871	.0646	.9289
CG81-811B	.5074	.2871	.1864	.0191	.3605	.1343	-	-	.3545	.6246
CG84-362	.5269	.2901	.1712	.0118	.4063	.1183	.0448	.5945	.3888	.5866
GF81-222	.3913	.3933	.2041	.0112	-	-	.0426	.5138	.6532	.3449
CF81-244A	.3893	.4423	.1576	.0108	.6119	.0311	.0996	.5813	.7046	.2680
GF81-246A	.5292	.2696	.1802	.0209	.3588	.2061	.0324	.4802	.3969	.5867
VO81-89A	.5119	.2790	.1795	.0295	.3601	.1161	-	-	.2719	.7281
VO81-188	.4599	.3844	.1349	.0207	.4536	.0886	.0024	.5299	.4827	.5115
VN84-229	.6858	.0892	.1675	.0574	.4683	.2598	.0346	.5178	.4387	.5528
VN84-431	.5848	.2054	.1825	.0273	.2824	.1827	.0323	.5222	.3663	.6222
CG84-100	-	-	-	-	.3438	.2146	.0468	.5662	.4563	.5267
GF81-121	-	-	-	-	.2261	.2357	.0263	.5093	.4760	.5212
VAN84-19	-	-	-	-	.3288	.2334	.0319	.5210	.4044	.5725
VN84-534	-	-	-	-	.4452	.1289	.0471	.5399	.4567	.5381

$Xi(\text{garnet}) = 1/Mg+Fe+Mn+Ca$

$Xi(\text{opx}) = 1/Mg+Fe$

$Xi(\text{cpx}) = 1/Mg+Fe$

$Xi(\text{plagioclase}) = 1/Ca+Na+K$

**APPENDIX 8.3** Activities of garnet - plagioclase - clinopyroxene - orthopyroxene  
and plagioclase in mafic rocks.

Sample #	Garnet		Plag		Cpx		Opx		$\ln K_a$	$\ln K_b$
	$a_{gr}$	$a_{py}$	$a_{an}$	$a_{di}$	$a_{en}$	$a_{fs}$	$a_{en}$	$a_{fs}$		
CG81-366	.2926	.3419	.4951	.5928	.0153	.0025	-	-	-	-2.59
CG81-488A	.2013	.2994	.4752	.5399	.0494	.0083	-	-	-2.67	-
CG81-641	.2502	.0582	.0588	.2871	.0067	.0197	.0568	.4717	-1.37	-1.55
CG81-811B	.2197	.3152	.4523	-	-	-	.3605	.1343	-2.01	-
CG84-362	.1967	.3336	.4951	.5945	.0448	.0051	.4063	.1183	-2.21	-2.59
GF81-222	.2596	.4331	.7083	.5138	.0426	.0043	-	-	-	-2.52
GF81-244A	.2059	.4688	.7171	.5813	.0996	.0035	.6119	.0311	-2.27	-2.65
GF81-246A	.2127	.2976	.5091	.4802	.0342	.0067	.3588	.2601	-2.27	-2.24
VO81-89A	.1979	.3066	.3375	-	-	-	.3601	.1161	-1.76	-
VO81-188	.2031	.4199	.4790	.5299	.0024	.0003	.4536	.0885	-1.80	-2.68
VN84-229	.2410	.2571	.3529	.5397	.0210	.0064	-	-	-	-2.83
VN84-431	.2076	.2295	.4591	.5222	.0176	.0070	.2824	.1827	-2.47	-3.18
CG84-100	-	-	-	.5662	.0468	.0078	.3438	.2164	-	-
GF81-121	-	-	-	.5093	.0263	.0084	.2261	.2357	-	-
VN84-19	-	-	-	.5210	.0319	.0094	.3288	.2333	-	-
VN84-534	-	-	-	.5399	.0471	.0058	.4452	.1289	-	-

APPENDIX 8.4 Composition of hornblende samples used in  $^{40}\text{Ar}/^{39}\text{Ar}$  dating. Hornblende structural formula calculated on the basis of 23 oxygen atoms.

	<u>17D</u>	<u>18A</u>	<u>14B</u>	<u>32A</u>	<u>23B</u>	<u>22B</u>	<u>21A</u>
Na <sub>2</sub> O	1.72	1.43	1.75	1.82	1.54	1.64	1.53
MgO	11.46	10.53	9.07	10.27	12.84	10.82	11.36
Al <sub>2</sub> O <sub>3</sub>	11.04	10.95	11.16	11.65	9.84	10.22	10.53
SiO <sub>2</sub>	42.12	42.61	41.90	42.13	43.69	42.64	43.23
K <sub>2</sub> O	1.43	1.52	1.05	1.38	1.19	1.07	1.10
CaO	11.93	12.01	11.69	11.78	11.59	11.35	11.67
TiO <sub>2</sub>	.71	.58	.65	.73	.92	1.04	.89
Cr <sub>2</sub> O <sub>3</sub>	.07	.03	.04	.05	.09	.01	.03
MnO	.21	.30	.20	.18	.19	.33	.27
FeO	14.62	15.75	18.51	14.35	13.20	16.52	15.35
Total	95.14	96.00	95.73	94.29	95.41	95.56	96.07
Na <sub>2</sub> O	.451	.440	.427	.436	.534	.456	.472
MgO	2.625	2.432	2.097	2.298	2.901	2.479	2.620
Al <sub>2</sub> O <sub>3</sub>	1.999	1.876	2.038	2.132	1.757	1.851	1.934
SiO <sub>2</sub>	6.474	6.576	6.497	6.489	6.625	6.562	6.583
K <sub>2</sub> O	.279	.285	.205	.267	.227	.208	.214
CaO	1.962	1.993	1.938	1.952	1.882	1.896	1.932
TiO <sub>2</sub>	.081	.069	.073	.086	.102	.117	.095
Cr <sub>2</sub> O <sub>3</sub>	.004	.002	.004	.005	.009	-	.003
MnO	.027	.032	.022	.020	.022	.022	.019
FeO	1.876	2.101	2.397	1.832	1.673	2.122	1.974
Total	15.779	15.797	15.699	15.517	15.731	15.704	15.846

APPENDIX 8.5 MICROPROBE ANALYSES

Minerals: GNT - Garnet  
          BIO - Biotite  
          PLA - Plagioclase  
          COR - Cordierite  
          OPX - Orthopyroxene  
          CPX - Clinopyroxene

Codes: R - Rim of grain  
          C - Core of grain  
          1 - Average of several grains

Oxygen Basis: Garnet - 12  
                  Biotite - 22  
                  Plagioclase - 8  
                  Cordierite - 18  
                  Orthopyroxene - 6  
                  Clinopyroxene - 6

SAMPLE# MINERAL Code	CG-148 GNT C	CG-148 GNT C	CG-148 BIO I	CG-148 PLA R
SiO2	38.24	37.89	37.12	61.79
TiO2	0.00	0.00	2.78	0.00
Al2O3	20.70	20.55	17.20	23.20
Cr2O3	0.00	0.00	0.01	0.00
FeO	27.67	28.00	18.00	0.04
MnO	6.78	6.88	0.00	0.00
MgO	5.46	5.13	13.48	0.00
CaO	1.80	1.77	0.00	5.51
Na2O	0.00	0.00	0.11	9.06
K2O	0.00	0.00	8.93	0.25
SUM	100.65	100.22	97.63	99.85
Si	3.018	3.013	2.726	2.754
Ti	0.000	0.000	0.154	0.000
Al	1.926	1.926	1.489	1.219
Cr	0.000	0.000	0.001	0.000
Fe	1.827	1.862	1.105	0.001
Mn	0.453	0.463	0.000	0.000
Mg	0.642	0.608	1.475	0.000
Ca	0.152	0.151	0.000	0.263
Na	0.000	0.000	0.016	0.783
K	0.000	0.000	0.837	0.014
SUM	8.018	8.024	7.802	5.035
Mg/Mg+Fe	0.260	0.246	0.572	0.000
Al4	0.000	0.000	1.274	0.246
Al6	1.926	1.926	0.215	0.973

SAMPLE# MINERAL Code	CG-155 GNT R	CG-155 GNT C	CG-155 BIO I	CG-155 PLA R
SiO2	39.14	39.58	38.54	62.00
TiO2	0.00	0.00	2.32	0.00
Al2O3	21.19	20.90	16.77	23.51
Cr2O3	0.00	0.00	0.00	0.00
FeO	23.99	23.64	10.74	0.04
MnO	5.63	5.33	0.09	0.04
MgO	8.67	9.44	17.36	0.00
CaO	1.67	1.64	0.01	6.34
Na2O	0.00	0.00	0.20	8.41
K2O	0.00	0.00	10.39	0.21
SUM	100.29	100.53	96.42	100.55
Si	3.024	3.040	2.789	2.745
Ti	0.000	0.000	0.126	0.000
Al	1.930	1.892	1.431	1.227
Cr	0.000	0.000	0.000	0.000
Fe	1.550	1.519	0.650	0.001
Mn	0.369	0.347	0.006	0.001
Mg	0.998	1.081	1.872	0.000
Ca	0.138	0.135	0.001	0.301
Na	0.000	0.000	0.028	0.722
K	0.000	0.000	0.959	0.012
SUM	8.010	8.013	7.863	5.009
Mg/Mg+Fe	0.392	0.416	0.742	0.000
Al4	0.000	0.000	1.211	0.255
Al6	1.930	1.892	0.220	0.971



SAMPLE/ MINERAL Code	CG-170B GNT R	CG-170B GNT C	CG-170B BIO I	CG-170B FLA R	CG-170B FLA C	CG-170B CCR R
SiO2	39.54	39.27	39.03	62.26	61.25	47.62
TiO2	0.00	0.00	1.91	0.03	0.00	0.00
Al2O3	21.34	21.23	16.92	23.59	23.36	32.14
Cr2O3	0.00	0.00	0.05	0.00	0.00	0.00
FeO	25.46	26.18	11.38	0.03	0.04	4.92
MnO	1.81	1.73	0.02	0.01	0.02	0.05
MgO	10.50	10.51	17.79	0.00	0.00	12.95
CaO	1.26	1.26	0.00	6.51	5.91	0.24
Na2O	0.00	0.00	0.27	7.77	9.31	0.17
K2O	0.00	0.00	8.09	0.07	0.09	0.21
SUM	99.91	100.18	95.46	100.27	99.98	98.30
Si	3.029	3.012	2.817	2.754	2.733	0.000
Ti	0.000	0.000	0.104	0.001	0.000	0.000
Al	1.927	1.919	1.440	1.230	1.229	0.000
Cr	0.000	0.000	0.003	0.000	0.000	0.000
Fe	1.631	1.679	0.687	0.001	0.001	0.000
Mn	0.117	0.112	0.001	0.000	0.001	0.000
Mg	1.199	1.201	1.914	0.000	0.000	0.000
Ca	0.103	0.104	0.000	0.309	0.283	0.000
Na	0.000	0.000	0.038	0.666	0.806	0.000
K	0.000	0.000	0.745	0.004	0.005	0.000
SUM	8.007	8.028	7.749	4.965	5.058	0.000
Mg/Mg+Fe	0.424	0.417	0.736	0.000	0.000	0.000
Al4	0.000	0.000	1.183	0.246	0.267	0.000
Al6	1.927	1.919	0.257	0.984	0.962	0.000

SAMPLE/ MINERAL Code	CG-239 GNT R	CG-239 GNT C	CG-239 BIO I	CG-239 FLA R	CG-239 FLA C
SiO2	38.66	38.92	38.07	62.16	59.47
TiO2	0.01	0.01	2.26	0.00	0.00
Al2O3	21.79	21.78	18.91	24.10	24.77
Cr2O3	0.02	0.00	0.01	0.02	0.01
FeO	19.77	19.93	11.36	0.06	0.04
MnO	13.55	13.92	0.34	0.01	0.00
MgO	5.91	6.33	15.13	0.00	0.00
CaO	2.14	1.47	0.00	5.67	5.93
Na2O	0.01	0.04	0.07	8.99	9.25
K2O	0.01	0.01	9.64	0.37	0.28
SUM	101.87	102.41	95.79	101.38	99.75
Si	2.993	2.996	2.763	2.732	2.668
Ti	0.001	0.001	0.123	0.000	0.000
Al	1.988	1.976	1.618	1.248	1.310
Cr	0.001	0.000	0.001	0.001	0.000
Fe	1.280	1.283	0.690	0.002	0.002
Mn	0.888	0.908	0.021	0.000	0.000
Mg	0.682	0.726	1.637	0.000	0.000
Ca	0.178	0.121	0.000	0.267	0.285
Na	0.002	0.006	0.010	0.766	0.805
K	0.001	0.001	0.893	0.021	0.016
SUM	8.013	8.018	7.755	5.037	5.086
Mg/Mg+Fe	0.348	0.361	0.704	0.000	0.000
Al4	0.007	0.004	1.237	0.268	0.332
Al6	1.981	1.973	0.381	0.980	0.979

SAMPLE/ MINERAL Code	CG-299A GNT R	CG-299A BIO I	CG-299A PLA R	CG-299A GNT C
SiO2	38.73	38.43	62.67	38.14
TiO2	0.00	0.31	0.00	0.01
Al2O3	20.95	19.51	24.46	21.05
Cr2O3	0.01	0.04	0.01	0.01
FeO	24.75	15.39	0.03	25.02
MnO	8.82	0.18	0.01	8.43
MgO	4.53	12.02	0.02	5.12
CaO	3.19	0.00	4.43	3.24
Na2O	0.01	0.09	9.32	0.01
K2O	0.01	8.86	0.17	0.00
SUM	101.00	94.83	101.12	101.03
Si	3.040	2.846	2.746	2.997
Ti	0.000	0.017	0.000	0.001
Al	1.939	1.703	1.264	1.950
Cr	0.001	0.002	0.000	0.001
Fe	1.625	0.953	0.001	1.644
Mn	0.586	0.011	0.000	0.561
Mg	0.530	1.326	0.001	0.600
Ca	0.268	0.000	0.208	0.273
Na	0.002	0.013	0.792	0.002
K	0.001	0.837	0.010	0.000
SUM	7.991	7.709	5.022	8.028
Mg/Mg+Fe	0.246	0.582	0.543	0.267
Al4	0.000	1.154	0.254	0.003
Al6	1.939	0.549	1.010	1.947

SAMPLE/ MINERAL Code	CG-476 GNT R	CG-476 GNT C	CG-476 BIO I	CG-476 PLA R	CG-476 PLA C
SiO2	38.99	38.35	38.07	60.84	61.52
TiO2	0.06	0.06	5.71	0.00	0.00
Al2O3	20.91	20.79	13.58	23.84	23.89
Cr2O3	0.00	0.03	0.02	0.00	0.00
FeO	28.64	28.52	14.30	0.04	0.00
MnO	1.39	1.45	0.03	0.01	0.00
MgO	6.84	7.14	14.49	0.00	0.00
CaO	3.75	3.63	0.00	6.54	6.41
Na2O	0.00	0.00	8.13	8.74	9.30
K2O	0.00	0.00	8.73	0.15	0.16
SUM	100.58	99.97	95.06	100.16	101.28
Si	3.031	3.004	2.829	2.712	2.715
Ti	0.004	0.004	0.319	0.000	0.000
Al	1.916	1.920	1.189	1.253	1.243
Cr	0.000	0.002	0.001	0.000	0.000
Fe	1.862	1.868	0.889	0.001	0.000
Mn	0.092	0.096	0.002	0.000	0.000
Mg	0.792	0.833	1.605	0.000	0.000
Ca	0.312	0.305	0.000	0.312	0.303
Na	0.000	0.000	0.019	0.755	0.796
K	0.000	0.000	0.828	0.009	0.009
SUM	8.008	8.032	7.680	5.043	5.066
Mg/Mg+Fe	0.299	0.308	0.644	0.000	0.000
Al4	0.000	0.000	1.171	0.288	0.285
Al6	1.916	1.920	0.018	0.965	0.958

SAMPLE/ MINERAL Code	CG-479 GNT R	CG-479 GNT C	CG-479 BIO I	CG-479 FLA R	CG-479 FLA C
SiO2	38.76	38.35	37.55	60.66	60.73
TiO2	0.02	0.02	4.39	0.00	0.00
Al2O3	21.13	21.25	15.46	23.65	24.25
Cr2O3	0.03	0.02	0.01	0.00	0.00
FeO	29.06	31.19	13.05	0.00	0.02
MnO	1.07	0.42	0.02	0.00	0.00
MgO	8.00	8.52	14.73	0.01	0.00
CaO	2.18	2.18	0.00	7.16	6.77
Na2O	0.00	0.00	0.08	6.92	8.63
K2O	0.00	0.00	8.74	0.25	0.28
SUM	100.25	101.95	94.03	98.65	100.68
Si	3.012	2.954	2.799	2.731	2.697
Ti	0.001	0.001	0.246	0.000	0.000
Al	1.936	1.929	1.358	1.255	1.269
Cr	0.002	0.001	0.001	0.000	0.000
Fe	1.889	2.009	0.813	0.000	0.001
Mn	0.070	0.027	0.001	0.000	0.000
Mg	0.927	0.978	1.636	0.001	0.000
Ca	0.182	0.180	0.000	0.345	0.322
Na	0.000	0.000	0.012	0.604	0.743
K	0.000	0.000	0.831	0.014	0.016
SUM	8.018	8.080	7.697	4.951	5.048
Mg/Mg+Fe	0.329	0.327	0.668	1.000	0.000
Al4	0.000	0.046	1.201	0.269	0.303
Al6	1.936	1.883	0.157	0.986	0.966

SAMPLE/ MINERAL Code	CG-749B GNT R	CG-749B GNT C	CG-749B BIO I	CG-749B FLA R	CG-749B FLA C
SiO2	37.57	36.89	37.75	63.92	63.68
TiO2	0.13	0.12	2.43	0.00	0.01
Al2O3	18.92	18.78	14.94	21.50	21.19
Cr2O3	0.00	0.00	0.00	0.01	0.00
FeO	18.48	18.77	19.54	0.11	0.09
MnO	10.18	9.50	0.57	0.03	0.00
MgO	1.57	1.56	10.84	0.02	0.00
CaO	12.61	12.62	0.00	3.89	3.77
Na2O	0.00	0.00	0.07	9.80	10.39
K2O	0.00	0.00	9.02	0.18	0.20
SUM	99.46	98.24	95.16	99.46	99.33
Si	3.031	3.016	2.876	2.844	2.843
Ti	0.008	0.007	0.139	0.000	0.000
Al	1.800	1.810	1.342	1.128	1.115
Cr	0.000	0.000	0.000	0.000	0.000
Fe	1.247	1.284	1.245	0.004	0.003
Mn	0.696	0.658	0.037	0.001	0.000
Mg	0.189	0.190	1.231	0.001	0.000
Ca	1.090	1.106	0.000	0.185	0.180
Na	0.000	0.000	0.010	0.845	0.900
K	0.000	0.000	0.877	0.010	0.011
SUM	8.061	8.071	7.757	5.020	5.054
Mg/Mg+Fe	0.131	0.129	0.497	0.245	0.000
Al4	0.000	0.000	1.124	0.156	0.157
Al6	1.800	1.810	0.218	0.972	0.959

SAMPLE# MINERAL Code	CG-756 QNT R	CG-756 QNT C	CG-756 BIO I	CG-756 PLA R	CG-756 PLA C
SiO2	38.06	37.95	38.41	61.42	60.95
TiO2	0.00	0.02	1.66	0.00	0.01
Al2O3	20.54	20.46	18.11	23.53	23.28
Cr2O3	0.00	0.00	0.00	0.00	0.00
FeO	24.32	25.24	12.52	0.01	0.01
MnO	9.29	7.26	0.05	0.00	0.02
MgO	5.37	6.27	15.58	0.00	0.00
CaO	2.25	1.63	0.00	6.03	5.79
Na2O	0.00	0.00	0.21	9.20	9.07
K2O	0.00	0.00	8.71	0.18	0.17
SUM	99.83	98.83	95.25	100.37	99.30
Si	3.023	3.027	2.801	2.730	2.736
Ti	0.000	0.001	0.091	0.000	0.000
Al	1.923	1.924	1.557	1.233	1.232
Cr	0.000	0.000	0.000	0.000	0.000
Fe	1.616	1.684	0.764	0.000	0.000
Mn	0.625	0.490	0.003	0.000	0.001
Mg	0.636	0.745	1.693	0.000	0.000
Ca	0.192	0.139	0.000	0.287	0.278
Na	0.000	0.000	0.030	0.793	0.789
K	0.000	0.000	0.810	0.010	0.010
SUM	8.015	8.010	7.749	5.054	5.047
Mg/Mg+Fe	0.282	0.307	0.689	0.000	0.000
Al4	0.000	0.000	1.199	0.270	0.264
Al6	1.923	1.924	0.358	0.964	0.968

SAMPLE# MINERAL Code	GF81-16 QNT R	GF81-16 QNT C	GF81-16 BIO I	GF81-16 PLA R	GF81-16 PLA C
SiO2	38.32	38.32	39.35	66.06	65.73
TiO2	0.01	0.00	2.05	0.00	0.00
Al2O3	20.81	20.64	17.03	22.20	21.14
Cr2O3	0.00	0.01	0.00	0.00	0.00
FeO	15.86	14.93	9.51	0.04	0.03
MnO	17.20	17.14	0.53	0.01	0.01
MgO	5.82	5.77	17.10	0.00	0.00
CaO	2.45	2.23	0.00	3.98	3.65
Na2O	0.00	0.00	0.09	8.98	9.25
K2O	0.00	0.00	9.33	0.11	0.07
SUM	100.47	99.04	94.99	101.38	99.88
Si	3.014	3.042	2.851	2.865	2.892
Ti	0.001	0.000	0.112	0.000	0.000
Al	1.929	1.932	1.454	1.135	1.097
Cr	0.000	0.001	0.000	0.000	0.000
Fe	1.043	0.991	0.576	0.001	0.001
Mn	1.146	1.153	0.033	0.000	0.000
Mg	0.682	0.683	1.846	0.000	0.000
Ca	0.206	0.190	0.000	0.185	0.172
Na	0.000	0.000	0.013	0.755	0.789
K	0.000	0.000	0.862	0.006	0.004
SUM	8.021	7.991	7.747	4.948	4.956
Mg/Mg+Fe	0.395	0.408	0.762	0.000	0.000
Al4	0.000	0.000	1.149	0.135	0.108
Al6	1.929	1.932	0.305	1.000	0.989

SAMPLE/ MINERAL Code	GF81-18 GNT R	GF81-18 GNT, C	GF81-18 BIO I	GF81-18 PLA R	GF81-18 PLA C
SiO2	39.86	39.36	39.27	65.30	63.46
TiO2	0.00	0.01	1.50	0.00	0.00
Al2O3	20.60	21.14	17.43	22.54	22.21
Cr2O3	0.00	0.00	0.00	0.00	0.00
FeO	17.66	18.35	11.13	0.00	0.03
MnO	14.98	13.90	0.36	0.04	0.01
MgO	4.82	6.01	16.58	0.02	0.00
CaO	2.56	2.45	0.00	4.24	4.20
Na2O	0.02	0.02	0.12	8.43	10.21
K2O	0.01	0.02	9.27	0.23	0.19
SUM	100.51	101.26	95.66	100.80	100.31
Si	3.115	3.050	2.842	2.849	2.809
Ti	0.000	0.001	0.082	0.000	0.000
Al	1.898	1.931	1.487	1.159	1.159
Cr	0.000	0.000	0.000	0.000	0.000
Fe	1.154	1.189	0.674	0.000	0.001
Mn	0.992	0.912	0.022	0.001	0.000
Mg	0.561	0.694	1.789	0.001	0.000
Ca	0.214	0.203	0.000	0.198	0.199
Na	0.003	0.003	0.017	0.713	0.876
K	0.001	0.002	0.856	0.013	0.011
SUM	7.938	7.986	7.769	4.935	5.055
Mg/Mg+Fe	0.327	0.369	0.726	1.000	0.000
Al4	0.000	0.000	1.158	0.151	0.191
Al6	1.898	1.931	0.330	1.008	0.968

SAMPLE/ MINERAL Code	GF81-23 GNT R	GF81-23 GNT C	GF81-23 BIO I	GF81-23 PLA C
SiO2	40.13	40.00	39.87	65.36
TiO2	0.02	0.00	1.84	0.03
Al2O3	20.99	21.42	17.24	21.88
Cr2O3	0.00	0.00	0.00	0.00
FeO	15.88	15.96	8.50	0.03
MnO	14.59	12.57	0.28	0.01
MgO	7.47	8.80	18.60	0.01
CaO	2.09	2.70	0.00	4.23
Na2O	0.02	0.06	0.06	8.43
K2O	0.01	0.02	9.17	0.11
SUM	101.20	101.53	95.56	100.09
Si	3.078	3.039	2.848	2.869
Ti	0.001	0.000	0.099	0.001
Al	1.898	1.918	1.452	1.132
Cr	0.000	0.000	0.000	0.000
Fe	1.019	1.014	0.508	0.001
Mn	0.948	0.809	0.017	0.000
Mg	0.854	0.996	1.980	0.001
Ca	0.172	0.220	0.000	0.199
Na	0.003	0.009	0.008	0.717
K	0.001	0.002	0.836	0.006
SUM	7.973	8.007	7.749	4.926
Mg/Mg+Fe	0.456	0.496	0.796	0.373
Al4	0.000	0.000	1.152	0.131
Al6	1.898	1.918	0.300	1.001

SAMPLE/ MINERAL Code	GF-141 GNT R	GF-141 GNT C	GF-141 BIO I	GF-141 FLA R	GF-141 FLA C
SiO2	38.47	37.97	37.51	61.50	61.58
TiO2	0.00	0.09	4.90	0.00	0.00
Al2O3	21.08	20.91	15.83	23.51	23.63
Cr2O3	0.02	0.00	0.03	0.00	0.00
FeO	31.17	30.85	14.18	0.00	0.00
MnO	0.38	0.36	0.02	0.00	0.00
MgO	7.86	7.76	13.64	0.02	0.00
CaO	1.41	1.36	0.00	5.79	6.42
Na2O	0.00	0.00	0.14	9.03	7.27
K2O	0.00	0.00	8.86	0.20	0.29
SUM	100.39	99.30	95.11	100.05	99.19
Si	3.000	2.994	2.780	2.738	2.751
Ti	0.000	0.005	0.273	0.000	0.000
Al	1.938	1.944	1.383	1.234	1.245
Cr	0.001	0.000	0.002	0.000	0.000
Fe	2.033	2.034	0.879	0.000	0.000
Mn	0.025	0.024	0.001	0.000	0.000
Mg	0.914	0.912	1.507	0.001	0.000
Ca	0.118	0.115	0.000	0.276	0.307
Na	0.000	0.000	0.020	0.780	0.630
K	0.000	0.000	0.838	0.011	0.017
SUM	8.030	8.028	7.683	5.040	4.949
Mg/Mg+Fe	0.310	0.310	0.632	1.000	0.000
Al4	0.000	0.006	1.220	0.262	0.249
Al6	1.938	1.938	0.163	0.972	0.996

SAMPLE/ MINERAL Code	GF-235B GNT R	GF-235B GNT C	GF-235B BIO I	GF-235B FLA R	GF-235B FLA C
SiO2	37.90	38.26	36.83	62.64	62.44
TiO2	0.00	0.00	3.55	0.00	0.00
Al2O3	20.71	20.54	17.23	23.19	22.99
Cr2O3	0.00	0.01	0.00	0.00	0.00
FeO	31.74	31.34	17.80	0.01	0.02
MnO	2.98	2.59	0.09	0.02	0.02
MgO	5.63	6.07	11.35	0.00	0.00
CaO	1.62	1.56	0.01	5.17	5.23
Na2O	0.00	0.00	0.11	9.55	9.44
K2O	0.00	0.00	8.34	0.14	0.16
SUM	100.58	100.37	95.31	100.72	100.30
Si	3.000	3.021	2.760	2.766	2.769
Ti	0.000	0.000	0.200	0.000	0.000
Al	1.932	1.912	1.522	1.207	1.202
Cr	0.000	0.001	0.000	0.000	0.000
Fe	2.101	2.070	1.116	0.000	0.001
Mn	0.200	0.173	0.006	0.001	0.001
Mg	0.664	0.714	1.268	0.000	0.000
Ca	0.137	0.132	0.001	0.245	0.248
Na	0.000	0.000	0.016	0.818	0.812
K	0.000	0.000	0.797	0.008	0.009
SUM	8.034	8.022	7.685	5.044	5.041
Mg/Mg+Fe	0.240	0.257	0.532	0.000	0.000
Al4	0.000	0.000	1.240	0.234	0.231
Al6	1.932	1.912	0.282	0.972	0.970

SAMPLE/ MINERAL Code	VAN-12H GNT R	VAN-12H GNT C	VAN-12H BIO I	VAN-12H PLA R
SiO2	38.57	37.95	37.31	62.71
TiO2	0.02	0.00	2.60	0.00
Al2O3	20.61	20.48	17.18	23.03
Cr2O3	0.00	0.00	0.04	0.01
FeO	28.06	28.39	16.81	0.03
MnO	6.87	6.02	0.14	0.00
MgO	3.93	4.23	11.28	0.00
CaO	2.08	1.97	0.00	5.72
Na2O	0.10	0.03	0.09	8.96
K2O	0.02	0.00	7.91	0.30
SUM	100.26	99.07	93.36	100.76
Si	3.063	3.048	2.829	2.769
Ti	0.001	0.000	0.148	0.000
Al	1.929	1.939	1.536	1.199
Cr	0.000	0.000	0.002	0.000
Fe	1.864	1.907	1.066	0.001
Mn	0.462	0.410	0.009	0.000
Mg	0.465	0.506	1.275	0.000
Ca	0.177	0.170	0.000	0.271
Na	0.015	0.005	0.013	0.767
K	0.002	0.000	0.765	0.017
SUM	7.979	7.984	7.643	5.023
Mg/Mg+Fe	0.200	0.210	0.545	0.000
Al4	0.000	0.000	1.171	0.231
Al6	1.929	1.939	0.364	0.967

SAMPLE/ MINERAL Code	VAN-12N GNT R	VAN-12N GNT C	VAN-12N BIO I	VAN-12N PLA R	VAN-12N PLA C
SiO2	39.32	39.22	38.73	63.22	62.56
TiO2	0.00	0.00	2.78	0.01	0.01
Al2O3	21.64	20.93	17.09	23.33	23.67
Cr2O3	0.00	0.00	0.02	0.02	0.00
FeO	27.93	27.91	13.00	0.03	0.01
MnO	4.72	4.59	0.09	0.00	0.02
MgO	6.98	7.22	14.95	0.00	0.01
CaO	1.55	1.37	0.00	5.52	5.45
Na2O	0.04	0.12	0.10	8.11	8.64
K2O	0.02	0.07	7.99	0.19	0.27
SUM	102.20	101.43	94.75	100.43	100.64
Si	3.017	3.035	2.834	2.784	2.759
Ti	0.000	0.000	0.153	0.000	0.000
Al	1.958	1.909	1.474	1.211	1.230
Cr	0.000	0.000	0.001	0.001	0.000
Fe	1.792	1.806	0.796	0.001	0.000
Mn	0.307	0.301	0.006	0.000	0.001
Mg	0.798	0.833	1.631	0.000	0.001
Ca	0.127	0.114	0.000	0.260	0.258
Na	0.006	0.018	0.014	0.693	0.739
K	0.002	0.007	0.746	0.011	0.015
SUM	8.008	8.023	7.655	4.961	5.003
Mg/Mg+Fe	0.308	0.316	0.672	0.000	0.641
Al4	0.000	0.000	1.166	0.216	0.241
Al6	1.958	1.909	0.309	0.995	0.989

SAMPLE/ MINERAL Code	VAN-16E GNT R	VAN-16E GNT C	VAN-16E BIO 1	VAN-16E PLA C
SiO2	39.46	40.25	38.11	65.50
TiO2	0.02	0.04	1.26	0.00
Al2O3	21.14	21.36	18.04	22.27
Cr2O3	0.01	0.02	0.00	0.02
FeO	16.13	16.46	11.11	0.07
MnO	17.09	15.75	0.44	0.00
MgO	4.95	6.71	16.50	0.00
CaO	2.48	1.68	0.04	3.51
Na2O	0.05	0.12	0.07	9.82
K2O	0.02	0.00	7.64	0.14
SUM	101.35	102.39	93.21	101.33
Si	3.067	3.069	2.809	2.850
Ti	0.001	0.002	0.070	0.000
Al	1.937	1.920	1.567	1.142
Cr	0.001	0.001	0.000	0.001
Fe	1.048	1.050	0.685	0.003
Mn	1.125	1.017	0.027	0.000
Mg	0.573	0.762	1.812	0.000
Ca	0.207	0.137	0.003	0.164
Na	0.008	0.018	0.010	0.829
K	0.002	0.000	0.718	0.008
SUM	7.968	7.977	7.702	4.996
Mg/Mg+Fe	0.354	0.421	0.726	0.000
Al4	0.000	0.000	1.191	0.150
Al6	1.937	1.920	0.376	0.993

SAMPLE/ MINERAL Code	VAN-34A GNT R	VAN-34A GNT C	VAN-34A BIO 1	VAN-34A PLA R	VAN-34A PLA C
SiO2	40.53	39.38	38.78	62.40	62.70
TiO2	0.02	0.00	2.77	0.00	0.03
Al2O3	20.78	22.04	16.41	23.11	23.69
Cr2O3	0.00	0.03	0.02	0.01	0.00
FeO	22.87	23.64	11.75	0.07	0.01
MnO	5.22	4.75	0.16	0.01	0.01
MgO	9.64	10.15	16.29	0.00	0.00
CaO	1.27	1.21	0.00	5.14	5.53
Na2O	0.01	0.00	0.05	8.64	8.37
K2O	0.02	0.00	8.43	0.20	0.25
SUM	100.36	101.20	94.66	99.58	100.59
Si	3.095	2.991	2.836	2.777	2.763
Ti	0.001	0.000	0.152	0.000	0.001
Al	1.871	1.973	1.414	1.212	1.231
Cr	0.000	0.002	0.001	0.000	0.000
Fe	1.461	1.502	0.719	0.003	0.000
Mn	0.338	0.306	0.010	0.000	0.000
Mg	1.097	1.149	1.775	0.000	0.000
Ca	0.104	0.098	0.000	0.245	0.261
Na	0.001	0.000	0.007	0.746	0.715
K	0.002	0.000	0.786	0.011	0.014
SUM	7.970	8.021	7.701	4.995	4.985
Mg/Mg+Fe	0.429	0.433	0.712	0.000	0.000
Al4	0.000	0.009	1.164	0.223	0.237
Al6	1.871	1.964	0.250	0.989	0.993



SAMPLE/ MINERAL Code	VN-35B GNT R	VN-35B GNT C	VN-35B BIO 11	VN-35B PLA R
SiO <sub>2</sub>	39.68	39.87	38.24	60.86
TiO <sub>2</sub>	0.00	0.04	3.08	0.00
Al <sub>2</sub> O <sub>3</sub>	21.08	21.02	15.96	23.90
Cr <sub>2</sub> O <sub>3</sub>	0.04	0.01	0.01	0.00
FeO	25.30	24.80	10.75	0.03
MnO	4.23	4.24	0.04	0.01
MgO	8.56	8.86	17.96	0.01
CaO	1.66	1.78	0.00	6.61
Na <sub>2</sub> O	0.07	0.00	0.15	8.07
K <sub>2</sub> O	0.02	0.02	12.45	0.23
SUM	100.64	100.64	98.64	99.71
Si	3.051	3.058	2.745	2.719
Ti	0.000	0.002	0.166	0.000
Al	1.911	1.901	1.351	1.259
Cr	0.002	0.001	0.001	0.000
Fe	1.627	1.591	0.645	0.001
Mn	0.276	0.275	0.002	0.000
Mg	0.981	1.013	1.922	0.001
Ca	0.137	0.146	0.000	0.316
Na	0.010	0.000	0.021	0.699
K	0.002	0.002	1.140	0.013
SUM	7.998	7.989	7.993	5.008
Mg/Mg+Fe	0.376	0.389	0.749	0.373
Al <sub>4</sub>	0.000	0.000	1.255	0.281
Al <sub>6</sub>	1.911	1.901	0.096	0.977

SAMPLE/ MINERAL Code	VAN-36 GNT R	VAN-36 GNT C	VAN-36 BIO 1	VAN-36 PLA R	VAN-36 PLA C
SiO <sub>2</sub>	39.56	39.93	39.57	62.12	62.26
TiO <sub>2</sub>	0.02	0.00	2.07	0.00	0.00
Al <sub>2</sub> O <sub>3</sub>	21.04	21.71	17.16	23.89	23.87
Cr <sub>2</sub> O <sub>3</sub>	0.02	0.01	0.02	0.00	0.00
FeO	21.69	20.61	10.85	0.03	0.04
MnO	7.11	7.09	0.05	0.00	0.00
MgO	8.98	9.67	17.08	0.00	0.00
CaO	1.66	1.31	0.00	6.07	6.42
Na <sub>2</sub> O	0.05	0.05	0.02	8.15	7.81
K <sub>2</sub> O	0.01	0.01	8.09	0.25	0.21
SUM	100.14	100.39	94.91	100.51	100.61
Si	3.048	3.045	2.857	2.744	2.747
Ti	0.001	0.000	0.112	0.000	0.000
Al	1.911	1.951	1.460	1.244	1.241
Cr	0.001	0.001	0.001	0.000	0.000
Fe	1.398	1.314	0.655	0.001	0.001
Mn	0.464	0.458	0.003	0.000	0.000
Mg	1.031	1.099	1.838	0.000	0.000
Ca	0.137	0.107	0.000	0.287	0.303
Na	0.007	0.007	0.003	0.698	0.668
K	0.001	0.001	0.745	0.014	0.012
SUM	7.999	7.983	7.674	4.989	4.973
Mg/Mg+Fe	0.425	0.455	0.737	0.000	0.000
Al <sub>4</sub>	0.000	0.000	1.143	0.256	0.253
Al <sub>6</sub>	1.911	1.951	0.317	0.989	0.988

SAMPLE# MINERAL Code	VN-102 GNT R	VN-102 GNT C	VN-102 BIO I	VN-102 PLA R
SiO2	40.03	36.12	39.79	61.99
TiO2	0.00	0.00	0.41	0.00
Al2O3	21.10	24.54	16.60	23.39
Cr2O3	0.02	0.00	0.03	0.01
FeO	22.76	22.58	9.65	0.04
MnO	5.54	5.50	0.08	0.00
MgO	9.82	9.82	18.54	0.00
CaO	0.52	0.82	0.00	5.99
Na2O	0.00	0.00	0.13	8.24
K2O	0.00	0.00	8.86	0.22
SUM	99.79	99.38	94.09	99.88
Si	3.073	2.802	2.896	2.756
Ti	0.000	0.000	0.022	0.000
Al	1.909	2.244	1.424	1.226
Cr	0.001	0.000	0.002	0.000
Fe	1.461	1.465	0.587	0.001
Mn	0.360	0.361	0.005	0.000
Mg	1.123	1.135	2.011	0.000
Ca	0.043	0.068	0.000	0.285
Na	0.000	0.000	0.018	0.710
K	0.000	0.000	0.823	0.012
SUM	7.971	8.076	7.789	4.992
Mg/Mg+Fe	0.435	0.437	0.774	0.000
Al4	0.000	0.198	1.104	0.244
Al6	1.909	2.046	0.320	0.962

SAMPLE# MINERAL Code	VN-150 GNT R	VN-150 GNT C	VN-150 BIO I	VN-150 PLA R
SiO2	38.74	38.79	37.18	61.35
TiO2	0.00	0.00	4.09	0.00
Al2O3	20.27	20.27	17.62	23.52
Cr2O3	0.02	0.01	0.07	0.00
FeO	28.95	28.59	16.84	0.04
MnO	6.24	6.20	0.11	0.02
MgO	4.86	5.30	10.62	0.00
CaO	1.20	1.06	0.00	6.12
Na2O	0.01	0.02	0.11	8.24
K2O	0.01	0.01	9.86	0.25
SUM	100.30	100.25	96.50	99.54
Si	3.071	3.069	2.760	2.741
Ti	0.000	0.000	0.228	0.000
Al	1.894	1.891	1.542	1.239
Cr	0.001	0.001	0.004	0.000
Fe	1.919	1.892	1.046	0.001
Mn	0.419	0.416	0.007	0.001
Mg	0.574	0.625	1.175	0.000
Ca	0.102	0.090	0.000	0.293
Na	0.002	0.003	0.016	0.714
K	0.001	0.001	0.934	0.014
SUM	7.983	7.987	7.713	5.003
Mg/Mg+Fe	0.230	0.248	0.529	0.000
Al4	0.000	0.000	1.240	0.259
Al6	1.894	1.891	0.303	0.980

SAMPLE/ MINERAL Code	VN-338 GNT R	VN-338 BIO I	VN-338 PLA R	VN-338 PLA C
SiO2	39.83	38.88	64.21	63.60
TiO2	0.88	3.00	0.04	0.03
Al2O3	20.86	16.09	21.80	21.77
Cr2O3	0.00	0.03	0.02	0.00
FeO	20.29	8.56	0.02	0.07
MnO	8.15	0.14	0.03	0.00
MgO	10.07	19.44	0.04	0.00
CaO	0.02	0.00	4.03	4.42
Na2O	0.02	0.10	9.61	9.23
K2O	0.00	9.43	0.21	0.27
SUM	100.12	95.67	100.01	99.39
Si	3.048	2.793	2.839	2.832
Ti	0.051	0.162	0.001	0.001
Al	1.882	1.363	1.136	1.143
Cr	0.000	0.002	0.001	0.000
Fe	1.299	0.514	0.001	0.003
Mn	0.528	0.009	0.001	0.000
Mg	1.149	2.081	0.003	0.000
Ca	0.002	0.000	0.191	0.211
Na	0.003	0.014	0.824	0.797
K	0.000	0.864	0.012	0.015
SUM	7.961	7.802	5.009	5.002
Mg/Mg+Fe	0.469	0.802	0.781	0.000
Al4	0.000	1.207	0.161	0.168
Al6	1.882	0.156	0.975	0.975

SAMPLE/ MINERAL Code	VO-77A GNT R	VO-77A GNT C	VO-77A BIO I	VO-77A PLA R	VO-77A PLA C
SiO2	39.45	39.43	37.73	62.48	62.77
TiO2	0.02	0.00	1.93	0.01	0.00
Al2O3	21.35	21.66	18.52	23.50	23.81
Cr2O3	0.04	0.01	0.01	0.01	0.02
FeO	22.58	23.00	12.02	0.03	0.01
MnO	6.49	6.22	0.23	0.02	0.01
MgO	7.37	7.34	14.75	0.00	0.01
CaO	3.27	2.47	0.00	4.71	4.97
Na2O	0.03	0.06	0.07	9.52	9.69
K2O	0.01	0.00	9.98	0.15	0.23
SUM	100.61	100.19	95.24	100.43	101.52
Si	3.042	3.046	2.771	2.762	2.751
Ti	0.001	0.000	0.107	0.000	0.000
Al	1.940	1.973	1.603	1.225	1.230
Cr	0.002	0.001	0.001	0.000	0.001
Fe	1.456	1.486	0.738	0.001	0.000
Mn	0.424	0.407	0.014	0.001	0.000
Mg	0.847	0.845	1.614	0.000	0.001
Ca	0.270	0.204	0.000	0.223	0.233
Na	0.004	0.009	0.010	0.816	0.823
K	0.001	0.000	0.935	0.008	0.013
SUM	7.988	7.971	7.793	5.037	5.052
Mg/Mg+Fe	0.368	0.363	0.686	0.000	0.641
Al4	0.000	0.000	1.229	0.238	0.249
Al6	1.940	1.973	0.374	0.987	0.980

SAMPLE# MINERAL Code	VO-518 GNT R	VO-518 BIO I	VO-518 PLA R
SiO2	37.89	36.64	61.89
TiO2	0.02	1.70	0.00
Al2O3	21.88	18.71	24.31
Cr2O3	0.03	0.06	0.00
FeO	33.44	16.45	0.03
MnO	1.31	0.03	0.00
MgO	5.79	12.70	0.02
CaO	1.20	0.00	5.59
Na2O	0.11	0.11	8.64
K2O	0.03	9.48	0.22
SUM	101.70	95.88	100.70
Si	2.959	2.726	2.730
Ti	0.001	0.095	0.000
Al	2.014	1.641	1.264
Cr	0.002	0.004	0.000
Fe	2.184	1.023	0.001
Mn	0.087	0.002	0.000
Mg	0.674	1.408	0.001
Ca	0.100	0.000	0.264
Na	0.017	0.016	0.739
K	0.003	0.900	0.012
SUM	8.041	7.814	5.013
Mg/Mg+Fe	0.236	0.579	0.543
Al4	0.041	1.274	0.270
Al6	1.973	0.367	0.995

SAMPLE/ MINERAL Code	CG-366 GNT R	CG-366 GNT C	CG-366 BIO I	CG-366 PLA R	CG-366 PLA C	CG-366 CPX I
SiO <sub>2</sub>	38.34	37.88	36.75	60.03	61.45	53.49
TiO <sub>2</sub>	0.05	0.03	4.46	0.00	0.01	0.07
Al <sub>2</sub> O <sub>3</sub>	21.44	21.69	15.20	25.46	25.05	1.29
Cr <sub>2</sub> O <sub>3</sub>	0.02	0.05	0.03	0.00	0.02	0.01
FeO	25.24	25.46	18.17	0.06	0.06	9.31
MnO	1.24	1.75	0.02	0.01	0.00	0.13
MgO	4.31	4.68	12.39	0.00	0.01	12.93
CaO	9.88	9.03	0.00	6.60	6.22	21.73
Na <sub>2</sub> O	0.00	0.02	0.01	8.24	7.74	1.45
K <sub>2</sub> O	0.00	0.00	8.65	0.29	0.33	0.00
SUM	100.52	100.59	95.68	100.69	100.82	100.41
Si	2.990	2.958	2.763	2.662	2.706	1.991
Ti	0.003	0.002	0.252	0.000	0.000	0.002
Al	1.971	1.997	1.347	1.331	1.300	0.057
Cr	0.001	0.003	0.002	0.000	0.001	0.000
Fe	1.646	1.663	1.142	0.002	0.002	0.290
Mn	0.082	0.116	0.001	0.000	0.000	0.004
Mg	0.501	0.545	1.388	0.000	0.001	0.717
Ca	0.826	0.756	0.000	0.314	0.293	0.866
Na	0.000	0.003	0.001	0.709	0.661	0.105
K	0.000	0.000	0.830	0.016	0.019	0.000
SUM	8.020	8.041	7.726	5.035	4.983	4.031
Mg/Mg+Fe	0.233	0.247	0.549	0.000	0.229	0.712
Al <sub>4</sub>	0.010	0.042	1.237	0.338	0.294	0.009
Al <sub>6</sub>	1.961	1.955	0.110	0.993	1.006	0.047

SAMPLE/ MINERAL Code	CG-488A GNT R	CG-488A GNT C	CG-488A PLA R	CG-488A CPX I
SiO <sub>2</sub>	39.43	39.29	58.96	52.22
TiO <sub>2</sub>	0.05	0.09	0.00	0.34
Al <sub>2</sub> O <sub>3</sub>	21.77	21.53	26.51	2.91
Cr <sub>2</sub> O <sub>3</sub>	0.00	0.00	0.02	0.00
FeO	29.86	24.36	0.06	9.73
MnO	2.21	2.20	0.00	0.37
MgO	6.73	7.13	0.00	13.27
CaO	5.93	6.07	7.98	20.41
Na <sub>2</sub> O	0.01	0.03	7.27	0.64
K <sub>2</sub> O	0.00	0.00	0.23	0.00
SUM	100.99	100.70	101.03	99.89
Si	3.024	3.019	2.611	1.948
Ti	0.003	0.005	0.000	0.010
Al	1.968	1.950	1.384	0.128
Cr	0.000	0.000	0.001	0.000
Fe	1.594	1.565	0.002	0.304
Mn	0.144	0.143	0.000	0.012
Mg	0.769	0.816	0.000	0.738
Ca	0.487	0.500	0.379	0.816
Na	0.001	0.004	0.624	0.046
K	0.000	0.000	0.013	0.000
SUM	7.990	8.003	5.015	4.001
Mg/Mg+Fe	0.325	0.343	0.000	0.708
Al <sub>4</sub>	0.000	0.000	0.389	0.052
Al <sub>6</sub>	1.968	1.950	0.996	0.076

SAMPLE/ MINERAL Code	CG-641 GNT R	CG-641 BIO I	CG-641 PLA R	CG-641 PLA C	CG-641 OPX I	CG-641 OPX I
SiO2	38.03	36.00	67.16	67.04	49.12	50.49
TiO2	0.05	4.45	0.00	0.00	0.02	0.08
Al2O3	20.85	13.17	20.79	20.01	0.23	1.23
Cr2O3	0.02	0.02	0.04	0.00	0.03	0.03
FeO	28.72	26.20	0.04	0.06	40.27	20.03
MnO	2.68	0.13	0.00	0.00	2.08	0.90
MgO	1.18	6.47	0.00	0.00	7.85	6.23
CaO	8.38	0.00	1.71	1.66	0.70	19.87
Na2O	0.00	0.06	12.07	12.02	0.01	1.09
K2O	0.01	8.97	0.15	0.18	0.01	0.01
SUM	99.92	95.47	101.96	100.97	100.32	99.96
Si	3.041	2.840	2.907	2.930	2.010	1.987
Ti	0.003	0.264	0.000	0.000	0.001	0.002
Al	1.965	1.225	1.061	1.031	0.011	0.057
Cr	0.001	0.001	0.001	0.000	0.001	0.001
Fe	1.921	1.728	0.001	0.002	1.378	0.659
Mn	0.182	0.009	0.000	0.000	0.072	0.030
Mg	0.141	0.761	0.000	0.000	0.479	0.365
Ca	0.718	0.000	0.079	0.078	0.831	0.838
Na	0.000	0.009	1.013	1.019	0.001	0.083
K	0.001	0.903	0.008	0.010	0.001	0.001
SUM	7.973	7.739	5.072	5.069	3.984	4.023
Mg/Mg+Fe	0.068	0.306	0.000	0.000	0.258	0.357
Al4	0.000	1.160	0.093	0.070	0.000	0.013
Al6	1.965	0.064	0.968	0.961	0.011	0.044

SAMPLE/ MINERAL Code	CG-811B GNT R	CG-811B PLA R	CG-811B OPX I
SiO2	39.59	59.70	51.84
TiO2	0.05	0.00	0.05
Al2O3	21.54	26.48	2.22
Cr2O3	0.05	0.02	0.02
FeO	23.80	0.18	23.55
MnO	0.99	0.04	0.96
MgO	7.61	0.01	21.65
CaO	6.96	7.59	0.45
Na2O	0.06	7.39	0.06
K2O	0.00	0.40	0.00
SUM	100.65	101.81	100.80
Si	3.026	2.624	1.932
Ti	0.003	0.000	0.001
Al	1.941	1.372	0.098
Cr	0.003	0.001	0.001
Fe	1.521	0.007	0.734
Mn	0.064	0.001	0.030
Mg	0.867	0.001	1.202
Ca	0.570	0.357	0.018
Na	0.009	0.630	0.004
K	0.000	0.022	0.000
SUM	8.004	5.015	4.020
Mg/Mg+Fe	0.363	0.090	0.621
Al4	0.000	0.376	0.068
Al6	1.941	0.996	0.029

SAMPLE/ MINERAL Code	CG-362 GNT R	CG-362 PLA 1	CG-362 OPX 1	CG-362 OPX 1
SiO2	39.68	59.01	52.69	52.87
TiO2	0.00	0.00	0.00	0.38
Al 2O3	20.86	25.13	1.69	2.91
Cr 2O3	0.04	0.00	0.02	0.03
FeO	25.08	0.06	22.29	8.41
MnO	0.55	0.00	0.17	0.08
MgO	7.74	0.00	22.97	13.92
CaO	6.36	8.23	0.39	21.63
Na2O	0.05	6.86	0.04	0.65
K2O	0.02	0.44	0.00	0.01
SUM	100.38	99.73	100.26	100.89
Si	3.049	2.648	1.953	1.944
Ti	0.000	0.000	0.000	0.011
Al	1.890	1.329	0.074	0.126
Cr	0.002	0.000	0.001	0.001
Fe	1.612	0.002	0.691	0.259
Mn	0.036	0.000	0.005	0.002
Mg	0.886	0.000	1.269	0.763
Ca	0.524	0.396	0.015	0.852
Na	0.007	0.597	0.003	0.046
K	0.002	0.025	0.000	0.000
SUM	8.009	4.998	4.011	4.005
Mg/Mg+Fe	0.355	0.000	0.647	0.747
Al4	0.000	0.352	0.047	0.056
Al6	1.890	0.978	0.027	0.070

SAMPLE/ MINERAL Code	GF-222 GNT R	GF-222 GNT C	GF-222 PLA R	GF-222 PLA C	GF-222 OPX 1
SiO2	40.08	40.63	51.54	51.07	50.36
TiO2	0.04	0.10	0.00	0.00	0.70
Al 2O3	21.88	22.29	30.08	30.45	5.15
Cr 2O3	0.05	0.03	0.00	0.02	0.04
FeO	18.88	17.18	0.09	0.15	7.45
MnO	0.56	0.47	0.01	0.01	0.11
MgO	10.63	10.25	0.00	0.00	13.17
CaO	7.69	7.81	13.88	14.51	21.86
Na2O	0.01	0.01	4.04	3.20	0.66
K2O	0.01	0.01	0.07	0.09	0.04
SUM	99.83	98.78	99.71	99.50	99.54
Si	3.019	3.061	2.354	2.337	1.877
Ti	0.002	0.006	0.000	0.000	0.020
Al	1.943	1.979	1.619	1.642	0.226
Cr	0.003	0.002	0.000	0.001	0.001
Fe	1.189	1.082	0.003	0.006	0.232
Mn	0.036	0.030	0.000	0.000	0.003
Mg	1.193	1.151	0.000	0.000	0.732
Ca	0.621	0.630	0.679	0.711	0.873
Na	0.001	0.001	0.358	0.284	0.048
K	0.001	0.001	0.004	0.005	0.002
SUM	8.007	7.944	5.018	4.986	4.014
Mg/Mg+Fe	0.501	0.515	0.000	0.000	0.759
Al4	0.000	0.000	0.646	0.663	0.123
Al6	1.943	1.979	0.973	0.979	0.103

SAMPLE# MINERAL Code	GF-244A GNT R	GF-244A PLA R	GF-244A OPX I	GF-244A CPX I
SiO2	42.02	49.77	54.66	51.80
TiO2	0.05	0.00	0.06	0.50
Al2O3	23.02	32.40	3.37	4.26
Cr2O3	0.04	0.02	0.01	0.04
FeO	14.03	0.04	12.00	5.44
MnO	0.39	0.00	0.19	0.09
MgO	15.94	0.00	29.86	16.16
CaO	5.68	15.44	0.28	19.30
Na2O	0.05	3.14	0.01	0.75
K2O	0.00	0.07	0.01	0.00
SUM	101.22	100.88	100.45	98.34
Si	3.023	2.256	1.925	1.918
Ti	0.003	0.000	0.002	0.014
Al	1.952	1.731	0.140	0.186
Cr	0.002	0.001	0.000	0.001
Fe	0.844	0.002	0.353	0.168
Mn	0.024	0.000	0.006	0.003
Mg	1.709	0.000	1.567	0.892
Ca	0.438	0.750	0.011	0.766
Na	0.007	0.276	0.001	0.054
K	0.000	0.004	0.000	0.000
SUM	8.001	5.018	4.004	4.001
Mg/Mg+Fe	0.669	0.000	0.816	0.841
Al4	0.000	0.744	0.075	0.082
Al6	1.952	0.986	0.065	0.104

SAMPLE# MINERAL Code	GF-246A GNT R	GF-246A GNT C	GF-246A BIO I	GF-246A PLA R	GF-246A PLA C	GF-246A OPX I	GF-246A CPX I
SiO2	39.46	39.55	37.71	58.06	58.38	51.93	51.26
TiO2	0.02	0.04	5.16	0.00	0.00	0.04	0.31
Al2O3	21.39	21.21	13.55	25.82	26.57	2.25	3.64
Cr2O3	0.02	0.00	0.00	0.02	0.04	0.00	0.02
FeO	25.21	24.85	13.61	0.13	0.07	22.98	9.82
MnO	0.96	1.07	0.03	0.01	0.01	0.25	0.13
MgO	6.95	7.23	15.14	0.00	0.00	21.42	12.40
CaO	6.47	6.32	0.00	8.53	8.66	0.49	21.29
Na2O	0.04	0.00	0.04	6.97	7.07	0.00	0.91
K2O	0.00	0.00	9.72	0.32	0.35	0.00	0.00
SUM	100.49	100.27	94.96	99.86	101.15	99.36	99.78
Si	3.035	3.044	2.815	2.609	2.592	1.950	1.923
Ti	0.001	0.002	0.290	0.000	0.000	0.001	0.009
Al	1.940	1.924	1.192	1.368	1.390	0.100	0.161
Cr	0.001	0.000	0.000	0.001	0.001	0.000	0.001
Fe	1.622	1.600	0.850	0.005	0.003	0.722	0.308
Mn	0.063	0.070	0.002	0.000	0.000	0.008	0.004
Mg	0.797	0.829	1.684	0.000	0.000	1.199	0.693
Ca	0.533	0.521	0.000	0.411	0.412	0.020	0.856
Na	0.001	0.000	0.006	0.607	0.609	0.000	0.066
K	0.000	0.000	0.926	0.018	0.020	0.000	0.000
SUM	7.993	7.991	7.765	5.019	5.027	3.999	4.021
Mg/Mg+Fe	0.329	0.341	0.665	0.000	0.000	0.624	0.692
Al4	0.000	0.000	1.185	0.391	0.408	0.050	0.077
Al6	1.940	1.924	0.007	0.977	0.982	0.050	0.084



SAMPLE# MINERAL Code	GF-121 PLA R	GF-121 PLA C	GF-121 OPX 1	GF-121 CPX 1
SiO2	56.47	56.79	50.46	52.46
TiO2	0.00	0.00	0.43	0.12
Al2O3	27.27	27.18	1.64	1.97
Cr2O3	0.03	0.00	0.02	0.02
FeO	0.10	0.07	30.21	11.80
MnO	0.03	0.00	0.83	0.34
MgO	0.00	0.00	16.61	11.70
CaO	10.05	9.69	0.74	21.26
Na2O	6.18	6.71	0.02	0.57
K2O	0.37	0.22	0.00	0.00
SUM	100.50	100.66	100.96	100.24
Si	2.534	2.542	1.940	1.973
Ti	0.000	0.000	0.012	0.003
Al	1.442	1.434	0.074	0.087
Cr	0.001	0.000	0.001	0.001
Fe	0.004	0.003	0.972	0.371
Mn	0.001	0.000	0.027	0.011
Mg	0.000	0.000	0.952	0.656
Ca	0.483	0.465	0.030	0.857
Na	0.538	0.582	0.001	0.042
K	0.021	0.013	0.000	0.000
SUM	5.024	5.038	4.010	4.000
Mg/Mg+Fe	0.000	0.000	0.495	0.639
Al4	0.466	0.458	0.060	0.027
Al6	0.976	0.976	0.015	0.060

SAMPLE# MINERAL Code	CG-100 PLA R	CG-100 OPX 1	CG-100 CPX 1
SiO2	58.07	52.87	51.70
TiO2	0.00	0.11	0.35
Al2O3	25.44	1.33	2.66
Cr2O3	0.00	0.00	0.05
FeO	0.09	23.39	9.65
MnO	0.02	1.42	0.61
MgO	0.00	21.14	13.21
CaO	8.55	0.56	21.28
Na2O	6.54	0.02	0.71
K2O	0.52	0.01	0.00
SUM	99.23	100.85	100.22
Si	2.624	1.968	1.933
Ti	0.000	0.003	0.010
Al	1.355	0.058	0.117
Cr	0.000	0.000	0.001
Fe	0.003	0.728	0.302
Mn	0.001	0.045	0.019
Mg	0.000	1.173	0.736
Ca	0.414	0.022	0.853
Na	0.573	0.001	0.051
K	0.030	0.000	0.000
SUM	5.000	4.000	4.023
Mg/Mg+Fe	0.000	0.617	0.709
Al4	0.376	0.032	0.067
Al6	0.979	0.027	0.051

SAMPLE/ MINERAL Code	VO-89A GNT R	VO-89A GNT C	VO-89A BIO I	VO-89A PLA R	VO-89A PLA C	VO-89A OPX I
SiO2	38.36	39.63	37.68	61.30	60.97	53.03
TiO2	0.00	0.01	5.08	0.00	0.12	0.02
Al2O3	22.36	21.54	14.21	24.27	23.89	1.10
Cr2O3	0.08	0.05	0.03	0.00	0.00	0.03
FeO	25.59	24.16	15.46	0.06	0.02	21.77
MnO	1.18	1.39	0.14	0.01	0.01	1.84
MgO	6.99	7.38	13.64	0.00	0.00	21.72
CaO	6.78	6.62	0.00	5.99	5.94	0.86
Na2O	0.01	0.07	0.01	8.91	8.87	0.04
K2O	0.02	0.01	9.90	0.23	0.29	0.01
SUM	101.37	100.86	96.15	100.77	100.11	100.42
Si	2.942	3.030	2.803	2.713	2.717	1.974
Ti	0.000	0.001	0.284	0.000	0.004	0.001
Al	2.022	1.941	1.246	1.266	1.255	0.048
Cr	0.005	0.003	0.002	0.000	0.000	0.001
Fe	1.641	1.545	0.962	0.002	0.001	0.678
Mn	0.077	0.090	0.009	0.000	0.000	0.058
Mg	0.799	0.841	1.512	0.000	0.000	1.205
Ca	0.557	0.542	0.000	0.284	0.284	0.034
Na	0.001	0.010	0.001	0.765	0.766	0.003
K	0.002	0.001	0.940	0.013	0.016	0.000
SUM	8.046	8.003	7.759	5.043	5.043	4.002
Mg/Mg+Fe	0.327	0.352	0.611	0.000	0.000	0.640
Al4	0.058	0.000	1.197	0.287	0.283	0.026
Al6	1.964	1.941	0.049	0.979	0.972	0.022

SAMPLE/ MINERAL Code	VO-188 GNT R	VO-188 GNT C	VO-188 PLA C	VO-188 OPX I	VO-188 CPX I
SiO2	39.68	39.16	57.72	50.37	50.83
TiO2	0.05	0.06	0.00	0.05	0.46
Al2O3	22.91	22.35	27.57	4.07	5.46
Cr2O3	0.01	0.06	0.02	0.05	0.02
FeO	22.48	21.82	0.07	19.57	8.01
MnO	1.02	0.86	0.00	0.11	0.14
MgO	10.53	11.10	0.00	25.08	12.80
CaO	5.16	5.10	9.24	0.43	21.17
Na2O	0.00	0.04	6.71	0.01	0.83
K2O	0.01	0.01	0.14	0.00	0.00
SUM	101.85	100.56	101.47	99.74	99.72
Si	2.960	2.955	2.554	1.861	1.889
Ti	0.003	0.003	0.000	0.001	0.013
Al	2.015	1.988	1.438	0.177	0.239
Cr	0.001	0.004	0.001	0.001	0.001
Fe	1.403	1.377	0.003	0.605	0.249
Mn	0.064	0.055	0.000	0.003	0.004
Mg	1.171	1.248	0.000	1.381	0.709
Ca	0.412	0.412	0.438	0.017	0.843
Na	0.000	0.006	0.576	0.001	0.060
K	0.001	0.001	0.008	0.000	0.000
SUM	8.030	8.049	5.018	4.048	4.008
Mg/Mg+Fe	0.455	0.475	0.000	0.695	0.740
Al4	0.040	0.045	0.446	0.139	0.111
Al6	1.975	1.943	0.993	0.038	0.129

SAMPLE# MINERAL Code	VAN-19 PLA R	VAN-19 PLA C	VAN-19 OPX 1	VAN-19 CPX 1
SiO2	57.32	56.95	51.80	50.55
TiO2	0.00	0.00	0.06	0.32
Al2O3	26.24	26.23	1.91	3.30
Cr2O3	0.00	0.00	0.02	0.03
FeO	0.08	0.09	23.79	9.82
MnO	0.00	0.00	0.92	0.38
MgO	0.01	0.02	20.39	12.20
CaO	9.00	9.37	0.55	21.89
Na2O	6.83	6.84	0.02	0.67
K2O	0.40	0.36	0.01	0.01
SUM	99.88	99.86	99.47	99.17
Si	2.581	2.570	1.958	1.916
Ti	0.000	0.000	0.002	0.009
Al	1.393	1.395	0.085	0.147
Cr	0.000	0.000	0.001	0.001
Fe	0.003	0.003	0.752	0.311
Mn	0.000	0.000	0.029	0.012
Mg	0.001	0.001	1.148	0.689
Ca	0.434	0.453	0.022	0.889
Na	0.596	0.598	0.001	0.049
K	0.023	0.021	0.000	0.000
SUM	5.032	5.042	3.999	4.025
Mg/Mg+Fe	0.182	0.284	0.604	0.689
Al4	0.419	0.430	0.042	0.084
Al6	0.974	0.965	0.043	0.064

SAMPLE# MINERAL Code	VN-534 OPX 1	VN-534 CPX 1
SiO2	52.99	50.84
TiO2	0.07	0.56
Al2O3	2.85	5.25
Cr2O3	0.05	0.09
FeO	19.67	8.22
MnO	0.30	0.03
MgO	24.64	13.07
CaO	0.01	20.86
Na2O	0.01	0.70
K2O	0.01	0.02
SUM	100.60	99.64
Si	1.931	1.891
Ti	0.002	0.016
Al	0.122	0.230
Cr	0.001	0.003
Fe	0.600	0.256
Mn	0.009	0.001
Mg	1.338	0.724
Ca	0.000	0.831
Na	0.001	0.050
K	0.000	0.001
SUM	4.006	4.003
Mg/Mg+Fe	0.691	0.739
Al4	0.069	0.109
Al6	0.054	0.121

SAMPLE# MINERAL Code	VN-229 GNT R	VN-229 PLA R	VN-229 CPX 1
SiO2	39.14	63.80	52.67
TiO2	0.00	0.00	0.02
Al2O3	19.57	22.40	1.82
Cr2O3	0.02	0.02	0.00
FeO	28.29	0.11	12.63
MnO	2.37	0.02	0.29
MgO	3.68	0.02	11.08
CaO	6.91	5.23	21.27
Na2O	0.02	8.40	0.85
K2O	0.01	0.16	0.01
SUM	100.01	100.16	100.64
Si	3.100	2.816	1.981
Ti	0.000	0.000	0.001
Al	1.827	1.166	0.081
Cr	0.001	0.001	0.000
Fe	1.874	0.004	0.397
Mn	0.159	0.001	0.009
Mg	0.434	0.001	0.621
Ca	0.586	0.247	0.857
Na	0.003	0.719	0.062
K	0.001	0.009	0.000
SUM	7.987	4.964	4.009
Mg/Mg+Fe	0.188	0.245	0.610
Al4	0.000	0.184	0.019
Al6	1.827	0.982	0.062

SAMPLE# MINERAL Code	VAN-431 GNT R	VAN-431 PLA R	VAN-431 OPX 1	VAN-431 CPX 1
SiO2	39.35	57.48	51.80	52.13
TiO2	0.03	0.01	0.07	0.25
Al2O3	21.67	25.88	1.39	2.97
Cr2O3	0.00	0.02	0.02	0.00
FeO	26.89	0.07	27.71	10.33
MnO	1.25	0.00	0.38	0.16
MgO	5.30	0.00	18.56	12.36
CaO	6.56	7.90	0.55	21.66
Na2O	0.01	7.41	0.05	0.50
K2O	0.00	0.23	0.00	0.01
SUM	101.06	99.00	100.53	100.37
Si	3.036	2.604	1.967	1.945
Ti	0.002	0.000	0.002	0.007
Al	1.971	1.382	0.062	0.131
Cr	0.000	0.001	0.001	0.000
Fe	1.735	0.003	0.880	0.322
Mn	0.082	0.000	0.012	0.005
Mg	0.609	0.000	1.051	0.687
Ca	0.542	0.383	0.022	0.866
Na	0.001	0.651	0.004	0.036
K	0.000	0.013	0.000	0.000
SUM	7.978	5.037	4.001	4.001
Mg/Mg+Fe	0.260	0.000	0.544	0.681
Al4	0.000	0.396	0.033	0.055
Al6	1.971	0.985	0.030	0.076





